

Fall 2012

Computational Ligand-Based CNS Therapeutic Design: The Search for Novel-Scaffold Norepinephrine Transporter Inhibitors

Anna Chaly

Follow this and additional works at: <https://dsc.duq.edu/etd>

Recommended Citation

Chaly, A. (2012). Computational Ligand-Based CNS Therapeutic Design: The Search for Novel-Scaffold Norepinephrine Transporter Inhibitors (Master's thesis, Duquesne University). Retrieved from <https://dsc.duq.edu/etd/389>

This Immediate Access is brought to you for free and open access by Duquesne Scholarship Collection. It has been accepted for inclusion in Electronic Theses and Dissertations by an authorized administrator of Duquesne Scholarship Collection. For more information, please contact phillips@duq.edu.

COMPUTATIONAL LIGAND-BASED CNS THERAPEUTIC DESIGN:
THE SEARCH FOR NOVEL-SCAFFOLD NOREPINEPHRINE TRANSPORTER
INHIBITORS

A Thesis

Submitted to the Graduate School of Pharmaceutical Sciences of Duquesne University

Mylan School of Pharmacy

Duquesne University

In partial fulfillment of the requirements for
the degree of Master of Pharmaceutical Sciences

By

Anna Chaly

December 2012

Copyright by

Anna Chaly

2012

COMPUTATIONAL LIGAND-BASED CNS THERAPEUTIC DESIGN:
THE SEARCH FOR NOVEL-SCAFFOLD NOREPINEPHRINE
TRANSPORTER INHIBITORS

By

Anna Chaly

Approved October 26, 2012

Christopher K. Surratt, Ph.D.
Professor of Pharmacology
Graduate School of Pharmaceutical
Sciences
(Committee Chair)

Jeffry D. Madura, Ph.D.
Professor of Chemistry and
Biochemistry
(Committee Member)

Lauren A. O'Donnell, Ph.D.
Assistant Professor of Pharmacology
Graduate School of Pharmaceutical
Sciences
(Committee Member)

Sciences

James K. Drennen, III, Ph.D.
Associate Dean, Research and
Graduate Programs
Mylan School of Pharmacy and
Graduate School of Pharmaceutical

J. Douglas Bricker, Ph.D.
Dean and Professor of Pharmacology
and Toxicology

ABSTRACT

COMPUTATIONAL LIGAND-BASED CNS THERAPEUTIC DESIGN: THE SEARCH FOR NOVEL-SCAFFOLD NOREPINEPHRINE TRANSPORTER INHIBITORS

By

Anna Chaly

December 2012

Thesis supervised by Christopher K. Surratt

Monoamine transporter (MAT) proteins are responsible for regulating cellular signal transduction through control of neurotransmitter reuptake in the synapse, and are therefore relevant to diseases including addiction, psychosis, anxiety and depression. MATs, specifically the serotonin transporter (SERT or 5-HTT), norepinephrine transporter (NET), and dopamine transporter (DAT), serve as the principal targets for antidepressant drugs, such as SSRIs (selective serotonin reuptake inhibitors), NRIs (norepinephrine reuptake inhibitors) and TCAs (tricyclic antidepressants), as well as psychostimulant drugs of abuse such as cocaine and the amphetamines. Due to a lack of crystallographic MAT data, it is unclear as to which of two MAT protein ligand binding sites these drugs bind, hindering knowledge of the specific binding modes of MAT ligands. In this study an *in silico* pharmacophore model was created using a ligand-based

method aimed at drug screening for the ability to specifically inhibit NET, using Molecular Operating Environment software. A group of four structurally-diverse compounds with high NET binding affinities comprised the training set used to generate the model. A test set, which included ten compounds with a range of known NET affinities, served in the validation of the model. The constructed pharmacophore model selected all high affinity NET inhibitors and one relatively inactive compound from the test set. Following model validation, the ZINC small molecule structural database was virtually screened to identify novel MAT inhibitor candidates. “Hit” compounds were ranked by an overlay score, which calculated how well novel compounds aligned to the original training set alignment. Six top-ranking compounds were purchased and evaluated via *in vitro* pharmacology to determine the binding affinity at the MATs. Although no significant inhibition was observed at the MATs, compound AC-1 showed a 15% inhibition at the DAT in radioligand binding assays. This result suggests that with further refinement of key pharmacophore features or alteration of the AC-1 structure, more potent MAT inhibitors could be discovered. Pharmacophore-based drug design has become one of the most important tools in drug discovery. Using the molecular modeling approaches described in this study, it is possible to rationally design novel and more selective central nervous system drugs.

DEDICATION

To my angel, my son - Valentin

ACKNOWLEDGEMENT

I would like to thank Dr. Christopher K. Surratt, my thesis advisor, for his support, ideas and for giving me the opportunity to work on such an interesting project. I have gained an appreciation of pharmacology and learned a lot from his guidance during my time as a graduate student in his lab.

I would also like to sincerely thank Dr. Jeffrey D. Madura for his creative ideas, for his ability to communicate difficult concepts in an easy and understandable form, but most of all, for him taking the time to mentor me. Dr. Madura has opened the grand metaphysical world of computational chemistry for me and for this I am grateful to him.

I wish to also thank my committee member, Dr. Lauren O'Donnell for her invaluable ideas and suggestions during the course of my graduate work.

I would like to especially thank Dr. Tammy L. Nolan for teaching me research techniques and for helping me troubleshoot problems at work.

I am grateful to my family for their support and understanding.

Finally, I wish to express my gratitude to my love, my husband, Yury - for everything.

TABLE OF CONTENTS

	Page
Abstract.....	iv
Dedication.....	vi
Acknowledgement.....	vii
List of Tables	xiii
List of Figures	xiv
List of Abbreviations.....	xvi
Chapter 1. Introduction.....	1
1.1 Statement of Problem	1
1.2 Monoamine Transporters (MATs)	3
1.2.1 MAT Structure	3
1.2.2 MAT Inhibitors.....	4
1.2.3 MAT Inhibitor Selectivity and Adverse Effects.....	4
1.2.4 Synaptic Transmission of the MATs	7
1.3 Norepinephrine Transporter (NET).....	9
1.3.1 Norepinephrine Synthesis and Function	10
1.3.2 NET Inhibitors.....	10
1.4 Leucine Transporter (LeuT).....	11
1.4.1 LeuT Structure.....	11
1.5 Drug Design	12
1.5.1 The Art of Drug Design	12
1.5.2 Pharmacophore Modeling: Yesterday and Today	13

1.5.3 Ligand-Based versus Structure-Based Pharmacophore Models	15
1.5.4 Guide to Generating a Pharmacophore Model.....	17
1.5.4.1 Generation of the Training Set (TS)	17
1.5.4.2 Alignment of TS compounds	17
1.5.4.3 Selecting the Optimal Pharmacophore Features.....	18
1.5.4.4 Validation.....	18
1.5.4.5 Virtual Screening (VS)	19
1.6 Ranking of Hit Compounds	20
1.7 Different Software Packages and Pharmacophore Features	22
1.8 Inactive Hit Compounds	24
1.9 Rational Drug Design	24
1.10 Conclusion	25
Chapter 2. Materials and Methods	26
2.1 Materials	26
2.1.1 Facilities	26
2.1.2 Cell Lines	26
2.1.3 Chemicals and Drugs	26
2.1.4 VS-Identified Compounds	28
2.1.5 Other Materials	29
2.1.6 Equipment	30
2.1.7 Computer Software.....	31
2.2 Methodology and Procedure	32
2.2.1 Computational Methods.....	32

2.2.2 Selecting and Building Active Set Structures	32
2.2.3 Alignment of Molecules	32
2.2.4 Generation of the Pharmacophore Model	34
2.2.5 Validating and Refining the Pharmacophore Query.....	35
2.2.6 Searching a Conformation Database	37
2.2.7 Sorting the Hit Database	39
2.3 Experimental Methods.....	40
2.3.1 hSERT and hNET Membrane Preparation.....	40
2.3.2 hSERT and hNET One-Point Binding Assays.....	40
2.3.3 hDAT Whole Cell Binding Assays	41
Chapter 3. Computational Chapter.....	43
3.1 Pharmacophore Model Generation and Virtual Screening	43
3.1.1 Introduction	43
3.1.2 Generation of the Training Set.....	44
3.1.2.1 Searching for Relevant Compounds: Literature Review	44
3.1.2.2 Examining Compound Combinations.....	52
3.1.3 Selecting the Optimal Alignment for Creationg of the Pharmacophore Query	54
3.1.4 Validation of the Pharmacophore Model.....	58
3.1.5 Refining the Pharmacophore Query	60
3.1.6 Second Refinement of the Pharmacophore Query	63
3.1.7 Virtual Screening of the ZINC Database	67
3.1.8 Sorting of Hit Compounds	69
Chapter 4. Pharmacologic Characterization	74

4.1 hNET.....	74
4.2 hSERT.....	76
4.3 hDAT	78
Chapter 5. Discussion and Future Directions.....	80
5.1 Pharmacophore-based Drug Design.....	80
5.2 Choosing Training Set Compounds.....	81
5.3 Pharmacophore Features.....	82
5.3.1 Choosing the Optimal Alignment Based on Pharmacophore Features	82
5.3.2 External Volumes	83
5.4 Validation Test Set	84
5.5 Influence of pKa on Pharmacophore Features.....	87
5.6 Virtual Screening.....	87
5.6.1 ZINC Database	87
5.7 Ranking of Hit Compounds	88
5.7.1 RMSD versus Overlay Methods.....	88
5.7.2 Strain Energy versus Overlay Methods	89
5.7.3 Clustering by Chemical Scaffold.....	90
5.8 Future Directions.....	90
5.8.1 Altering the Training Set	90
5.8.2 NET-Selective TS Compounds	91
5.8.3 Examining Analogs of AC-1.....	93
5.8.4 Amine Groups in CNS Drugs.....	96
5.8.5 Revisions to Pharmacophore Model.....	99

5.8.6 Rescreening the ZINC Database	105
5.8.7 Selecting Compounds Based on RMSD versus Overlay Score	111
5.8.8 Unique Structure of Hit Compounds	111
5.8.9 Refining the Structure of New Hit Compounds	112
5.9 Conclusion	114

LIST OF TABLES

	Page
3.1 Binding affinities of NET inhibitors from radioligand competition binding assays ...	45
3.2. Compound combinations explored prior to choosing final training set	53
3.3. Training set NET ligands used to generate pharmacophore model.....	54
3.4. List of high affinity and low affinity compounds at the NET used in validation studies	59
3.5. Retrieved compounds from the validation database screening after refining the pharmacophore model	62
3.6. Six structurally-distinct hits chosen based on S Score and characterized in vitro	70
5.1. The four training set compounds and their IUPAC names	82
5.2. IUPAC names of test set compounds	85
5.3. MAT binding affinities of training set compounds, and the selectivity of each compound relative to NET.....	92
5.4. Analogs of compound AC-1	94
5.5. Analogs of AC-1 with an “S” score better than -114	95
5.6. Structures and “S” Scores of the top three new hit compounds.....	106

LIST OF FIGURES

	Page
1.1 A monoaminergic synaptic terminal showing the role of the SLC6 NTTs in synaptic transmission.....	9
1.2 Schematic illustration of a ligand-based pharmacophore screening	21
1.3 Hydrophobic features defined by different software packages.....	23
2.1 Generation of the pharmacophore query from a molecular alignment.....	34
2.2 Pharmacophore query refinement and validation.....	36
2.3 Pharmacophore searching in MOE.....	38
3.1 Optimal alignment of training set compounds mazindol, milnacipran, reboxetine and 8d.....	56
3.2 Preliminary pharmacophore features generated by MOE, based on training set alignment of mazindol, milnacipran, reboxetine, and 8d	57
3.3. The refined pharmacophore model containing four pharmacophore features, mapped onto the four training set compounds	65
3.4. Refined pharmacophore model with excluded volume feature.....	66
3.5. Generation of ZINC Database.....	68
3.6. Superposition of AC-1 (orange) on the original training set alignment	71
3.7. Superposition of AC-1 on the pharmacophore points	73
4.1. VS hit compound one-point screening assay at hNET	75
4.2. VS hit compound one-point screening assay at hSERT	77
4.3. VS hit compound one-point screening assay at hDAT.....	79
5.1. Comparison of the structures of reboxetine and its analogue, compound “3”.....	86

5.2. Compound AC-2 demonstrating the distances in Angstroms from the donor feature to the two aromatic features	98
5.3. Semi-refined model	102
5.4. Comparison of three generated models with the original query, refined query and semi-refined query	104
5.5. Overlay of top new hits from the semi-refined query to the alignment of the original training set compounds	107
5.6. Overlay of AC-1 to the original training set alignment	108
5.7. Illustration of poorest alignment	110
5.8. Compound AC-7 demonstrating the distances in Angstroms from the acceptor feature to the two aromatic features	113

LIST OF ABBREVIATIONS

5-HT: Serotonin

ADHD: Attention-Deficit Hyperactivity Disorder

CNS: Central Nervous System

DA: Dopamine

DAT: Dopamine Transporter

HTVS: High-Throughput Virtual Screening

LBP: Ligand-Based Pharmacophore

LeuT: Leucine Transporter

MAO: Monoamine Oxidase

MAT: Monoamine Transporter

MDD: Major Depressive Disorder

MOE: Molecular Operating Environment software

NE: Norepinephrine

NET: Norepinephrine Transporter

NRI: Norepinephrine Reuptake Inhibitor

NSS: Neurotransmitter:Sodium Symporter

RMSD: Root Mean Square Deviation

SBP: Structure-Based Pharmacophore

SERT: Serotonin Transporter

SLC: Solute Carrier

SSRI: Selective Serotonin Reuptake Inhibitor

TCA: Tricyclic Antidepressant

TM: Transmembrane

TS: Training Set

VMAT: Vesicular Monoamine Transporter

VS: Virtual Screen

WHO: World Health Organization

Chapter 1. Introduction

1.1 Statement of the Problem

Mental health illnesses are associated with human suffering, social alienation, disability and poor quality of life. One of the most prevalent and burdening public health problems is major depressive disorder (MDD). According to the World Health Organization (WHO), depression will be the second most debilitating illness next to heart disease by the year 2020 (Lin et al., 2011). MDD is one of the most investigated diseases by disciplines including neuropharmacology and genetics, and believed to be a combination of hereditary, environmental and developmental factors (Mill and Petronis, 2007). As defined in the DSM-IV, MDD is characterized by periods of depressed mood lasting for more than two weeks, accompanied by some or all of the following symptoms: hopelessness, worthlessness, disturbed appetite, weight gain or loss, disturbed sleep rhythm (insomnia or hypersomnia), reduced concentration, psychomotor agitation or retardation and recurrent suicidal thoughts (Mill and Petronis, 2007). However, the molecular mechanisms underlying depression are not fully understood. Studying the interaction between drugs and their targets, and thereby developing more effective treatments are the primary goals of research in this study. New treatment options are crucial to not only reducing the number of people living with such conditions, but to treat the substantial population that is either resistant to existing pharmacotherapies or cannot tolerate their adverse effects.

There are currently a variety of options to treat depressed patients, including

psychotherapy, electroconvulsive therapy, light therapy and pharmacotherapy with antidepressants (Haenisch and Bonisch, 2011). Regarding the latter, almost all clinically used antidepressants were developed after the chance discovery in the 1950s that the tricyclic compound imipramine (Azima and Vispo, 1958; Kuhn, 1958) and the antituberculosis drug iproniazid were effective in treating depression. Both drugs elevate extracellular monoamine levels by either inhibiting the neuronal serotonin and/or norepinephrine transporters (Brown and Gershon, 1993; Nemeroff and Owens, 2002) (imipramine and its active metabolite desipramine) or by blocking the enzyme monoamine oxidase (MAO) (iproniazid) (Haenisch and Bonisch, 2011).

Based on the mechanism of action of these drugs, it is believed that abnormal monoaminergic neurotransmission in the brain is present in depressed patients. However, it remains unknown why it takes between one and six weeks for antidepressant drugs to exert their clinical effects (Duman and Monteggia, 2006). One possible explanation for the delayed onset of antidepressant action is the requirement for neuronal adaptive mechanisms such as postsynaptic receptor downregulation (Haenisch and Bonisch, 2011). The latency in the onset of antidepressant action is still a problem in the therapy of MDD since depressive states are often associated with a high risk of committing suicide. Furthermore, only about 50% of patients with MDD show full remission while receiving currently available antidepressants (Haenisch and Bonisch, 2011) underscoring the necessity to find more effective pharmacological treatments for depression and related conditions.

1.2 Monoamine Transporters (MATs)

1.2.1 MAT Structure

The monoamine transporters belong to the SLC6 family of solute carriers of sodium / chloride coupled transporters (Kristensen et al., 2011). The SLC6 family is among the largest of the SLC families, containing 20 genes that encode a group of highly similar transporter proteins, including those for dopamine (DAT; SLC6A3), serotonin [5-hydroxytryptamine (5-HT); SERT; SLC6A4] and norepinephrine (NET; SLC6A2) (Chen et al., 2004; Hoglund et al., 2005). All SLC6 neurotransmitter transporters are expressed in the central nervous system (CNS), where their primary physiological function is neurotransmitter homeostasis (Macdougall and Griffith, 2008).

Different designations for the SLC family are often used, such as the “neurotransmitter:sodium symporter (NSS),” the “sodium-neurotransmitter symporter family,” or the “Na/Cl neurotransmitter transporter” family (Nelson, 1998; Beuming et al., 2006). These proteins transport amino acids and their derivatives into cells, using the electrochemical membrane potential difference of sodium as the energy source. The role of chlorine in the transport process is not fully understood, but for most MATs, one or more chlorine ions are hypothesized to be cotransported with sodium and the substrate (Kristensen, et al., 2011).

1.2.2 MAT Inhibitors

MAT inhibitors (*e.g.*, GBR-12909, mazindol, fluoxetine, paroxetine, reboxetine, amoxapine, desipramine, imipramine, bupropion and nisoxetine) have been developed to treat MDD, psychostimulant dependence, addiction and abuse, attention-deficit hyperactivity disorder (ADHD), anxiety disorders, mood disorders, personality disorders, psychosexual disorders, schizophrenia, eating disorders, premenstrual dysphoria, Parkinson's disease, Alzheimer's disease, bipolar disorder, chronic pain, migraine, epilepsy, multiple sclerosis, stroke, trauma, mania, obsessive-compulsive disorder, obesity and narcolepsy (J. Zhou, 2004). Tricyclic antidepressants (TCAs), including imipramine and clomipramine, were developed in the 1950s as the first generation of monoamine transporter drugs. The structure of the TCAs is conserved in that there is a tricyclic system containing a cycloheptane ring flanked by two phenyl moieties. The central ring is substituted with an aminopropyl chain, with the amino group being mono- or dimethyl substituted (Andersen et al., 2009). However, the TCAs have shown to act on a variety of receptors (Gillman, 2007), resulting in major adverse physiological effects.

1.2.3 MAT Inhibitor Selectivity and Adverse Effects

In recent years, the development of newer monoamine transporter inhibitors has been aimed at compounds with an improved selectivity toward SERT and/or NET, as demonstrated by the selective serotonin reuptake inhibitors (SSRIs), the selective norepinephrine reuptake inhibitors (NRIs), as well as the dual inhibitors of SERT and NET (SNRIs) (Andersen et al., 2011). These drugs are among the most frequently

prescribed for treatment of depression and anxiety disorders (Andersen et al., 2009) and have far fewer adverse side effects as compared to the TCAs or MAO inhibitors (Anderson, 2000). Although rare, SSRIs may be accompanied by a potentially lethal condition known as serotonin syndrome (SS). SS results from excessive serotonergic activity and is characterized by autonomic instability and neuromuscular abnormalities. Many drugs have been linked to SS, which typically develops in patients within hours of initiating treatment, after dosage increase, or overdose (Boyer and Shannon, 2005; Sun-Edelstein et al., 2008).

A study published by Schlessinger et al. (2011) found that the adverse side effects generally associated with antidepressants may be, in part, due to the administration of drugs for the treatment of diseases that are seemingly unrelated to MAT function, such as diabetes, which additionally act to inhibit NET activity. This finding may point to the involvement of the MATs, and in particular NET, in the progression of entirely dissimilar illnesses (Schlessinger et al., 2011). For example, about 80 –90% of the released norepinephrine is taken up again by postganglionic adrenergic neurons through the NET. Therefore, changes in NET function may have serious cardiovascular and metabolic side effects (Boschmann et al., 2002). Moreover, it is believed that long-term treatment with antidepressants which inhibit the NET causes down-regulation of α -adrenoceptors (Beer et al., 1987; Vetulani and Nalepa, 2000; Gould et al., 2003).

Norepinephrine's effects are mediated by three families of adrenergic receptors: α 1, α 2, and β (Bylund et al., 1994). The α 1-adrenergic family is mostly postsynaptic and excitatory. Alpha1-adrenergic receptors are coupled to phospholipase C and phosphoinositol secondary messengers through Gq proteins and are responsible for the

contraction of vascular smooth muscle. Therefore, an imbalance in the α 1-adrenergic receptors can lead to an increase in blood pressure. In the CNS, α 1 receptors are found in both neurons and glial cells and are involved in motor control, learning, memory, and fear (Tanoue et al., 2003).

The α 2-adrenergic family includes the α 2A, α 2B, and α 2C subtypes, which are located both pre- and post-synaptically (Bylund, et al., 1994). Alpha2-adrenergic receptors are coupled through Gi/o proteins to the second messenger adenylate cyclase, which is involved in regulating concentration of cyclic adenosine monophosphate (cAMP). Alpha2A receptors are linked to different adverse effects, including analgesia, hypothermia, sedation, and control of noradrenergic activity (Crassous et al., 2007). The alpha2B receptors generally mediate vasoconstriction (Starke, 2001).

Regarding the α 2C receptors, although their role is not fully understood they are associated with motor behavior, mood and memory (Starke, 2001). The α 2 agonist and antischizophrenia drug, clonidine, is administered for different conditions such as hypertension, opioid withdrawal, and ADHD (Raistrick et al., 2005; Posey and McDougle, 2007). Clozapine binds to a variety of serotonergic, dopaminergic, muscarinic, adrenergic, and other receptors that contributes to its high efficacy, yet simultaneously, leads to serious side effects including agranulocytosis, seizure, weight gain and as mentioned above, diabetes (Roth et al., 2004; Keiser et al., 2007).

Beta-adrenergic receptors include the β 1, β 2, and β 3 subtypes (Bylund, et al., 1994), which are coupled via Gs to adenylate cyclase (Ramos and Arnsten, 2007). Stimulation of β 1-adrenergic receptors increases heart rate and cardiac contractility; stimulation of β 2-adrenergic receptors, which are located in smooth muscle, causes

vasodilatation and bronchial relaxation. These receptor subtypes are also found in the brain, but their functions there are not well known (Ramos and Arnsten, 2007). Medications that block the β -adrenergic receptors are commonly used for a wide variety of conditions including hypertension, ischemic heart disease, migraine, and performance anxiety (Limmroth and Michel, 2001; Ong, 2007).

Furthermore, the TCA antidepressant, imipramine, is a dual-acting inhibitor of SERT and NET, while inhibiting cardiac Na⁺ channels and G protein-coupled receptors, including those for acetylcholine, norepinephrine and histamine. The lack of selectivity of TCA drugs is responsible for their serious adverse effects and toxicity (Iversen, 2000). These examples suggest that it is necessary to seek new NET inhibitors that would act more selectively on a particular receptor.

1.2.4 Synaptic Transmission of the MATs

Reuptake of a monoamine neurotransmitter by its transporter protein is the primary mechanism by which the biological effects in the synapse are terminated (J. Zhou, 2004). Figure 1.1 illustrates a monoaminergic neuron in synaptic transmission.

In the presynaptic terminals of monoaminergic neurons, a vesicular monoamine transporter (VMAT) carries the cytoplasmic neurotransmitter (either serotonin, dopamine, or norepinephrine) into synaptic vesicles, where it is stored and released from nerve terminals into the synapse once the neuron fires (Cooper et al., 2003). The activity of 5-HT, DA or NE in the synapse is most often terminated by rapid MAT uptake of the neurotransmitter into presynaptic terminals. Neurotransmitter metabolism is a second termination mechanism, achieved through monoamine oxidase

(Dostert et al., 1989; Bonisch and Bruss, 2006) or catechol-O-methyl transferase (COMT) (Huotari et al., 2002).

Monoaminergic Neuron

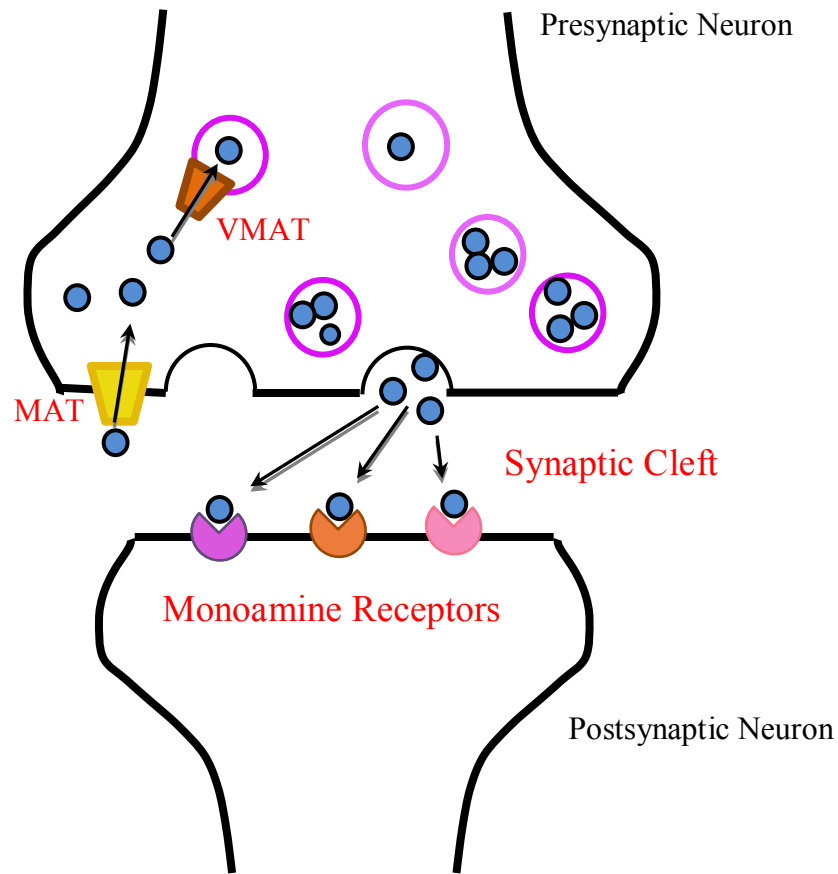


Figure 1.1. A monoaminergic synaptic terminal showing the role of the SLC6 NTTs in synaptic transmission. In the presynaptic terminals of monoaminergic neurons, vesicular monoamine transporters (VMATs) sequester either serotonin, dopamine or norepinephrine (blue spheres) into synaptic vesicles (purple circles). The MATs are responsible for reuptake of monoaminergic neurotransmitters in the synaptic cleft which terminates their action. After reuptake by the MAT some of the neurotransmitter is restored in vesicles, after the uptake by the VMAT. Released neurotransmitter activates receptors located on the postsynaptic neuron membrane.

Synaptic monoamine concentrations can be affected by medications that target their synthesis or degradation. For example, MAO, COMT and MAT inhibitors all act by increasing synaptic monoamine levels and are used to treat many neuropsychiatric disorders (Keating and Lyseng-Williamson, 2005).

1.3 Norepinephrine Transporter (NET)

Two major noradrenergic neuronal clusters in the brain, the locus coeruleus and the lateral tegmental group, provide extensive innervation to the striatum, amygdala, hypothalamus, thalamus, cerebellum, and neocortex (Moore and Bloom, 1979). The NET is located in the plasma membrane of the noradrenergic neurons, where it functions to take up synaptically released norepinephrine (NE) (Pacholczyk et al., 1991).

1.3.1 Norepinephrine Synthesis and Function

Despite the large body of data available for the monoamine SLC6 family, the NET remains the least explored MAT. Norepinephrine (NE), also known as noradrenaline, is a neurotransmitter found in the sympathetic nervous system and biosynthesized from the amino acid tyrosine, which is sequentially hydroxylated to generate dihydroxyphenylalanine (Dopa), decarboxylated to produce dopamine, and finally, hydroxylated to form NE (Axelrod, 1974). It is involved in a variety of physiological functions, including mood and sleep regulation, expression of behavior, alertness and arousal (Young et al., 1998). Norepinephrine also exerts central control over the endocrine and autonomic nervous systems (Tellioglu and Robertson, 2001),

which play a fundamental role in the anxiety and stress response (Tsigos and Chrousos, 2002).

1.3.2 NET Inhibitors

NET is an established molecular target for the treatment of conditions such as attention-deficit/hyperactivity disorder, substance abuse, Alzheimer's and Parkinson's diseases (Macdougall and Griffith, 2008). Low levels of NET mRNA and protein have been found in brains of suicidal patients with major depression (Hahn and Blakely, 2007).

Unlike the relatively nonspecific tricyclic antidepressants, newer-scaffold NET inhibitors can exert their effects rather selectively. For example, the ADHD drug atomoxetine (Strattera®) is a norepinephrine reuptake inhibitor (NRI) that is highly specific for NET (Schlessinger, et al., 2011). Certain high affinity NET ligands also inhibit the SERT, which enhances antidepressant properties e.g., SNRIs such as venlafaxine (Effexor®) and duloxetine (Cymbalta®) (Hahn and Blakely, 2007).

1.4 Leucine Transporter (LeuT)

Attempts to determine the tertiary structures of SLC6 transporters were unsuccessful for the first 25 years following the cloning of cDNAs encoding these proteins. This was due to the inability to obtain sufficiently pure and stable transporter protein in quantities essential for protein crystallization (Tate and Blakely, 1994; Tate, 2001; Tate et al., 2003; Rasmussen and Gether, 2005) as well as the additional difficulty of crystallizing membrane (nonsoluble) proteins. Before the determination of the first

high-resolution X-ray crystal structure of a bacterial SLC6 homolog, structural knowledge of SLC6 MATs was based on indirect observations derived from extensive biochemical and mutagenesis studies that provided valuable information into transporter topology and secondary structure, but limited data on the tertiary structure. This was transformed in 2005 when Yamashita et al. (2005) revealed a high-resolution X-ray structure of a prokaryotic homolog to the SLC6 transporters, the leucine transporter LeuT, from the thermophilic bacterium *Aquifex aeolicus* (Kristensen, et al., 2011).

1.4.1 LeuT Structure

The structure confirmed certain predictions made for the SLC6 transporter architecture by demonstrating 12 transmembrane (TM) regions connected by short intra- and extracellular loops with intracellular N and C termini (Kristensen, et al., 2011), along with a high-affinity substrate binding site (denoted the S1 site) centrally located in the core of the transporter protein. Unexpected were the two bundles of TMs 1 – 5 and 6 – 10, the centrally-hinged TM 1 and TM 6 α -helices, and a second substrate binding site (S2) in the extracellular vestibule (Z. Zhou et al., 2009; Piscitelli et al., 2010).

The LeuT provided the first credible template to better characterize MAT drug binding regions and has shown to be an excellent structural template for construction of MAT homology models, aiding in the discovery of ligand binding pockets and general binding requirements of substrates, ions, and inhibitors (Andersen, et al., 2011). Although there is modest homology between the MATs and LeuT, residues that comprise their ligand binding sites are not identical. Therefore, new approaches still need to be

developed in order to gain more insight into the structure and function of the monoamine transporters, specifically the NET.

1.5 Drug Design

1.5.1 The Art of Drug Design

Before the era of computational chemistry, new drugs were discovered through experimental (wet lab) trial and error (Lee et al., 2011). With scientific progress, active compounds were isolated and purified, from which researchers were able to infer their chemical structures (Sneader, 2005). Further advancements in the fields of molecular biology and biochemistry defined the notion of a so-called “ligand-receptor relationships” (Drews, 2000). Soon after, molecular modeling programs were created that were capable of discovering novel ligands relevant for a particular binding site. With this, the art of drug design emerged.

The objective in drug design is to identify a protein target that has been implicated in a certain disease, and discover compounds that activate or inhibit that target (Moon and Howe, 1991; Drews, 2000). The discovered compounds should show high target affinity, triggering a series reactions that lead to an improvement in the condition (Sleno and Emili, 2008). Progress in the field of drug design allowed the binding mode of a protein-ligand complex to be better understood using *in vitro* and *in silico* approaches. The *in vitro* method, known as high-throughput virtual screening (HTVS), is an effective computational approach for evaluating large chemical structure libraries with the goal of

discovering hit compounds that interact with a specific biological target (Schneider et al., 2008). Combinatorial chemistry and HTVS represent an important step in drug discovery, reducing costs, increasing time efficiency, and a new weapon in identifying potentially high affinity novel compounds (Gasteiger et al., 2003; Varnek et al., 2008).

1.5.2 Pharmacophore Modeling: Yesterday and Today

The German-born physician and scientist Paul Ehrlich introduced the pharmacophore concept and coined its definition as “a molecular framework that carries the essential features responsible for a drug’s biological activity” (Ehrlich, 1909). Several decades later, the pharmacophore notion was elaborated by Kier, who stated that a drug must possess “those atomic features suitable for the requisite drug–receptor interaction phenomena,” and “... the appropriate spatial disposition of these features necessary to bring about the required simultaneous or required sequential interaction events with the receptor” (Kier, 1967; Kier, 1973). Kier’s definition was refined by Gund, who defined a pharmacophore as “a set of structural features in a molecule that is recognized at a receptor site and is responsible for that molecule’s biological activity” (Gund, 1977). The official IUPAC definition of a pharmacophore is “the ensemble of steric and electronic features that is necessary to ensure the optimal supramolecular interactions with a specific biological target structure and to trigger (or to block) its biological response.” (Wermuth et al., 1998). This is a purely abstract concept that describes the common steric and electrostatic properties of bioactive compounds with the target of interest (Seidel et al., 2010). From these collective definitions, a

pharmacophore, in short, identifies important features that should comprise an active ligand (Lee, et al., 2011).

In early pharmacophore-based studies, computational models of pharmacophores were developed manually with the aid of simple molecular graphics visualization programs. More sophisticated computer programs have since been designed specifically for pharmacophore modeling (Markt et al., 2011). Today, 3D pharmacophore modeling is a conventional *in silico* technique imparting numerous advantages in drug design. Pharmacophore models are capable of detecting chemical features that are necessary for protein-ligand interactions and therefore for biological activity. Further, pharmacophore-based screening makes possible the retrieval of compounds with structurally diverse scaffolds that might not have been otherwise revealed (Markt et al., 2011).

The goal of pharmacophore-based drug design is to discover novel structural scaffolds that orient their biologically important groups similarly to the active compounds comprising the training set, termed *scaffold hopping*. Its importance is based on the ability to open new synthetic pathways after many of the analogs of a certain scaffold have been examined and to discover novel ligands with high binding affinities to a particular target (Horvath, 2011) and at the same time are more selective.

1.5.3 Ligand-Based versus Structure-Based Pharmacophore Models

There are two approaches in developing pharmacophore models: structure- (SBP) and ligand-based (LBP) (Wermuth, 1993; Guner, 2000). The structure-based method reveals chemical features based on the association between a ligand and its binding site. This technique requires obtaining structural information about the macromolecule and the

active conformation of the binding ligand. As such, there are three benefits of SBPs over LBPs:

- (1) SBPs can identify novel scaffolds with less bias towards existing ligand chemotypes.
- (2) SBPs can be used as suitable tools for structure-based ligand optimization.
- (3) SBPs lead to better understanding of ligand binding sites within the macromolecular structure (Sanders et al., 2012b).

Despite these advantages of SBPs, their use is limited to cases in which the target structure information is available (Horvath, 2011). A frequently encountered problem for SBP drug design is that too many pharmacophore features can be identified for a specific binding site in a macromolecular target. However, a pharmacophore model comprised of too many pharmacophore features (*i.e.*, more than seven) may not be appropriate for applications such as virtual screening (Yang, 2010). Therefore, it is important to select a limited number of pharmacophore features (typically three to seven) to construct a pharmacophore query (Yang, 2010).

If there is no structural information of the target protein available, pharmacophore models can be derived in a ligand-based way. This approach uses common chemical features within set of ligands (known as a training set) that show desired biological activity at the target. It is believed that a ligand-based method delivers good results if enough ligand information is available, and if the training set compounds are known to bind to the protein at a specific site (Evers et al., 2005).

Although in LBP generation procedures there is always uncertainty about the binding modes of a ligand-protein structure, there have been a number of studies

comparing the quality of hit compounds using a ligand-based approach versus a structure-based approach. In a comparative study of LBPs and SBPs for novel histone deacetylase 8 inhibitors, the LBP model contained four features and retrieved 117 compounds, of which 87 were active. The SBP model contained six features and retrieved 74 compounds, of which 63 were active (Thangapandian et al., 2010). These data demonstrate that the ligand-based method can be just as useful as the structure-based method in producing a high hit rate. LBP modeling has become a key computational strategy for facilitating drug discovery when a macromolecular target structure is not obtainable (Yang, 2010). Although structure-based drug design is an attractive approach, a ligand-based method is useful for finding pharmacophoric features that could facilitate the discovery of novel high-affinity ligands (Dash et al., 2012).

1.5.4 Guide to Generating a Pharmacophore Model

1.5.4.1 Generation of the Training Set (TS)

The first step in developing a ligand-based pharmacophore model is to collect an active compound set (or training set), generally from literature searches (Lee, et al., 2011). Ligand-based pharmacophores can be created from one or multiple active ligands (Leach et al., 2010). When choosing a training set, all selected molecules must exert their biological effect through the same mechanism (van Drie, 2003). Furthermore, the type of training set molecule, the size of the dataset and its chemical diversity have a great effect on the created pharmacophore model (Yang, 2010). A training set including active molecules with the same chemical scaffold can cause the so-called *analog bias*. In

this case, the pharmacophore model will ignore all compounds different from the single scaffold from which it has been derived. This bias contributes to inaccurate predictions and leads to an increase in the number of false positives and false negatives, and certainly less true positives. Therefore, an important aspect to consider when choosing training set compounds is structural diversity (Markt et al., 2011).

1.5.4.2 Alignment of TS compounds

The next step is to build the pharmacophore model from the common features found among the training set ligands (Yang, 2010). To find common features, the ligands comprising the active set are aligned and conformations of each compound are generated. Once all training set compounds have been aligned, pharmacophore models are created through a pharmacophore elucidation algorithm. This algorithm works by compiling common features among all active set compounds (Molecular Operating Environment 2010). More than one model is commonly produced from this procedure, and selecting the best one is a significant task (Guner, 2002).

1.5.4.3 Selecting the Optimal Pharmacophore Features

The first and most crucial step in pharmacophore modeling is selecting the right chemical feature types for the development of a high quality pharmacophore model (Wolber et al., 2008). Classically, pharmacophore feature designation has several rules: alkyl chains and halide groups are labeled as hydrophobes; aromatic rings may either be placed into a specific “aromatic” category or classified with the hydrophobes (Horvath, 2011). It is also desirable to choose specific pharmacophore features such as “Hydrogen

Bond Donor” or “Hydrogen Bond Acceptor” to denote a particular chemical group rather than selecting a nonspecific pharmacophore feature such as “Hydrogen Bond Donor or Hydrogen Bond Acceptor or Hydrophobe”.

1.5.4.4 Validation

Once the best model is chosen it should undergo a validation process using ligands that are not included in the training set. It is ideal for a validation database to contain structurally diverse active and inactive compounds (Rohrer and Baumann, 2009). A good model should maximally select the active and ignore the inactive compounds. If a pharmacophore model cannot pass this validation, it should be discarded and the modeling process refined (Lee, et al., 2011). Only after a model has satisfactorily passed the validation step can the virtual screen be initiated.

1.5.4.5 Virtual Screening (VS)

Pharmacophore-based screening is a virtual screening (VS) method that can automatically evaluate millions of compounds with the use of a computer program (Walters et al., 1998). Virtual screening works by matching each molecule in the virtual database to the pharmacophore model. A search algorithm aligns the molecule to the query using rigid-body superposition. Each match (known as a hit) is based on the mapping between the database molecule annotation points and the features of the model. For an efficient virtual screen, MOE discards conformers that do not match feature types or appropriate inter-feature distances of the pharmacophore model (Molecular Operating

Environment 2008). The search then outputs all matches that satisfy the constraints of the query (Seidel et al., 2010).

The first part of the VS process involves assessing how “druglike” are the virtual database molecules. Compounds are usually considered drug-like if they fulfill the Lipinski’s Rule of Five requirements (Bielska et al., 2011). To obtain more of these “druglike” molecules in a database, reactive, toxic or otherwise unsuitable compounds should be removed using specific filters. Examples of some common reactive functional groups include alkyl halide peroxide and carbazide. Unsuitable molecules may include crown ethers, disulfides, aliphatic chains of seven or more methylene groups, quinones, polyenes and cycloheximidine derivatives (Vyas et al., 2008).

1.6 Ranking of Hit Compounds

From the virtual screen, an algorithm calculates a score to describe the quality of the match between the pharmacophore model and each molecule of the VS hit list (Langer et al., 2006). In MOE this score is a root mean square deviation (RMSD) calculation, based on the superposition of the pharmacophore features and the output hit. A low RMSD score corresponds to a good alignment between model and conformer features (Molecular Operating Environment 2008). Alternatively, another approach to score compounds is based on their overlay to the alignment of the original training set compounds, known as an “S” score. The overall step-by-step scheme of a pharmacophore-based virtual screen is represented in Figure 1.2.

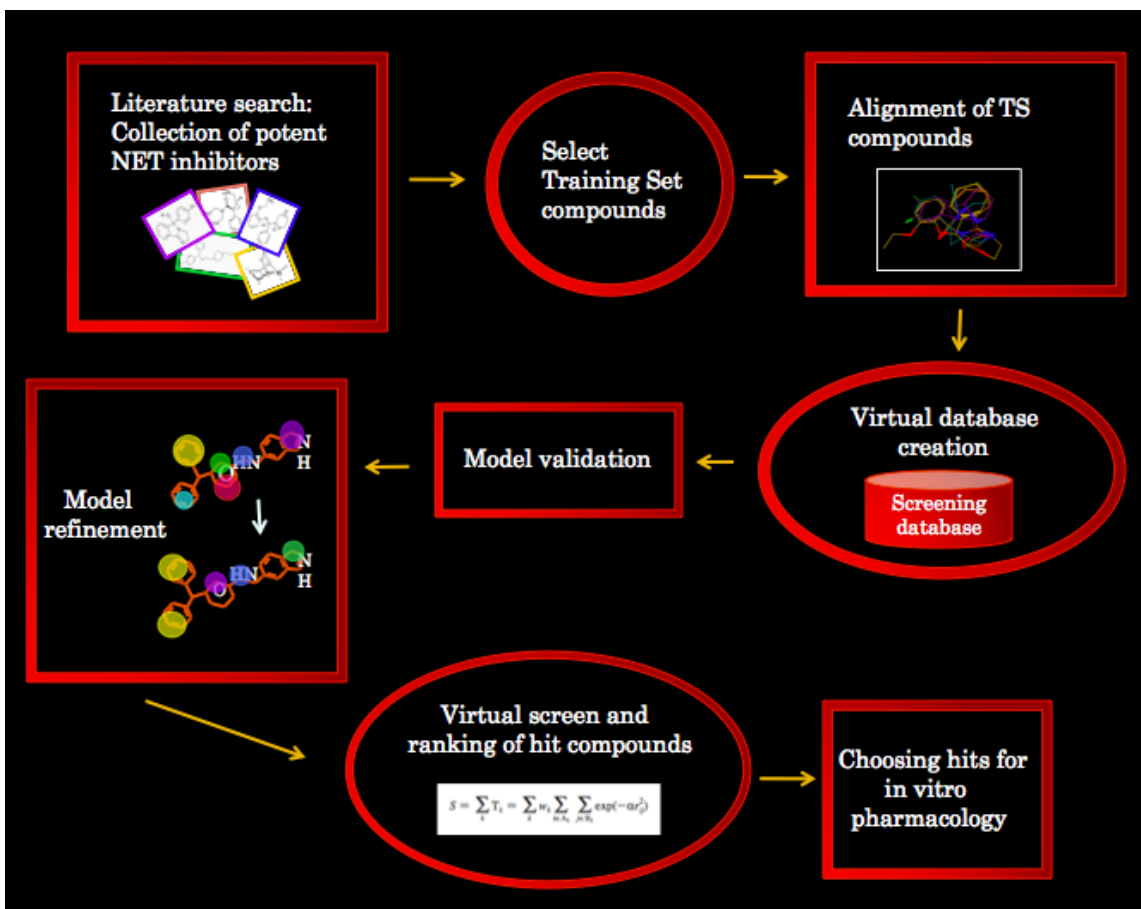


Figure 1.2. Schematic illustration of a ligand-based pharmacophore screening. The first step involved a literature search for active NET inhibitors. From these NET inhibitors, a group of compounds were selected to comprise the Training Set (TS). The TS compounds were aligned in Molecular Operating Environment (MOE). A virtual database was then created, which was used for screening by the created pharmacophore model. Based on the alignment of TS compounds, MOE output pharmacophore features which were validated and refined. The refined model was then used to virtually screen the database of compounds. The hit compounds that MOE retrieved were sorted and chosen for pharmacological assessment.

1.7 Software Packages and Pharmacophore Features

An important point to note when creating the pharmacophore query and assessing hit compounds is that the output may be a function of the software package. Software packages besides MOE used for pharmacophore-based screening include Phase, Catalyst and LigandScout. Each software uses its own classification to define particular features (Wolber et al., 2008). Figure 1.3 (as adapted from Wolber et al., 2008) illustrates two molecules containing several hydrophobic centers uniquely defined by each software program.

Taking the pentane molecule in the first example, both Catalyst and MOE assigned three similar hydrophobic centers; Phase and LigandScout generated two hydrophobic centers for the same compound, also in a similar space with respect to one another. In the pentylbenzene molecule, LigandScout and Catalyst both assigned three hydrophobic centers in the same spatial orientation. Conversely, MOE designated two points, but not in the benzene ring. Phase created only one hydrophobic point, located between the third and fourth carbons of the pentyl moiety. From these two molecules in Figure 1.3, it can be seen that different software packages uniquely designate pharmacophore centers. While there are similarities among these four programs in terms of pharmacophore feature designation, each software distinctly situates the number and orientation of these features, ultimately leading to the retrieval of different hits compounds.

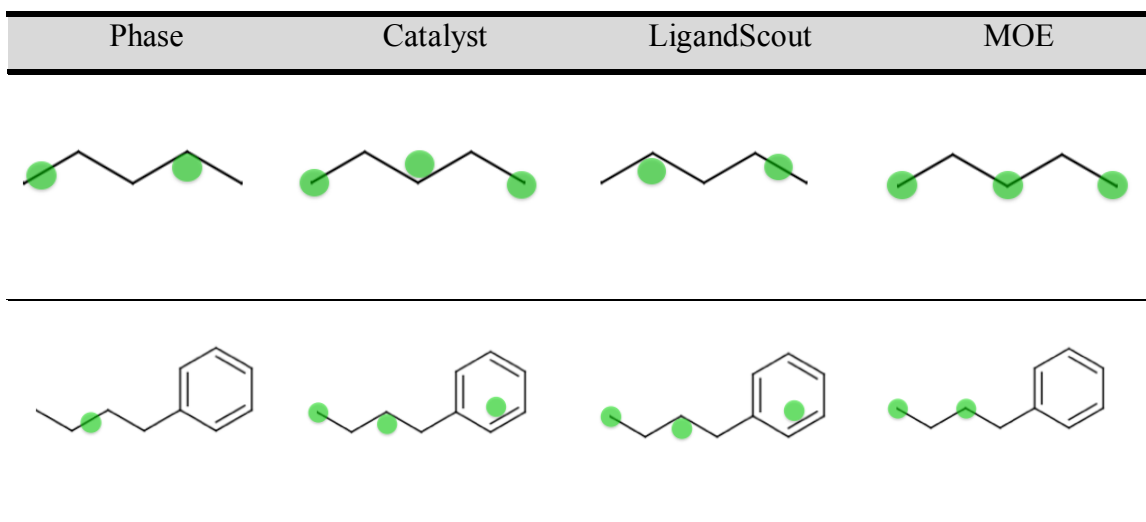


Figure 1.3 Hydrophobic features defined as a function of the software packages. Green spheres represent a hydrophobic pharmacophore feature. The top row illustrates a pentane molecule; the bottom row, a pentylbenzene. From this figure it can be seen that each software program has a unique way of designating the location and number of hydrophobic centers in each molecule.

1.8 Inactive Hit Compounds

After analyzing different aspects that could affect the type of hit retrieved in a pharmacophore-based screening, some matches still do not show activity at a particular target, as was seen in this investigation. There are several reasons for the inactivity of a VS hit compound. According to Martin:

1. A compound can contain groups that sterically prevent interactions despite its ability to satisfy the pharmacophore query.
2. A compound can contain groups that are unfavorable to activity.
3. A compound may be less soluble than its bioactive conformation (Martin, 2000).

1.9 Rational Drug Design

In this study, rational drug design will be used to discover novel NET inhibitors. It is rational because computational models will guide pharmacological analysis. A pharmacophore model based on NET inhibitors will be created *in silico*, using the MOE software package, comprising a series of structurally diverse compounds chosen from the literature. The created model will then be used to virtually screen an extensive compound database. “Hit” compounds, which are structures predicted to have high affinity at the NET, will be evaluated by *in vitro* pharmacology. Unlike conventional HTS, which involves pharmacologically evaluating a vast number of compounds until a hit is found, the prospective approach is much less expensive, less time-consuming, and

certainly more rational. Using the proposed pharmacophore model, novel, high affinity NET ligands could be discovered for the treatment of disorders mentioned above, including anxiety, depression, drug abuse, and attention deficit hyperactivity disorder.

1.10 Conclusion

Researchers from a variety of disciplines ranging from biological psychology to biophysics investigate the mechanisms involved in depression, anxiety and addiction. This study seeks to understand the basis of such conditions by exploring one of the most targeted proteins associated with these illnesses – the monoamine transporters (MATs). The discovery of novel ligands that vary both in their selectivity profiles and potency at the three MAT proteins may be of value in unraveling the relevant pharmacological mechanisms, aiding in the discovery of new therapies with fewer side effects (J. Zhou, 2004). Specifically, the approach in this study involves the use of computer-generated models to better understand molecular structure and function of the MATs, with a particular focus on the norepinephrine transporter (NET) as well as search for novel inhibitors of the MATs. Relying on these models, in vitro experiments could be performed to test the affinities of the potential MAT inhibitors. The continued interest in the development of new NET inhibitors combined with the lack of available MAT crystallographic structures prompted us to explore the possibility of developing ligand-based pharmacophore model(s) for NET inhibitors. It is the hope to be able to identify a novel class of potent NET inhibitors.

Chapter 2. Materials and Methods

2.1 Materials

2.1.1 Facilities

Laboratories – Mellon Hall of Science, Rooms 214, 456, 414.

2.1.2 Cell Lines

HEK-293 human embryonic kidney cells, stably transfected with wild type NET

(University of Pittsburgh, Pittsburgh, PA)

HEK-293 cells, stably transfected with wild type SERT

(University of Pittsburgh, Pittsburgh, PA)

N2A (murine neuroblastoma) cells, stably transfected with wild type DAT

(University of Michigan, Ann Arbor, MI)

2.1.3 Chemicals and Drugs

[3H]-Nisoxetine

Perkin Elmer, Foster City, CA

[3H]-Paroxetine

Perkin Elmer, Foster City, CA

[3H]-WIN 35,428

Perkin Elmer, Foster City, CA

Dimethylsulfoxide (DMSO)

Sigma Chemical Co., St. Louis, MO

Dulbecco's Modified Eagle Medium (DMEM)

Hyclone, Logan, UT

HBSS/modified

Hyclone, Logan, UT

Opti-MEM 1

Invitrogen, Carlsbad, CA

ScintiSafe scintillation fluid

Fisher Scientific, Pittsburgh, PA

Trizma base

Fisher Scientific, Pittsburgh, PA

Trypsin-EDTA (1x)

Invitrogen, Carlsbad, CA

2.1.4 VS-identified Compounds

AC-1

2-(3-fluorobenzoyl)-1-(4-methoxyphenyl)octahydro-4a(2H)-isoquinolinol

Aurora Fine Chemicals, San Diego, CA

AC-2

2-[(4-ethylphenyl)-(2-methoxy-5-methylphenyl)sulfonylamino]acetamide

Aurora Fine Chemicals, San Diego, CA

AC-3

5-(furan-2-yl)-3,3-dimethyl-2,4,5,6-tetrahydrobenzo[b]phenanthridin-1-one

Aurora Fine Chemicals, San Diego, CA

AC-4

3-[1-(2-methoxybenzyl)-1H-benzimidazol-2-yl]-1-propanol

Aurora Fine Chemicals, San Diego, CA

AC-5

[4-hydroxy-6-(4-methylphenyl)-2-thioxo-4-(trifluoromethyl)hexahydro-5-pyrimidinyl](phenyl)methanone

Aurora Fine Chemicals, San Diego, CA

AC-6

2-(3-hydroxypropyl)-1-(3-methoxyphenyl)-1,2-dihydrochromeno[2,3-c]pyrrole-3,9-dione

Aurora Fine Chemicals, San Diego, CA

2.1.5 Other Materials

Cell culture flasks, 75 cm²

Corning Inc., NY

Centrifuge tubes, 15 ml

Corning Inc., NY

Falcon tubes, 14 ml

Fisher Scientific, Pittsburgh, PA

Falcon tubes, 50 ml

Fisher Scientific, Pittsburgh, PA

Eppendorf microcentrifuge tubes, 1.5 ml

Fisher Scientific, Pittsburgh, PA

Pipette tips, disposable Redi-Tips (1,10, 200, 1000 μ l)

Fisher Scientific, Pittsburgh, PA

Scintillation vials

Fisher Scientific, Pittsburgh, PA

2.1.6 Equipment

Analytical balance

Mettler Toledo Inc., OH

Cell culture incubator

Forma Scientific, MA

Centrifuge, Model 228

Fisher Scientific, Pittsburgh, PA

Centrifuge, Model 5415 C

Eppendorf Scientific Inc., NY

Inverted microscope

Olympus, PA

Lab freezers and refrigerators

Forma Scientific, MA

Liquid nitrogen tank

Millipore Milli-Q and Elix water purification system

Millipore Corporation, MA

pH meter AB15

Fisher Scientific, Pittsburgh, PA

Water bath, 180 series

Precision Scientific, Winchester, VA

Weighing scale

Denver Instruments Co., CO

2.1.7 Computer Software

Molecular Operating Environment (MOE) software, Version 2008.09

Montreal, Canada

Microsoft Office Word and Excel 2008

Microsoft Corporation

2.2 Methods

2.2.1 Computational Methods

Molecular modeling studies were performed using a dual-core 3.06 GHz iMac and 2.66 GHz quad-core Intel Xeon macro computer. Construction and evaluation of pharmacophore models were performed using MOE 2008.09.

2.2.2 Selecting and Building Active Set Structures

Active NET inhibitors to comprise the training (or active) set were chosen from literature PubChem and SciFinder searches. The 2D structures of compounds included in the training set were built using the “molecule builder” function of MOE.

2.2.3 Alignment of Molecules

FlexAlign, an alignment method in MOE that explores the conformational space of a molecular set based on common chemical features, was used to generate conformers and align the training set compounds (Esposito et al., 2004). For each active set molecule, bonds were randomly rotated and chiral centers inverted, followed by energy minimization that created “new” molecular conformations. Once minimized, the molecules were held rigid and aligned using a similarity function based on the atomic coordinates. The following equation was used in the alignment process:

$$\text{Similarity Function} = -kt \cdot \log F + U,$$

where $-kT$ is approx 0.6 kcal/mol, F is the similarity measure derived from the atomic coordinates, and U is the average potential energy of the system (Esposito et al., 2004).

The FlexAlign alignment search was terminated once the number of consecutive failed attempts to generate a new molecular configuration based on the initial parameters was reached (Esposito et al., 2004).

2.2.4 Generation of the Pharmacophore Model

Once training set molecules were aligned, a query of points, which is a compilation of features, group constraints, and volumes common among all active set compounds, was generated. The role of the query is to select a subset from common ligand conformations such that all restrictions of the query are satisfied (Molecular Operating Environment 2010). A general diagram illustrating the creation of the pharmacophore query is shown in Figure 1.

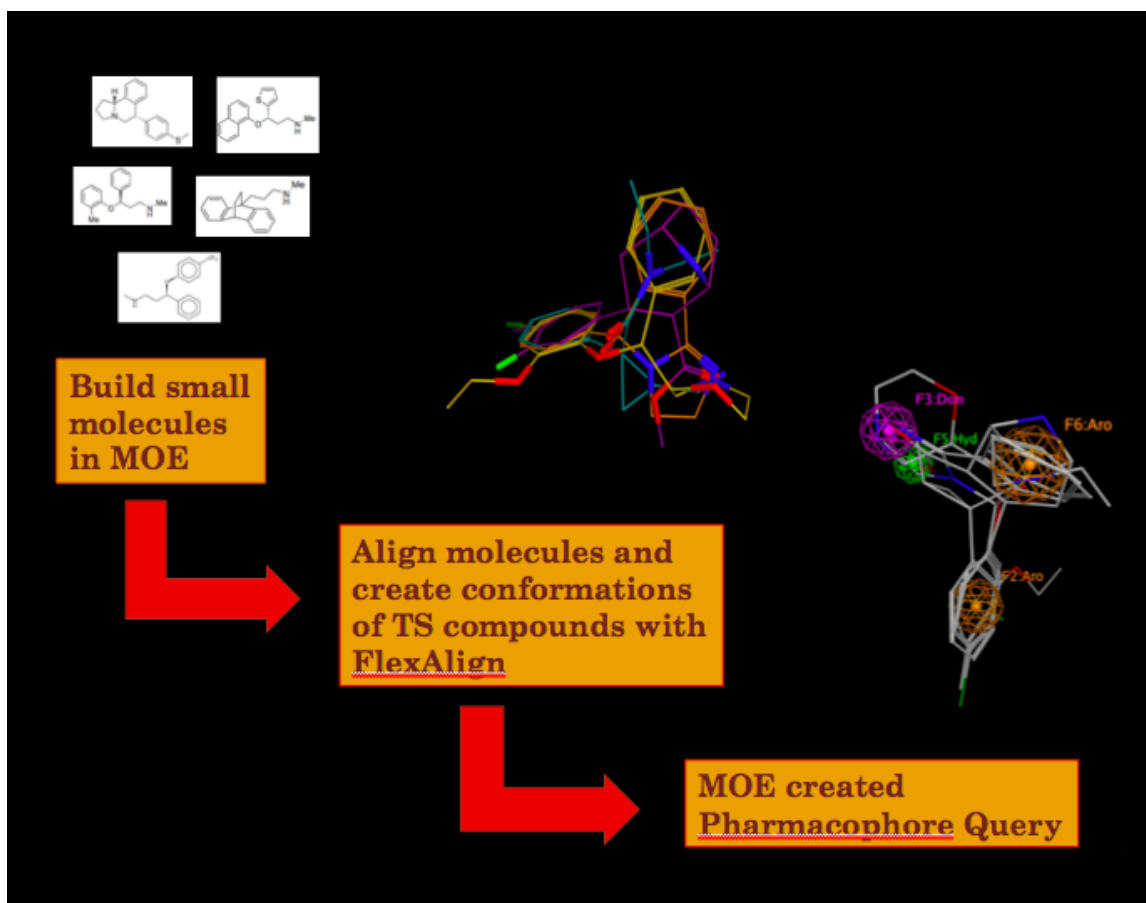


Figure 2.1. Generation of the pharmacophore query from a molecular alignment. Small molecules to comprise the training set were chosen from the literature and built in MOE. The MOE FlexAlign feature was used to create conformations and align training set compounds. Based on the alignment of the training set compounds, MOE found common features among all molecules: a donor group (purple sphere), a hydrophobic group (green sphere) and two aromatic groups (orange spheres). Common features were represented by colored spheres. Together, all features comprised the pharmacophore query.

The “pharmacophore query editor” was used to create and revise a query consisting of a set of constraints of ligand annotations. Pharmacophoric structural features were represented by points in space that reflected the presence or absence of biologically important atomic features at those locations, known as *ligand annotations* (Molecular Operating Environment 2010). The set of pharmacophore features among all active set compounds created the *pharmacophore query* (or *pharmacophore model*).

2.2.5 Validating and Refining the Pharmacophore Query

After the pharmacophore query was generated, it was validated in order to determine whether it could retrieve active and ignore inactive compounds from a *test set database*. All features were amended in a way to maximally retrieve active compounds at the NET while ignoring inactive compounds. A diagram representing the validation and refinement scheme is illustrated in Figure 2.

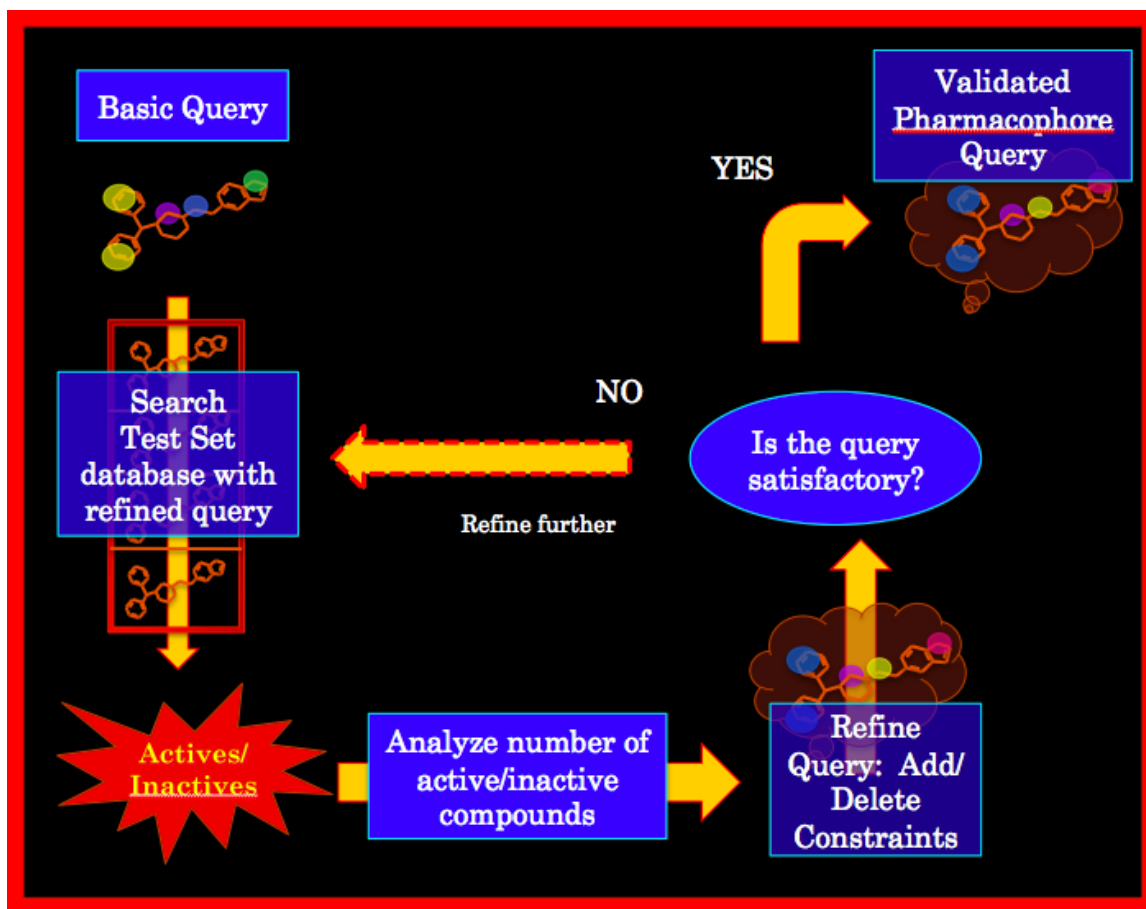


Figure 2.2. Pharmacophore query refinement and validation. A basic query consisting of features determined by MOE was created based on the alignment of the training set compounds. A test set database comprising active and inactive compounds was searched to determine how the query should be refined in order to maximally retrieve active and minimally retrieve inactive compounds. The features in the query were refined accordingly until a satisfactory retrieval ratio of active:inactive compounds was reached, thus generating the validated and refined pharmacophore query.

2.2.6 Searching a Conformation Database

The “pharmacophore search” feature of MOE was used to screen the extensive, virtual ZINC conformational database for compounds that satisfy the pharmacophore query features. Each ligand conformation from the ZINC database that complies with all restrictions of the pharmacophore query, known as a *hit (or match; Figure 2.3)*, was stored in an output *hit database*. In general, atomic centers within each hit must be within the radius of the pharmacophore feature to be considered a match (Molecular Operating Environment 2010).

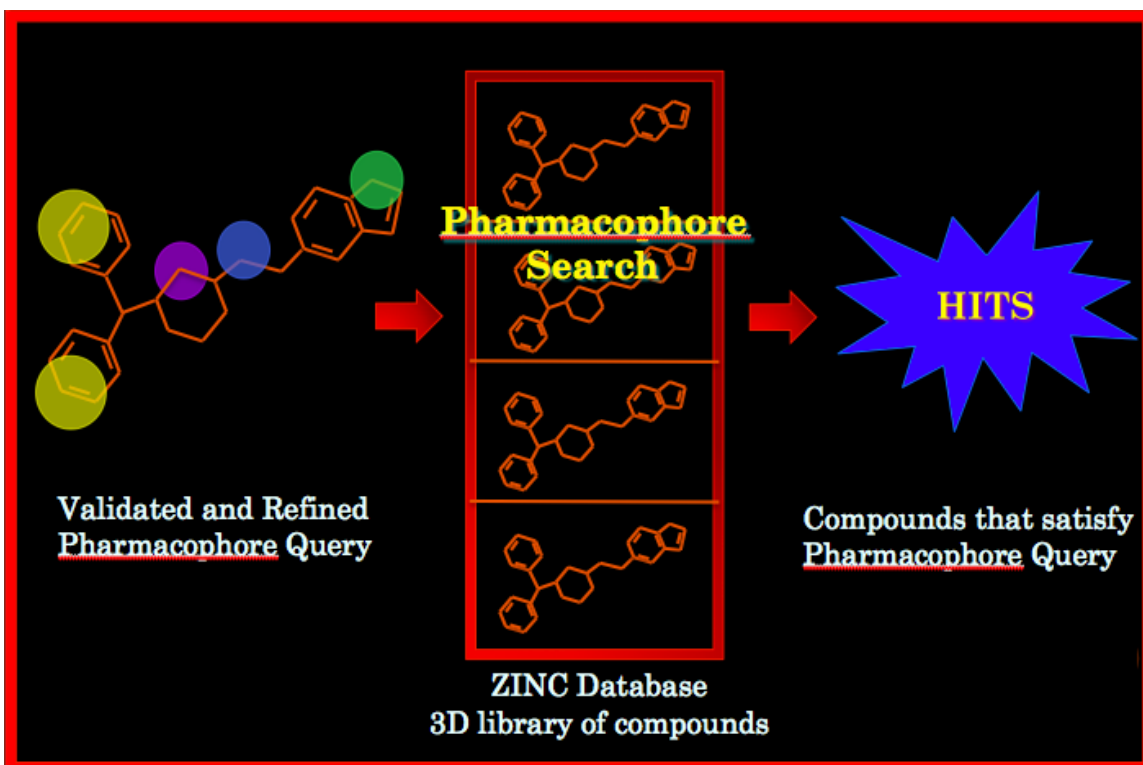


Figure 2.3. Pharmacophore searching in MOE. The pharmacophore query, illustrated with different colored spheres known as pharmacophore features, was used to search the ZINC database. Compounds that satisfied all features of the query were returned as hit compounds.

2.2.7 Sorting the Hit Database

A Gaussian-based scoring algorithm, informally called an “S” score, was used to rank the compounds in the hit database based on how well hits align to the original alignment of the four training set compounds. When the four active set molecules were aligned, the score consisted of a sum of terms that were based on intermolecular atom pairs. Each intermolecular atom pair with similar properties was calculated using the Gaussian scoring term:

$$w \exp(-Rr^2),$$

in which r is the distance between the two atoms, R is a parameter controlling the range of the interaction, and w is the weight of this term (Chan and Labute, 2010).

A scoring function S was constructed based on the sum of Gaussian terms:

$$S = \sum_k T_k = \sum_k w_k \sum_{i \in A_k} \sum_{j \in B_k} \exp(-\alpha r_{ij}^2)$$

In the above formula, T_k represents the overlap of a particular pair of atom types or features (A_k, B_k); w_k is the weight of the term; i and j are atoms/features from the two molecules; r_{ij} is the distance between the intermolecular atom/feature pair; and α is a parameter controlling the range of this type of interaction (Chan et al., 2010). For details on the “T” terms, please refer to Chan and colleagues (2010).

2.3 Experimental Methods

2.3.1 hNET and hSERT Membrane Preparation

Membranes were prepared from stably transfected HEK293-hNET and HEK293-hSERT cells grown at 37°C in a 5% CO₂ environment on 150 x 25 mm plates. At 95% confluence (3 days of growth), cells were washed twice with 10 mL cold phosphate-buffered saline (DPBS). An additional 10 mL of DPBS was added to the plates, and cells were detached by scraping and transferred to cold centrifuge tubes (15 mL). Cells were centrifuged for 10 min at low speed (700 x g). The supernatant was removed and the cell pellet was resuspended in 500 µL cold TE buffer (50 mM Tris, 1 mM EDTA, pH 7.5). Following centrifugation for 30 min at 100,000 x g at 4°C, the supernatant was discarded and the pellet was frozen and stored at -20°C for later use.

2.3.2 hNET and hSERT One-Point Binding Assays

Membrane one-point binding assays were performed for hNET and hSERT using stable hNET-HEK293 and hSERT-HEK293 cell lines, respectively. hNET and hSERT membrane pellets were resuspended in ice-cold binding buffer (50 mM Tris, pH 7.5, 100 mM NaCl). The membranes were sonicated until the pellet dissolved. Each compound identified from the virtual screen was dissolved in 100% DMSO to a concentration of 10 mM. Initial one-point competition binding assays were conducted using 10 µM final concentration of VS hit compounds and 10 nM of radiolabeled [³H]-nisoxetine and [³H]-paroxetine for NET and SERT, respectively. Reactions were carried out in 12 x 75 mm

borosilicate glass tubes. Each tube contained 240 μ L membrane, 30 μ L radioligand (10 nM [3 H]-nisoxetine or [3 H]-paroxetine), and 30 μ L cold competitor VS compound (to final concentration of 10 μ M). To measure non-specific binding, an additional tube contained similar amounts of membrane fraction, radioligand, and 10 μ M non-specific competitor (desipramine or paroxetine for hNET or hSERT, respectively). Tubes were gently shaken at room temperature for 1 hr. GF/B filters (Schleicher and Schuell, Keene, NH) were presoaked in 0.5% polyethylenimine solution (v/v). Solutions were rapidly filtered through GF/B filters using a Brandel harvester. Filters were washed twice with 5 mL cold 50 mM Tris buffer. Each filter was transferred to scintillation vials containing 5 ml of ScintSafe and radioactivity was counted using a liquid scintillation counter. Screening results were analyzed using Microsoft Office Excel software. Data were compared using Student's t-test; values less than 0.05 were considered to be statistically significant.

2.3.3 hDAT Whole Cell Binding Assays

Whole-cell one-point binding assays were performed for hDAT using stable hDAT-N2A cell lines, grown at 37°C in a 5% CO₂ environment. Cell monolayers were grown in 24-well plates to >90% confluence. Cells were washed twice with 1 mL of KRH buffer (25 mM HEPES, pH 7.3, 125 mM NaCl, 4.8 mM KCl, 1.3 mM CaCl₂, 1.2 mM MgSO₄, 1.2 mM KH₂PO₄, 5.6 mM glucose) supplemented with 50 mM ascorbic acid (KRH/AA). Each compound identified from the virtual screen was dissolved in 100% DMSO to a concentration of 10 mM. Cells were incubated for 15 min with 10 nM [3 H]-WIN 35,428 (total volume of 500 μ L) along with 10 μ M VS hit compound or 10 μ M mazindol.

Following incubation, cells were washed twice with 1 mL KRH/AA buffer, then treated with 1 mL 1% SDS with gentle shaking at room temperature for 1 hr. Cell lysates were transferred into vials. Radioactivity was determined in a liquid scintillation counter. Screening results were analyzed using Microsoft Office Excel software. Data were compared using Student's t-test and values less than 0.05 were considered to be statistically significant.

Chapter 3. Computational Studies

3.1 Pharmacophore Model Generation and Virtual Screening

3.1.1 Introduction

A pharmacophore model demonstrates the interaction between the active site of a target protein and a ligand. Yet, this is not entirely a new concept. The expression “pharmacophore” was first coined by Paul Ehrlich and defined as: “a molecular framework that carries the essential features responsible for a drug’s biological activity” (Ehrlich, 1909). Pharmacophore features include important functional groups involved in intermolecular interactions; the combination of these features in three-dimensional space represents the necessary components for a ligand to be active against a certain target (Pandit et al., 2006). A pharmacophore model demonstrates the interaction between the active site of a target protein and a ligand. In this study, because the 3-D structure of the NET (or any of the monoamine transporters) is not available, high-affinity NET inhibitors were used to generate the pharmacophore model in an approach known as “ligand-based drug design”.

Several steps were involved in generating the pharmacophore model. The first was to select known receptor ligands to comprise the “training set”. The 2-D structures of each ligand were built in MOE. The next step involved aligning common features found among all of the compounds in the training set. Upon completion of this alignment, pharmacophore models were generated using the MOE algorithm, and the more favorable

set of pharmacophore features in each model were selected. The model deemed best was subjected to a validation and refinement process using ligands not present in the training set; models that did not pass this validation step were rejected. The constructed pharmacophore model was then used to virtually screen the extensive ZINC database. “Hits” from the screening were ranked using a MOE scoring function, and the highest-ranked compounds were analyzed in vitro at the NET, DAT and SERT.

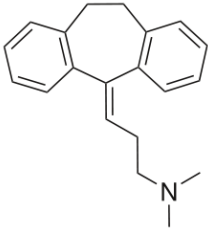
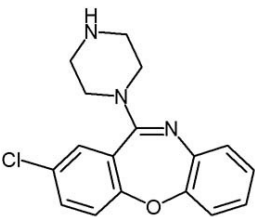
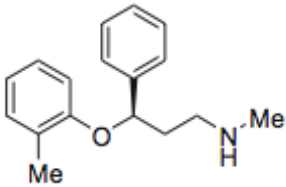
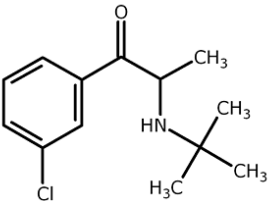
3.1.2 Generation of the Training Set

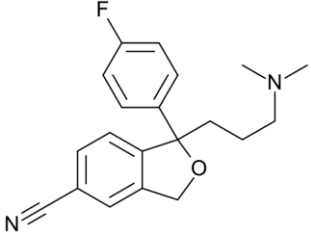
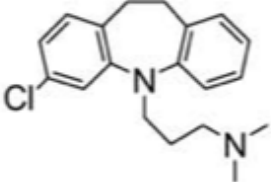
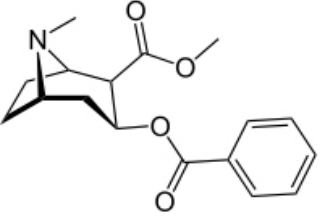
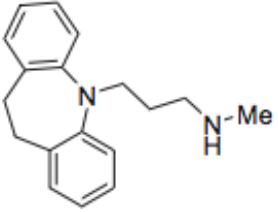
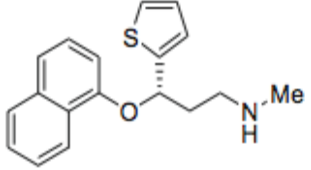
The training set is comprised of structurally diverse compounds of known biological activity.

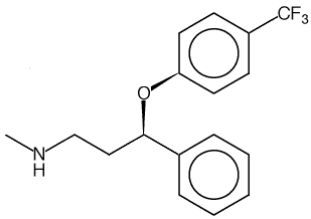
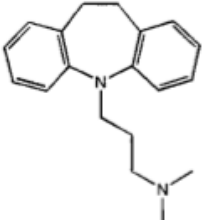
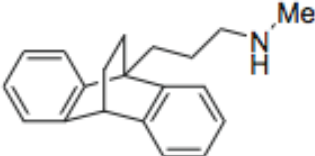
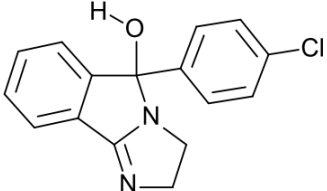
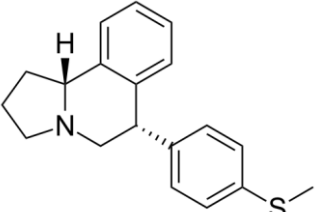
3.1.2.1 Searching for Relevant Compounds: Literature Review

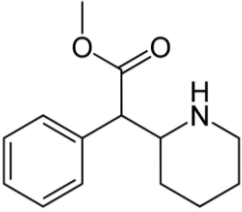
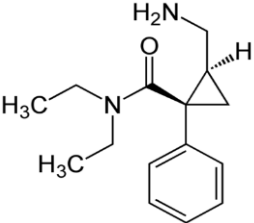
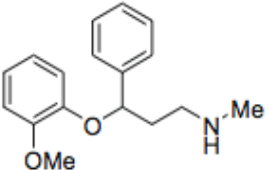
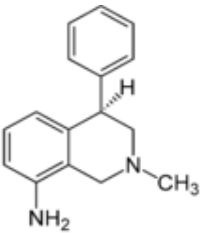
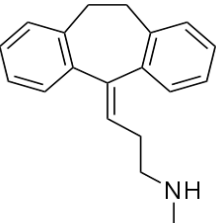
A thorough literature search was performed to seek out compounds with experimentally determined K_i values at the NET. Table 3.1 shows these compounds from a variety of studies. Considered investigations involved the use of either membrane fractions or whole cells of HEK-293 or MDCK cell lines, both stably transfected with NET as well as cells from male rat Sprague-Dawley cerebral cortex. Only literature sources using tritiated nisoxetine as the radioligand in each experiment at the NET were considered and shown in Table 3.1.

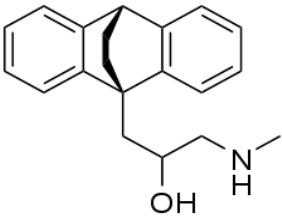
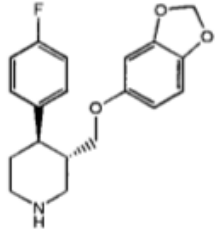
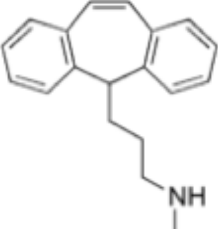
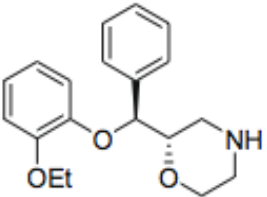
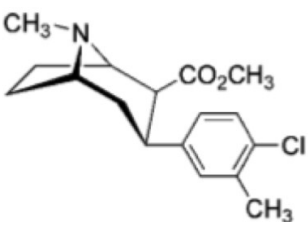
Table 3.1. Binding affinities of NET inhibitors from radioligand competition binding assays. In each case [³H]-nisoxetine was used as the radioligand. Whole cells or membrane fractions were prepared from stably transfected HEK293-hNET, MDCK-hNET or cerebral cortex sections from male Sprague-Dawley rat cells.

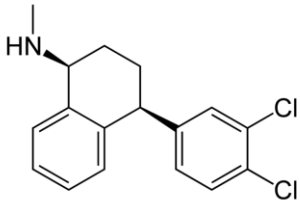
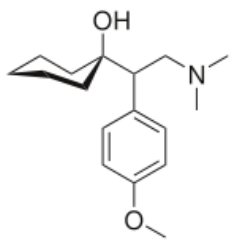
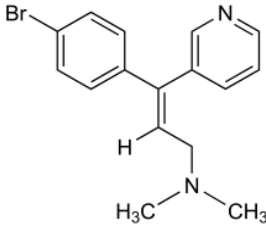
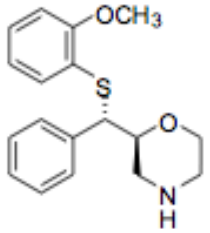
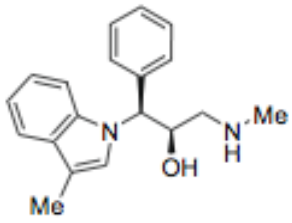
Compound	Ki for hNET (nM) ^a	Cell type
Amitriptyline 	19±1 13.3±1.54	HEK-293 ¹ HEK-293 ⁴
Amoxapine 	16 2	HEK-293 ⁵ HEK-293 ⁶
Atomoxetine 	5 3.5±0.3	MDCK ² HEK-293 ⁷
Bupropion 	>10,000 185,000±17,000	MDCK ² HEK-293 ¹⁰

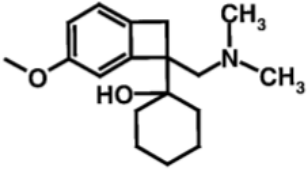
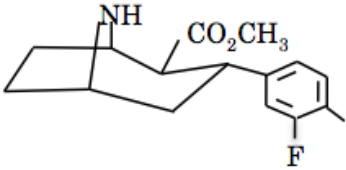
<p>Citalopram</p> 	<p>7865±304 4870±149 4070</p>	<p>HEK-293¹ HEK-293⁴ HEK-293⁵</p>
<p>Clomipramine</p> 	<p>38 79 144±21 53.7</p>	<p>HEK-293⁵ HEK-293⁶ HEK-293⁷ MDCK⁸</p>
<p>Cocaine</p> 	<p>20,000±2500 1990</p>	<p>HEK-293¹⁰ Cerebral cortex (male Sprague-Dawley rats)¹³</p>
<p>Desipramine</p> 	<p>0.63±0.03 3.8 1.58 0.83 2.3±0.2 0.6</p>	<p>HEK-293¹ MDCK² HEK-293⁶ HEK-293⁵ HEK-293⁷ MDCK⁹</p>
<p>Duloxetine</p> 	<p>7.5± 0.3 1.17±0.11 7.3±0.5 6.3</p>	<p>MDCK³ HEK-293⁴ HEK-293⁷ HEK-293⁶</p>

<p>Fluoxetine</p> 	<p>777±37 1022</p>	<p>HEK-293¹ MDCK²</p>
<p>Imipramine</p> 	<p>20±0.54 98 98±22</p>	<p>HEK-293¹ MDCK² HEK-293¹⁰</p>
<p>Maprotiline</p> 	<p>11.1 12</p>	<p>HEK-293⁵ MDCK⁹</p>
<p>Mazindol</p> 	<p>0.46±0.004 3.42±0.67</p>	<p>HEK-293¹ HEK-293¹⁰</p>
<p>MCN5652</p> 	<p>15.8</p>	<p>HEK-293⁶</p>

<p>Methylphenidate</p> 	<p>339</p>	<p>MDCK²</p>
<p>Milnacipran</p> 	<p>22±2.58</p> <p>50.1</p>	<p>HEK-293⁴</p> <p>HEK-293⁶</p>
<p>Nisoxetine</p> 	<p>6</p> <p>6±0.5</p>	<p>MDCK⁹</p> <p>HEK-293¹⁰</p>
<p>Nomifensine</p> 	<p>29</p> <p>71±6</p>	<p>MDCK²</p> <p>HEK-293¹⁰</p>
<p>Nortriptyline</p> 	<p>1.8±0.07</p> <p>1.49±0.17</p> <p>4.35</p> <p>17±0.5</p>	<p>HEK-293¹</p> <p>HEK-293⁴</p> <p>HEK-293⁵</p> <p>HEK-293¹⁰</p>

<p>Oxaprotiline</p> 	<p>4.9</p>	<p>HEK-293⁵</p>
<p>Paroxetine</p> 	<p>85±5 40 63</p>	<p>HEK-293¹ HEK-293⁵ HEK-293⁶</p>
<p>Protriptyline</p> 	<p>1.41</p>	<p>HEK-293⁵</p>
<p>Reboxetine</p> 	<p>0.3 15.8 11</p>	<p>MDCK⁹ MDCK⁸ MDCK³</p>
<p>RTI-112</p> 	<p>21.8±0.6</p>	<p>Cerebral cortex (male Sprague-Dawley rats)¹³</p>

<p>Sertraline</p> 	<p>817±80</p>	<p>HEK-293¹</p>
<p>Venlafaxine</p> 	<p>2269±84 2480±43 1920±158 3346 6310</p>	<p>HEK-293¹ MDCK³ HEK-293⁴ HEK-293⁶ MDCK⁸</p>
<p>Zimelidine</p> 	<p>9400±100*</p>	<p>HEK-293⁵</p>
<p>3</p> 	<p>0.76 ± 0.06</p>	<p>HEK-293¹¹</p>
<p>14</p> 	<p>9</p>	<p>MDCK⁹</p>

<p>S3305</p> 	<p>1510</p>	<p>MDCK⁸</p>
<p>8d</p> 	<p>0.43±0.02</p>	<p>Cerebral cortex (male Sprague-Dawley rats)¹²</p>

Data are expressed as geometric means \pm standard deviation of at least three separate experiments performed in triplicate.

^aRadioligand competitive binding using [³H]nisoxetine in cells transfected with a human norepinephrine transporter cDNA plasmid.

*Value shown as K_D

1: Owens et al., 1997

7: Wagstaff et al., 2007

2: Bymaster et al., 2002

8: Millan et al., 2001

3: Bymaster et al., 2001

9: Heffernan et al., 2009

4: Vaishnavi et al., 2004

10: Eshleman et al., 1999

5: Tatsumi et al., 1997

11: Zeng et al., 2008

6: Tsuruda et al., 2010

12: Carroll et al., 2005

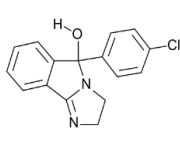
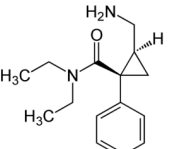
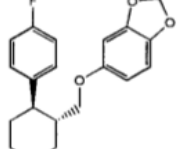
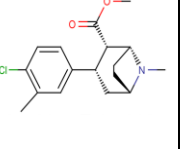
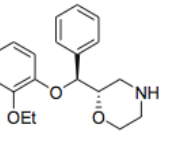
3.1.2.2 Examining compound combinations

All compounds used in the training set were high-affinity NET inhibitors. A variety of compound combinations were explored before the final set was selected. Table 3.2 depicts the diverse groupings of training set compounds. The first training set attempt included five chemically unique compounds. The second set comprised compounds with the highest affinity at the NET. The third set consisted of two TCA and two non-TCA high-affinity NET ligands. The tactic used for choosing the training set compounds is based on the “one group—one type” policy (Horvath, 2011), meaning that a pharmacophore feature should contain one chemical feature type such as “Donor” or “Hydrophobic”, rather than a “one group—many types” approach such as a “Donor or Hydrophobic” group (elaborated in more detail in section 2.1.3 and in section 5.4.2 of discussion).

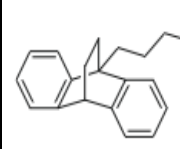
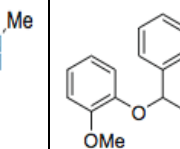
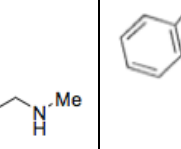
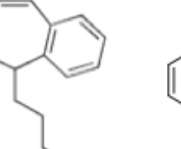
Table 3.2. Compound combinations explored prior to choosing final training set.

All compounds used in the training set are high-affinity NET inhibitors. The first training set attempt included five chemically distinct compounds (a). The second set consisted of compounds with the highest affinity at the NET (b). The third set comprised two TCA and two non-TCA high-affinity NET ligands (c).

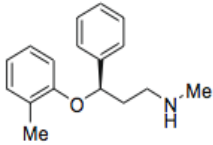
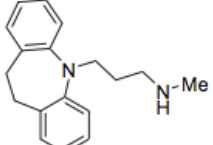
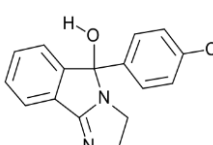
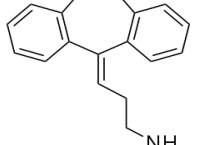
(a) Training Set 1

Chemically distinct structures					
Compound	Mazindol	Milnacipran	Paroxetine	RTI-112	Reboxetine
					
Ki (nM)	3.42	50	63	21.8	0.2

(b) Training Set 2

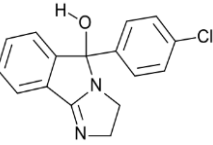
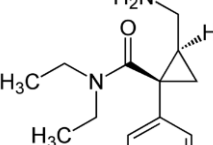
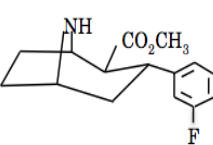
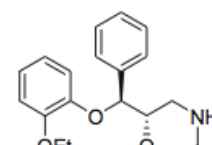
High-affinity NET ligands				
Compound	Maprotiline	Nisoxetine	Protriptyline	Reboxetine
				
Ki (nM)	11	50	1.4	0.2

(c) Training Set 3

Two TCA/two non-TCA compounds				
Compound	Atomoxetine	Desipramine	Mazindol	Nortriptyline
				
Ki (nM)	5	1.58	3.42	1.8

Four compounds with nanomolar inhibition potency were chosen as the final training set: mazindol, milnacipran, reboxetine and “8d” (Table 3.3). The 2D molecular structures of all ligands used to create the pharmacophore model in the training set were built and imported into MOE. These compounds were converted into 3D single conformer representations using the FlexAlign feature in MOE, which energetically minimized and aligned all four compounds (Figure 3.1).

Table 3.3. Training set NET ligands used to generate pharmacophore model.

Training Set Compounds				
Compound	Mazindol	Milnacipran	8d	Reboxetine
				
Ki (nM)	3.42	50	0.43	0.2

3.1.3 Selecting the Optimal Alignment for Creation of the Pharmacophore Query

Different compound combinations were examined, and the best set was chosen based on alignment (Figure 3.1) and pharmacophore feature composition. The FlexAlign feature in MOE was used to align the training set compounds. In selecting the best alignment, it is ideal to include features which are used alone, such as Acc (hydrogen bond acceptor) or Don (hydrogen bond donor), or in combination such as Acc|Don (hydrogen bond acceptor or hydrogen bond donor); it is best to avoid “or” features such as Aro|Acc|Don|Hyd (Aromatic or Hydrogen Bond Acceptor or Hydrogen Bond Donor or Hydrophobic). The Acc|Don feature is much more specific than the “or” Aro|Acc|Don|Hyd feature, which could encompass just about any chemical substituent.

From alignment of the training set compounds MOE generated an aromatic/hydrophobic feature on the aligned aromatic rings of the four training set compounds (F2; orange), two projected PiN features on either side of the Aro|Hyd feature (F1 and F4; red) representing pi bonding from the aromatic ring, an acceptor feature on the nitrogen or oxygen moieties (F3; cyan), a non-aromatic hydrophobic feature (F5; green), and a larger aromatic/hydrophobic feature on the aromatic rings of the TS compounds, located on the opposite side of the first Aro|Hyd feature (F6; orange) (Figure 3.2).

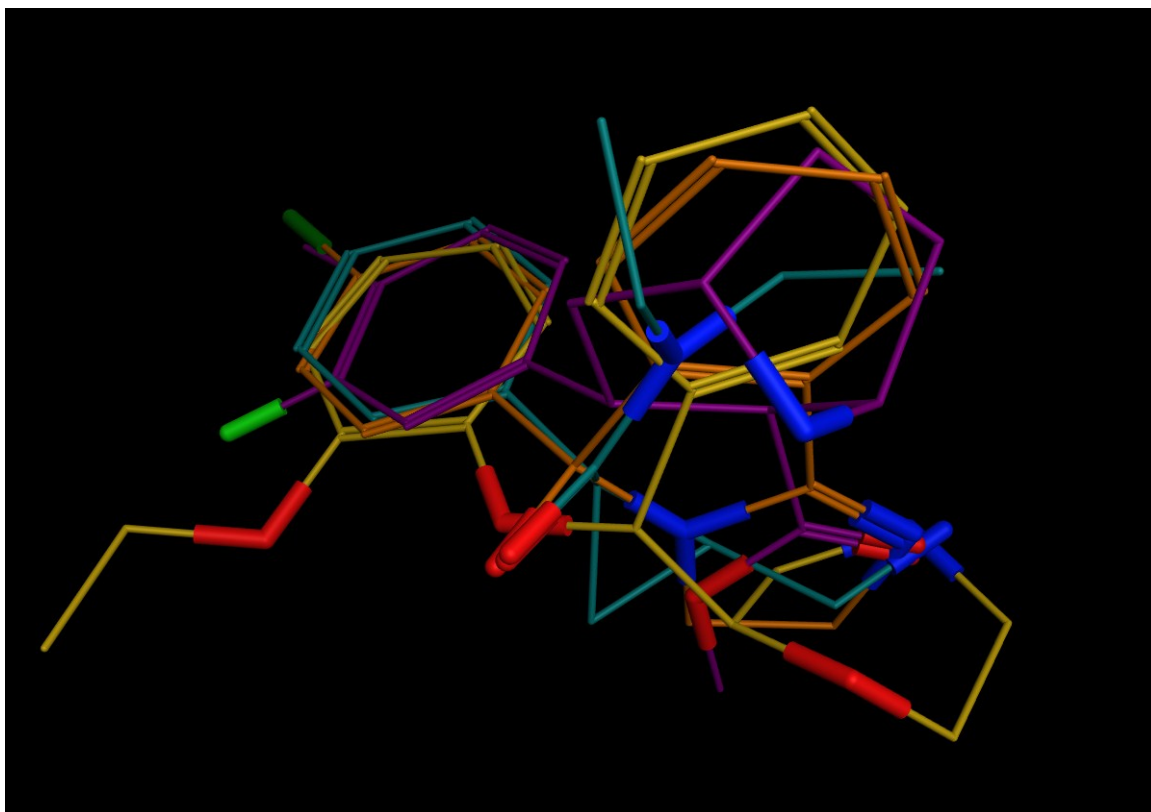


Figure 3.1. Optimal alignment of training set compounds mazindol (orange), milnacipran (cyan), reboxetine (yellow) and 8d (purple). Nitrogen (blue caps), oxygen (red caps) and halogen (green caps) atoms are indicated. From this figure it can be seen how the acceptor/donor groups align.

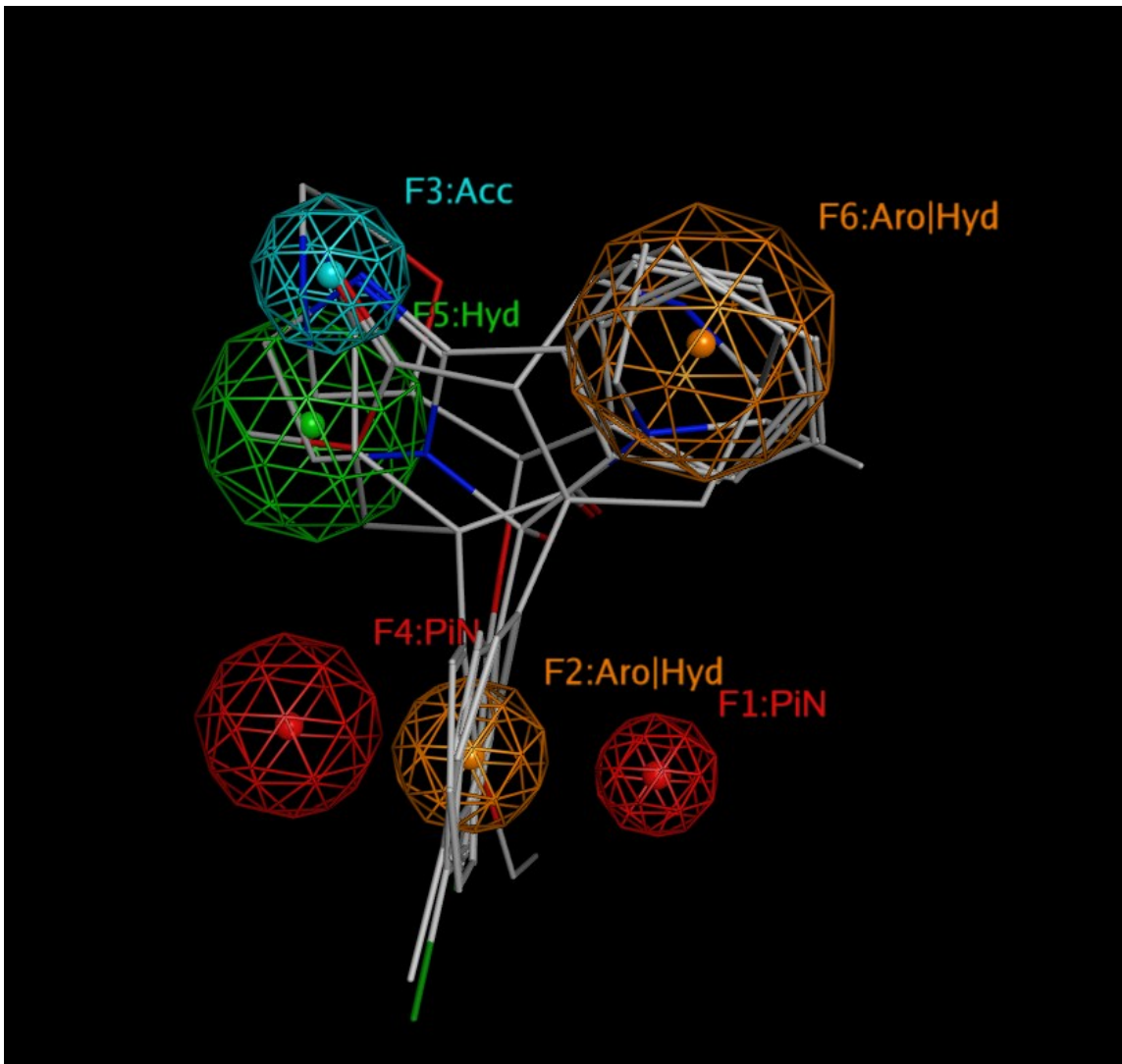


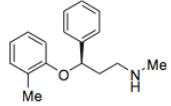
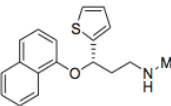
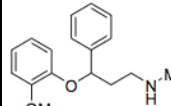
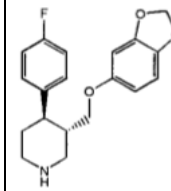
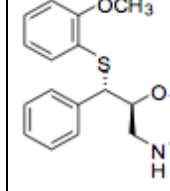
Figure 3.2. Preliminary pharmacophore features generated by MOE, based on training set alignment of mazindol, milnacipran, reboxetine, and 8d. In the alignment, MOE grouped common features together. The sky blue sphere represents an acceptor group located on nitrogen and oxygen moieties (cyan, of 0.91 Å radius). hydrophobic features (green, of 1.41 Å radius); groups that are either aromatic or hydrophobic in character (orange, with radii of 0.89 Angstroms). PiN groups (red, of

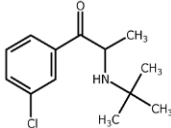
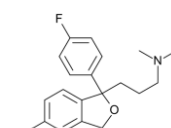
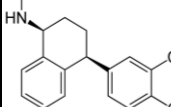
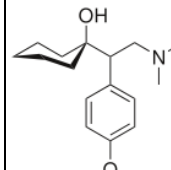
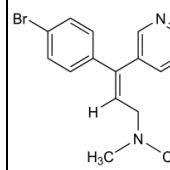
radii 0.70 and 1.07 Å) are projected pi-bond hydrogens which usually accompany the aromatic features.

3.1.4 Validation of the Pharmacophore Model

In order to discern whether the created model could retrieve active compounds and ignore inactive compounds from a database, validation of the constructed pharmacophore model was performed. A test set was created by randomly choosing 1000 compounds from the ZINC database and seeding it with 10 structurally diverse compounds of known affinities, including five active (high affinity) and five inactive (low affinity) at the NET (Table 3.4). Conformational analysis for each compound in the validation dataset was performed, with a maximum number of 100 conformations per molecule. From Table 3.4 it can be seen that both sertraline and venlafaxine have K_i values that are relatively not large, approximately 0.8 μM and 2 μM , respectively. In this study, a question of where to draw the line between active and inactive compounds arose. Generally, compounds that were approximately 1 μM or higher at the NET were deemed inactive.

Table 3.4. List of high affinity and low affinity compounds at the NET used in validation studies. The numbers represent K_i values (nM).

Active					
Compound	Atomoxetine	Duloxetine	Nisoxetine	Paroxetine	3
					
K_i (nM)	3.5^1	7.3^1	6^2	40^3	0.3^4

Inactive					
Compound	Bupropion	SCitalopram	Sertraline	Venlafaxine	Zimelidine
					
K_i (nM)	$185,000^2$	4070^3	817^5	2269^5	9400^3

1: Wagstaff et al. (HEK-293 cells)

2: Eshleman et al. (HEK-293 cells)

3: Tatsumi et al. (HEK-293 cells)

4: Zeng et al. (HEK-293 cells)

5: Owens et al. (HEK-293 cells)

The original model selected two inactive compounds (zimeclidine and venlafaxine) and two active compounds (nisoxetine and a reboxetine derivative, “3”). It was necessary, therefore, to refine the model in such a way so that it would pick out a greater number of active compounds and ignore inactive compounds, particularly ignoring extremely low affinity compounds at the NET such as zimelidine or bupropion.

3.1.5 Refining the Pharmacophore Query

In order to maximize the number of active and minimize inactive retrieved compounds, the pharmacophore features were modified. This was done by trial and error, systematically making one alteration at a time and screening the test set database to identify which known compounds were retrieved.

The first modification was to ignore both of the PiN features in order to broaden searching criteria. Although this change retrieved all five active compounds, four inactives (zimeclidine, bupropion, citalopram and venlafaxine) were also picked out. This is a general improvement in the number of active compounds since the screening with original pharmacophore query retrieved only two active compounds (nisoxetine and “3”), as described in section 2.1.4, above. At the same time, ignoring the PiN features also increased the number of inactives from two (zimeclidine and venlafaxine) to four. From this screening, it appeared that although the PiN features should remain ignored, as in their absence all active compounds were retrieved, there needed to be an adjustment that would narrow searching criteria, such that only the five actives would be selected. Of particular interest was to exclude in the validation screen zimelidine and bupropion, two compounds with very low NET affinity.

The structures of zimelidine and bupropion were overlaid with the pharmacophore points in order to discern how the features could be modified. The large “Aro|Hyd” feature, located opposite of the smaller “Aro|Hyd”, appeared to be in zimelidine’s hydrophobic rather than aromatic region. Therefore, both “Aro|Hyd” features were amended to “Aro” so that zimelidine would not be selected in the validation screening. Favorably, this change did not retrieve any inactive compounds. Yet, of the active compounds, only three of the five were selected. The two changes made at this point - ignoring the two PiNs and changing the “Aro|Hyd” features to “Aro” - were following the right path (i.e. retrieval of more actives and ignoring inactives). The next step involved, again, broadening search criteria in order for more active compounds to be retrieved.

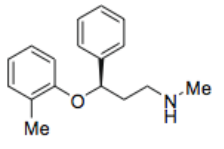
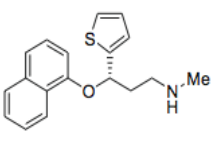
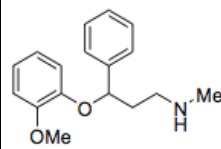
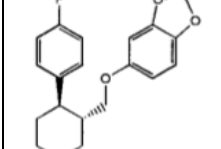
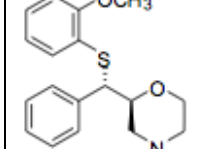
The acceptor feature is spatially located predominantly on amino groups, as well as on one of the carboxyl moieties of the training set (Figure 3.2). It was interesting to see what change would occur if it were to be changed to a donor group. From this adjustment, all five actives and three inactive compounds (zimelidine, sertraline and venlafaxine) were retrieved. Again, the next step involved narrowing search criteria so that little or no inactive compounds would be selected from the validation screening.

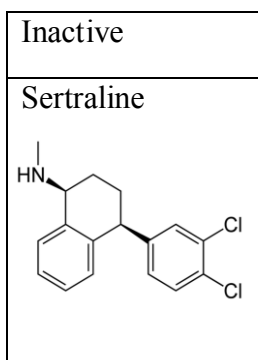
An exterior volume was placed about the training set compounds, with a radius of 1.49 Å. This change retrieved two active (atomoxetine and 3) and two inactive (zimelidine and venlafaxine) compounds. The exterior volume constraint was incrementally increased by 0.1 Å. At a radius of 2.5 Å, three actives and the two inactives remained; at a radius of 2.7 Å, four actives and the two inactives were retrieved.

Further increasing this radius did not produce any changes. Temporarily, the exterior volume radius was left at 2.7 Å.

The next change was to decrease the radius of the large “Aro” feature from 1.55 Å. It was systematically decreased every 0.1 Å until no more changes were observed. At a radius of 1.0 Å, four active compounds and one inactive (sertraline) compound were obtained. The large hydrophobic feature was also altered in size. It was observed that retrieved hits depended on the combination of exterior volume radius and the size of this hydrophobic feature. Decreasing the hydrophobic radius to 0.6 Å and exterior volume to 2.2 Å retrieved all five active compounds and one inactive (sertraline) compound. Since sertraline is moderately inactive regarding NET affinity (unlike zimilidine or bupropion), it was deemed an acceptable compromise that the model selected it.

Table 3.5. Retrieved compounds from the validation database screening after refining the pharmacophore model. Five active compounds (atomoxetine, duloxetine, nisoxetine, paroxetine and #3) and one inactive compound (sertraline) were retrieved.

Active				
Atomoxetine	Duloxetine	Nisoxetine	Paroxetine	3
				



3.1.6 Second Refinement of Pharmacophore Query

In order to determine whether the model required further refining and if a manageable number of hits would be retrieved, a preliminary screen of a portion of the ZINC database was performed. The filtered ZINC database (as discussed in Section 2.1.7 and shown in Figure 3.5) was divided into ten separate databases, each containing a range of 20,000 to 2 million entries. Database #2 was screened, which contained approximately 42,000 molecules. After the screen with the initially refined model, about 400 molecules were retrieved. Although this was a manageable hit return, it was only one small database screened out of ten even larger ones. Therefore, before any further screening, it was necessary to further revise the pharmacophore features in order to decrease the hit rate.

To this point, the model had been modified such that it could retrieve five active compounds and one inactive compound (Table 3.5). Each feature was next made more stringent by decreasing its radius, given that the selected compounds from the validation screen should not change. After each change, the validation database was rescreened.

The radius of each feature was decreased until a change in the number of retrieved compounds was observed. If the number of selected active or inactive compounds was altered, the change was reversed. At last, the features were amended to the following (Figures 3.3 and 3.4):

Aro – 0.78 A (formerly near the PiNs)

Don – 0.8 A

Hyd – 0.55 A

Aro – 1 A

Exterior volume – 2.14 A

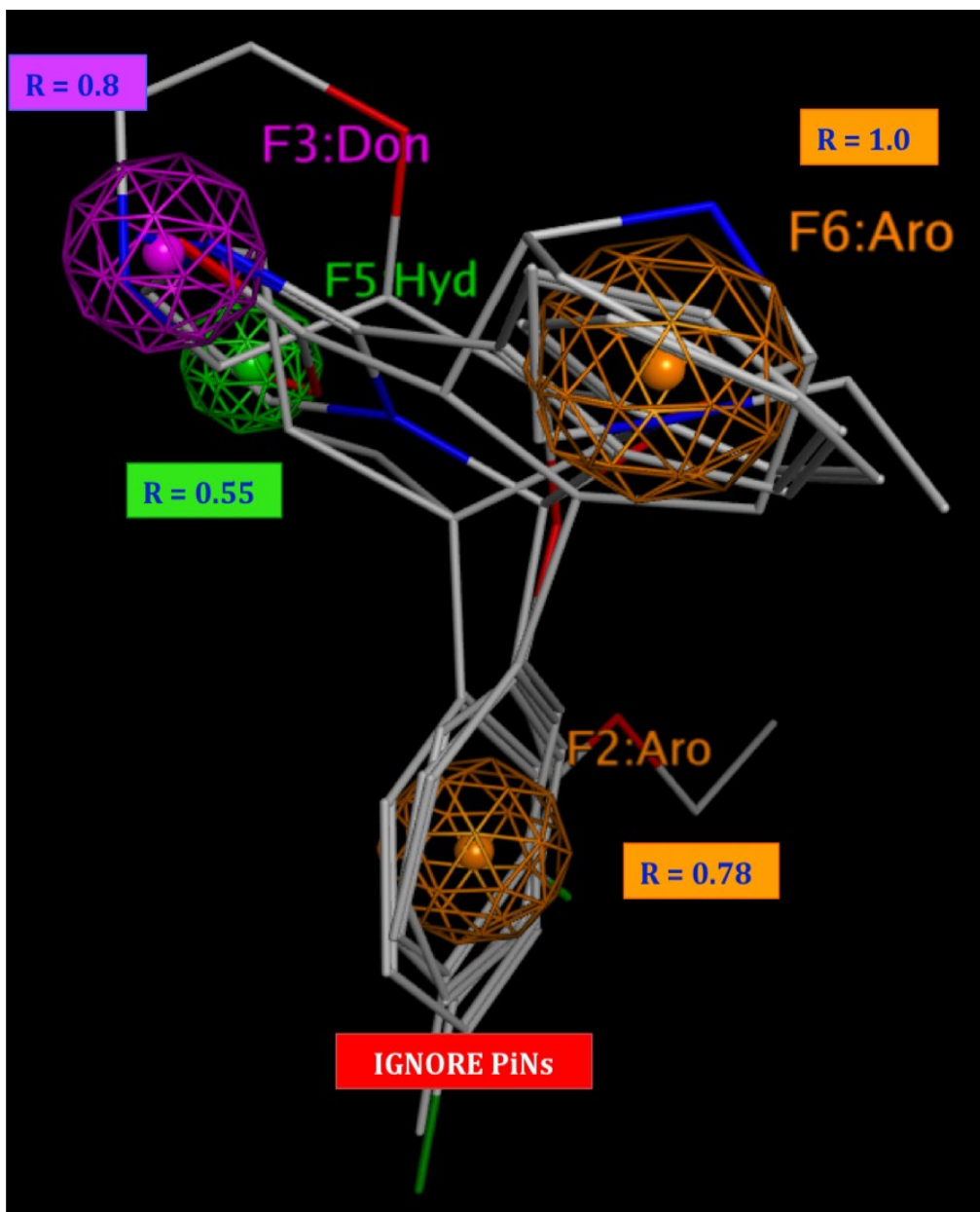


Figure 3.3. The refined pharmacophore model containing four pharmacophore features, mapped onto the four training set compounds. Features include: an aromatic feature with radius of 0.78 Å (orange, closer to bottom), another aromatic feature with radius of 1.0 Å (orange, larger sphere), a donor feature with radius of 0.8 Å (purple), hydrophobic feature with radius of 0.55 Å (green).

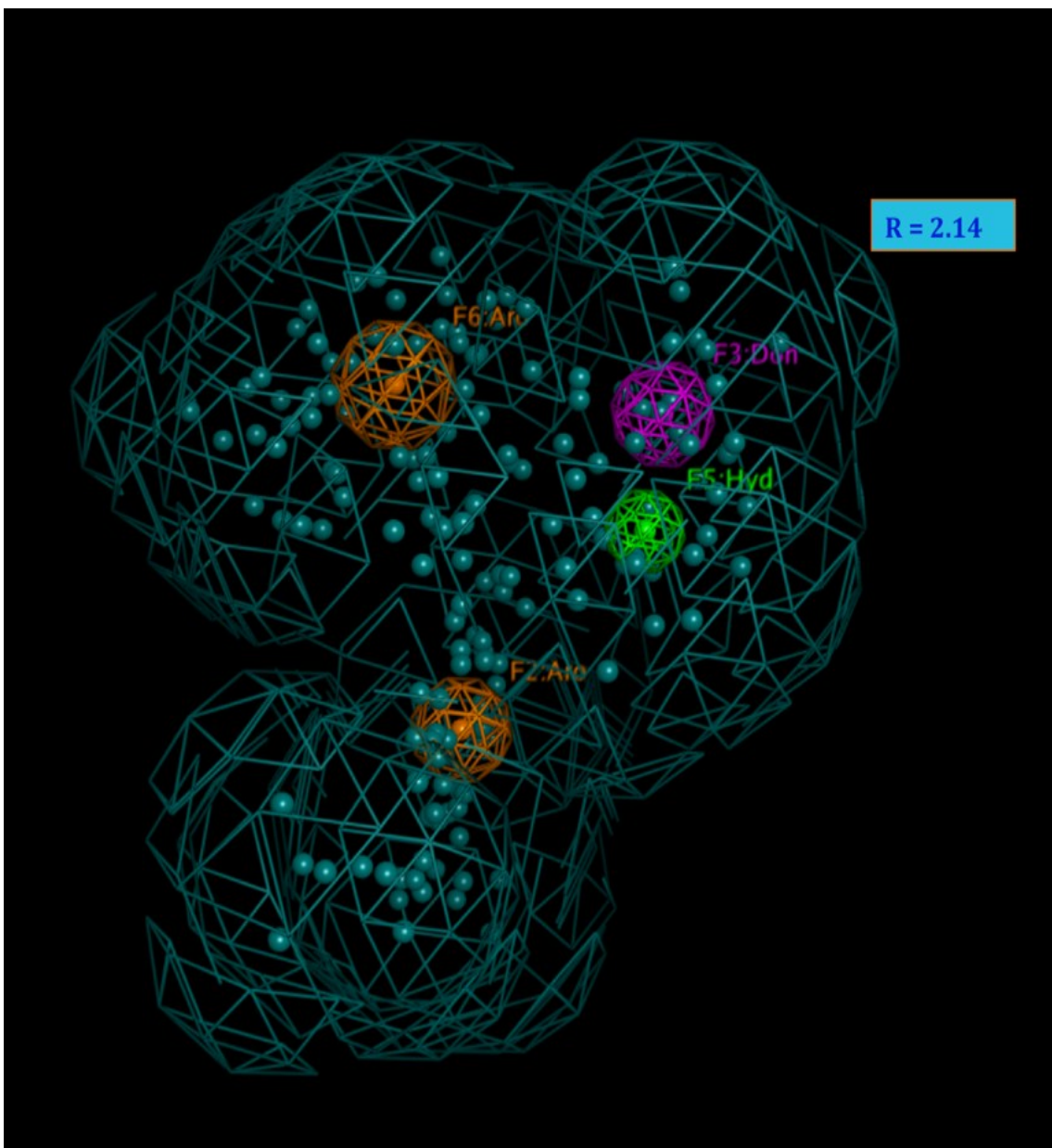


Figure 3.4. Refined pharmacophore model with excluded volume feature, shown in blue, with a radius of 2.14 Å. The volume is enclosed around the initial four training set compounds. Blue spheres represent atoms from these compounds.

All changes to the pharmacophore points gave a maximum number of five active compounds and a minimum number of one inactive compound, retrieved from the test set database. At this point, the model appeared acceptable and virtual screening could be performed.

3.1.7 Virtual Screening of the ZINC Database

Virtual screening is a fast and economic approach to effectively identify biologically active compounds, or “hits”, from a pool of millions of commercially available compounds (Waszkowycz, 2002; Shoichet, 2004). The database used in virtual screening was created in accordance to Manepalli et al. (Manepalli et al., 2011). An 18 million entry “all-purchasable” subset of the ZINC database was downloaded. Using the MOE software, the compounds were “washed” by removing salts, ions, and disconnected molecular fragments. To remove non-drug like molecules, The Lipinski’s Rule of Five descriptor was applied to the database. Compounds containing reactive groups were removed with a toxic moiety descriptor filter. From the approximate million remaining compounds, tautomers and protomers were generated. Conformational analysis was performed on these compounds using the “import conformation” module of MOE, with the MMFF94x force field. Conformations with strain energy 4 kcal/mol or greater were discarded (Figure 3.5). This final database was screened with the created pharmacophore model.

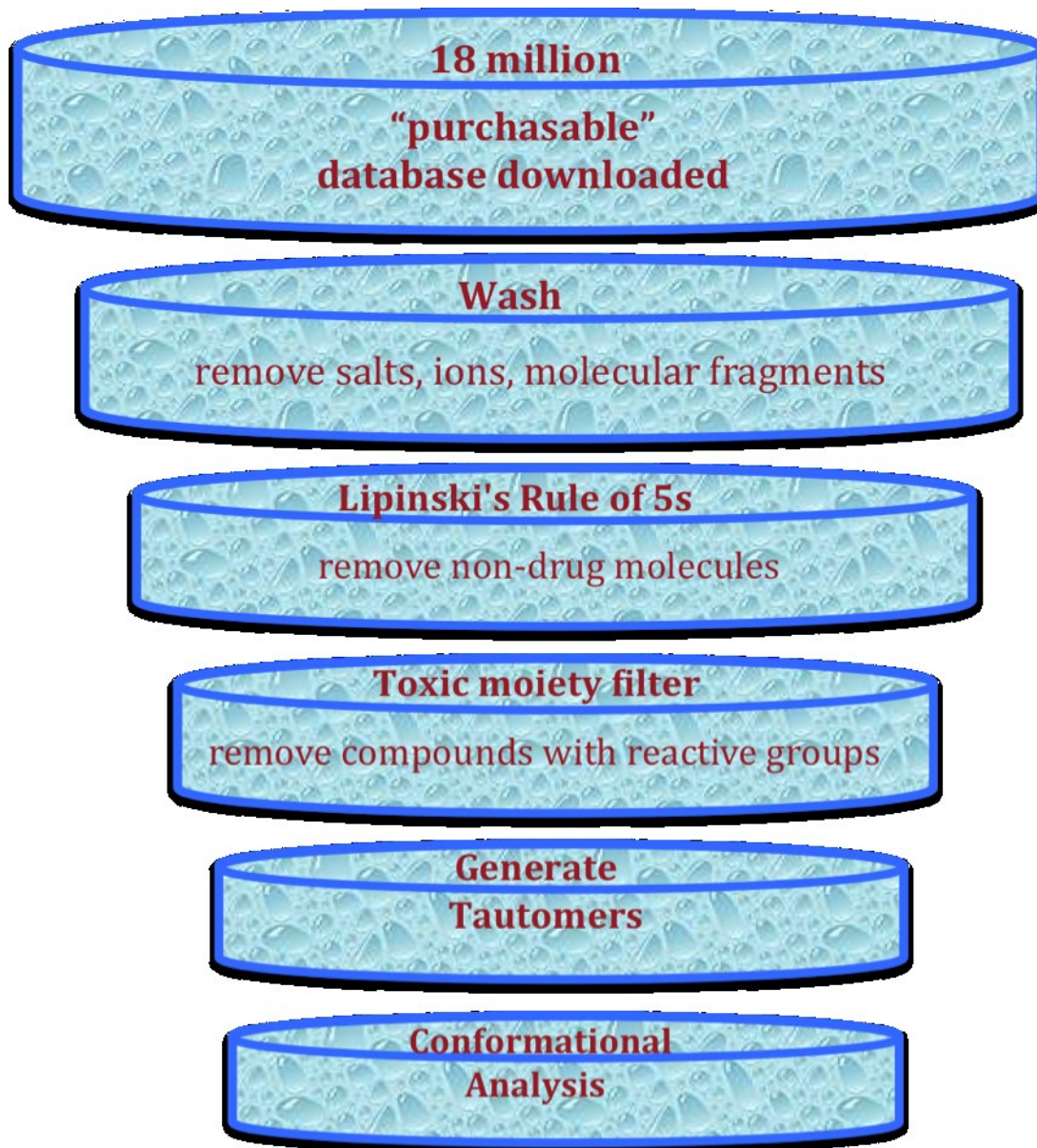


Figure 3.5. Generation of ZINC Database. Sequential filtering steps employed in screening the ZINC database to attain hit compounds including removing salts, ions, and molecular fragments; removing non-drug molecules based on the Lipinski's Rule of Fives; removing compounds with reactive groups by applying a toxic moiety filter; generating tautomers and performing conformational analysis.

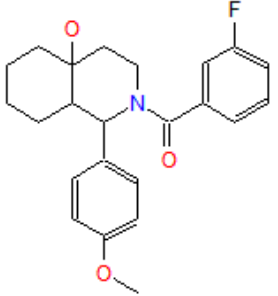
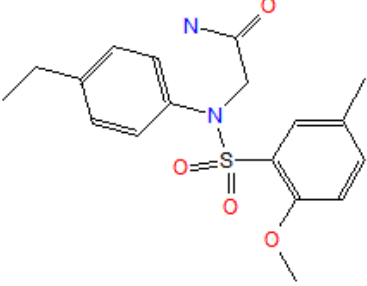
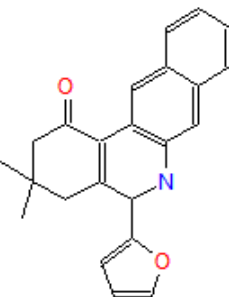
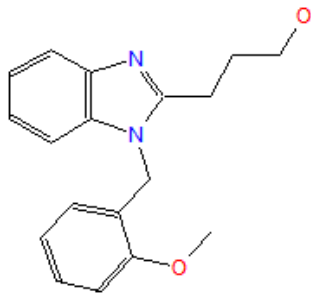
3.1.8 Sorting of Hit Compounds

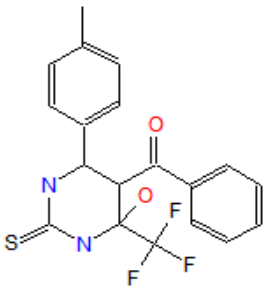
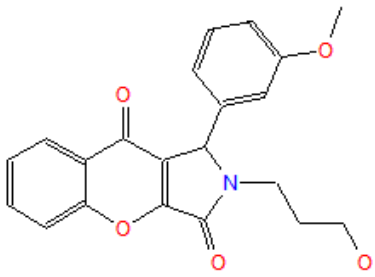
The virtual screen produced 868 hits. Although this was a manageable hit quantity, it was necessary to find an approach to rank the hits to determine which compounds should be chosen and synthesized for further in vitro pharmacological studies. One scheme was to create clusters based on scaffold similarity. The MOE clustering feature was used to organize hits by their scaffold constitution into different groups. Unfortunately, there were so many unique structures that over 200 clusters were generated, an unacceptably high number.

Another approach was to rank hits by RMSD (root mean square deviation) score, which is a statistical calculation of how well the pharmacophore centers of the hit compounds align with the training set pharmacophore centers. The RMSD is a score given by MOE upon completing the virtual screen. This approach was considered, but a more relevant method as opposed to RMSD ranking was used known as an overlay (or “S”) score. The “S” score is a measure of how hit compounds align to the training set alignment. A rationale for using an overlay-based method is that it provides the more appropriate biophysical binding mode of hit compounds, compared to RMSD ranking (Sanders et al., 2012a).

From visual inspection, it was found that compounds with an overlay score less than -113 aligned well to the training set alignment. As a result, 32 compounds possessed the best (lowest value) “S” score, in a range of about -113 to -116. Out of these 32 compounds, six unique scaffolds were selected and purchased for in vitro pharmacological characterization (Table 3.6).

Table 3.6. Six structurally-distinct hits chosen based on S Score and characterized in vitro.

Structure	S score	Name of Compound
	-116	AC-1 2-(3-fluorobenzoyl)-1-(4-methoxyphenyl)octahydro-4a(2H)-isoquinolinol
	-115	AC-2 2-[(4-ethylphenyl)-(2-methoxy-5-methylphenyl)sulfonylamino]acetamide
	-114	AC-3 5-(furan-2-yl)-3,3-dimethyl-2,4,5,6-tetrahydrobenzo[b]phenanthridin-1-one
	-113	AC-4 3-[1-(2-methoxybenzyl)-1H-benzimidazol-2-yl]-1-propanol

	-113	AC-5 [4-hydroxy-6-(4-methylphenyl)-2-thioxo-4-(trifluoromethyl)hexahydro-5-pyrimidinyl](phenyl)methanone
	-113	AC-6 2-(3-hydroxypropyl)-1-(3-methoxyphenyl)-1,2-dihydrochromeno[2,3-c]pyrrole-3,9-dione

Of the six hits, compound AC-1 seemed to be the most promising due to its S score and unique chemical composition. When superimposed on the original four training set compounds as well as the pharmacophore points, AC-1 appeared to align well (Figures 3.6 and 3.7).



Figure 3.6. Superposition of AC-1 (orange) on the original training set alignment.

Compound AC-1 exhibited the best overlay score of -116.

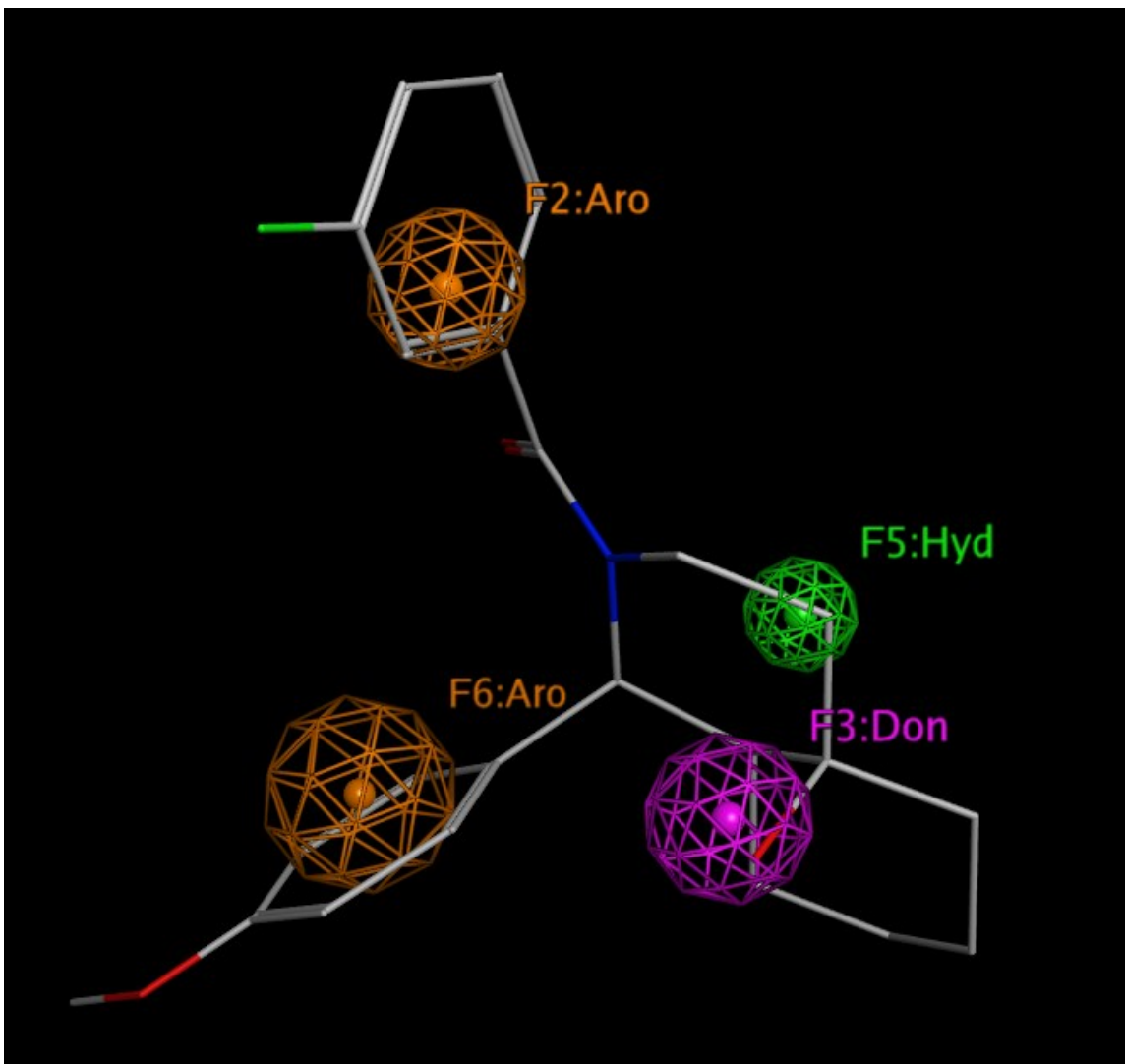


Figure 3.7. Superposition of AC-1 on the pharmacophore points. The pharmacophore points represent the refined pharmacophore model.

Chapter 4. Pharmacologic Characterization

4.1 hNET

To examine the VS hits attained from computational studies, the six highly scored compounds labeled AC-1 to AC-6 were tested for human NET affinity in single point, in vitro binding assays. The reagents were dissolved in DMSO as described in Materials and Methods and assessed for their ability to displace 10 nM [³H]-nisoxetine from the NET in membrane homogenates of hNET HEK293 cells. VS compounds were screened at a single concentration of 10 μM (1000-fold molar excess relative to the radioligand).

As shown in Figure 4.1 all compounds did not significantly displace the binding of radiolabeled ligand from the hNET in membrane homogenates (Student's t-test, $p > 0.05$), indicating no hNET affinity. In a parallel control, 10 μM of the established NET ligand desipramine inhibited the binding of [³H]-nisoxetine by $87 \pm 8\%$ ($p < 0.05$).

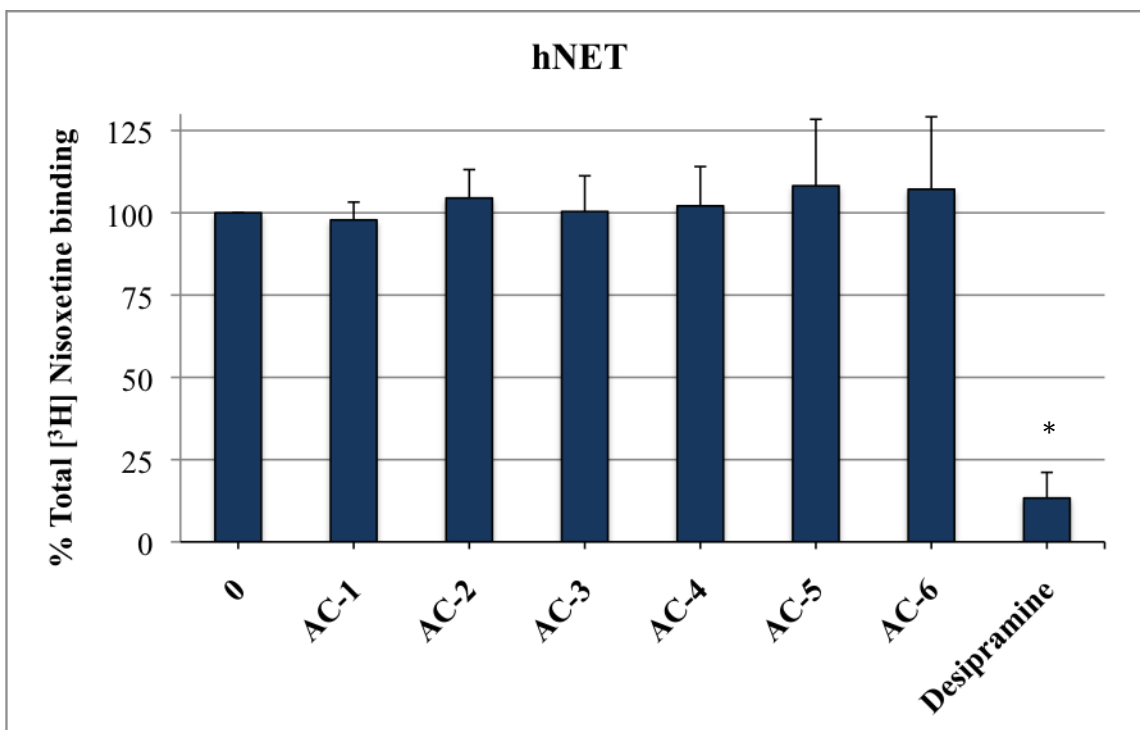


Figure 4.1. VS hit compound one-point screening assay at hNET. Membrane homogenates of HEK-293 cells stably transfected with hNET were used in the binding assay. hNET binding affinities were obtained by displacement of [³H]-nisoxetine. All VS compounds were added at a final concentration of 10 μ M. To measure non-specific binding, 10 μ M desipramine was used. * $p < 0.05$

4.2 hSERT

The six VS hits attained from computational studies (AC-1 to AC-6) were tested for human SERT affinity in single point, in vitro binding assays. VS compounds were assessed for their ability to displace 10 nM [³H]-paroxetine from the SERT in membrane homogenates of HEK293 cells expressing human SERT. VS compounds were screened at a single concentration of 10 μM (1000-fold molar excess relative to radioligand).

Figure 4.2 shows that all compounds did not significantly displace the binding of radiolabeled ligand from the hSERT in membrane homogenates (Student's t-test, $p > 0.05$), indicating no hSERT affinity. The positive control SSRI sertraline (10 μM) was used to assess non-specific radioligand binding, reducing [³H]-paroxetine binding by $77 \pm 8\%$ ($p < 0.05$).

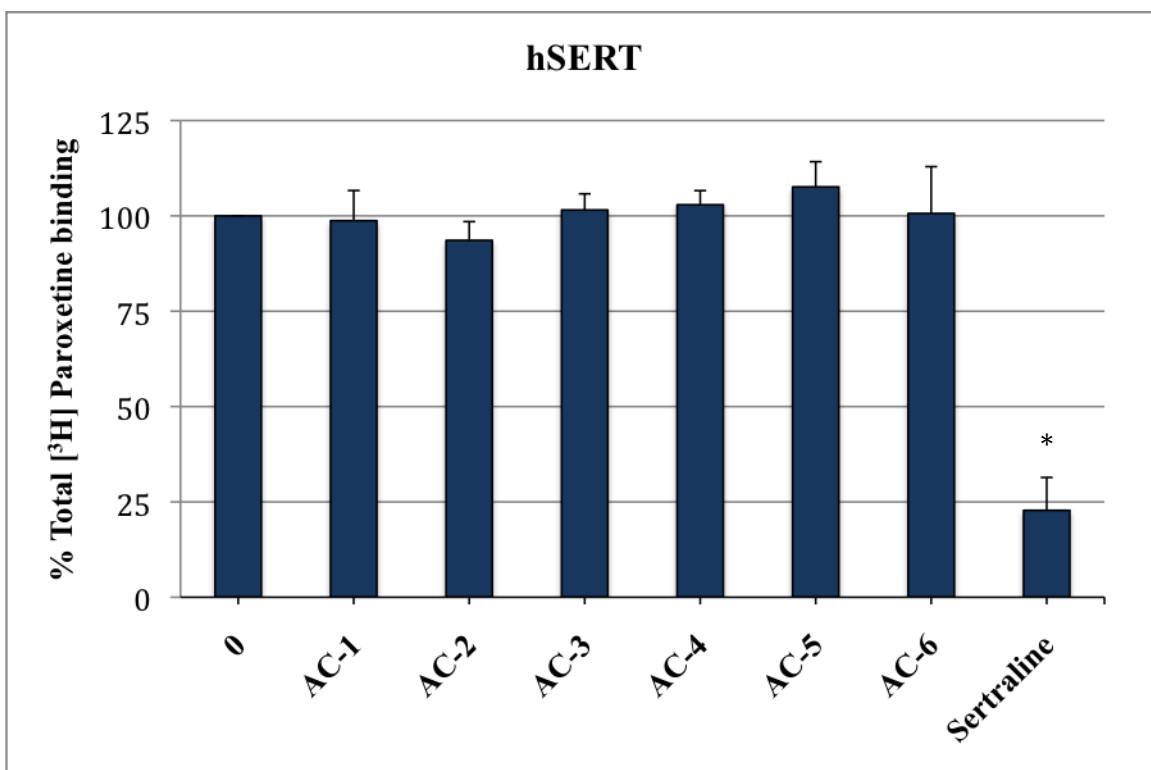


Figure 4.2. VS hit compound one-point screening assay at hSERT. Membrane homogenates of HEK-293 cells, stably transfected with hSERT, were used in the binding assay. hSERT binding affinities were obtained by displacement of [³H] paroxetine. All VS compounds were added at a final concentration of 10 μ M. To measure non-specific binding, 10 μ M sertraline was used. * $p < 0.05$

4.3 hDAT

The six VS hits attained from computational studies (AC-1 to AC-6) were tested for human DAT affinity in single point in vitro binding assays. Compounds were assessed for their ability to displace 10 nM [³H]-WIN 35,428 in N2A-hDAT whole-cell ligand binding assays. VS compounds were screened at a single concentration of 10 μM (1000-fold molar excess relative to radioligand).

As shown in Figure 4.3, compound AC-1 displayed a trend of 15% inhibition of [³H]-WIN binding, although this was not statistically significant based on the Student's t-test (p=0.13). None of the other compounds showed any significant displacement of the radiolabeled ligand in whole cells (Student's t-test, p>0.05), indicating no hDAT affinity. In a control experiment, 10 μM mazindol inhibited the binding of [³H]-WIN to DAT by 83±7% (p<0.05).

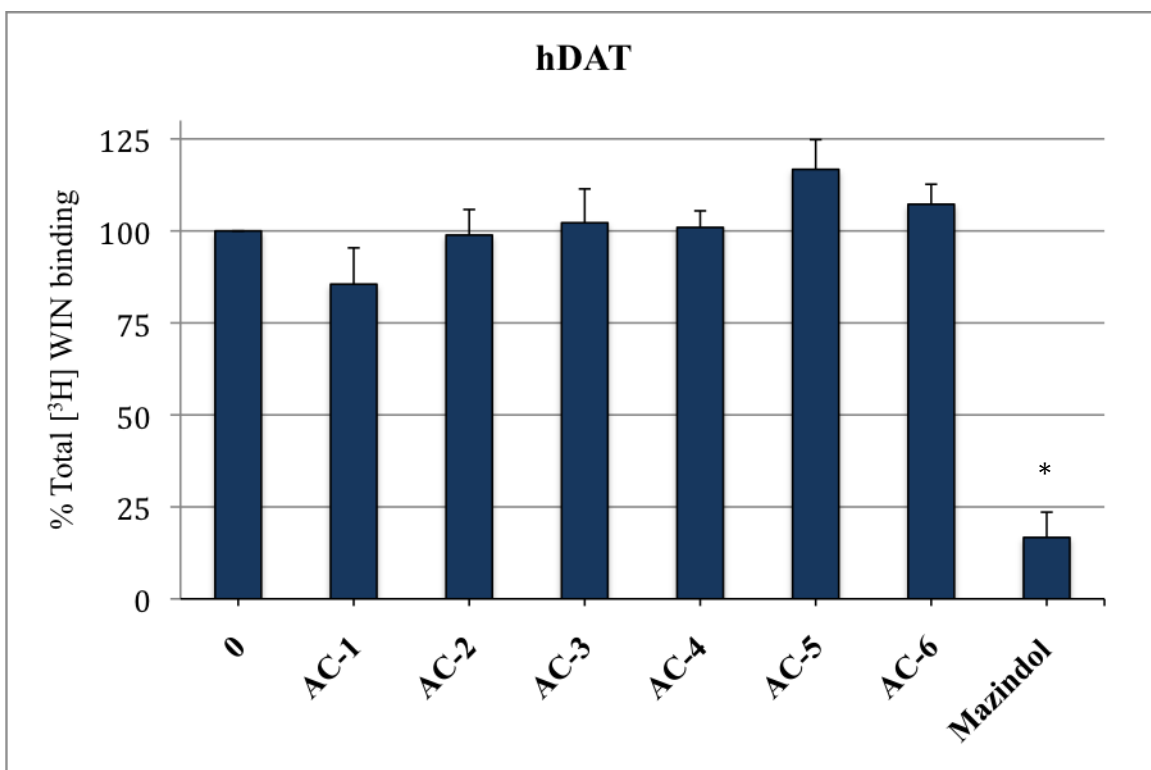


Figure 4.3. VS hit compound one-point screening assay at hDAT. Whole cells of stably transfected hDAT-N2A cell line were used. hDAT binding affinities were obtained by displacement of [³H]-WIN 35,428. All VS compounds were added at a final concentration of 10 μ M. To measure non-specific binding, 10 μ M mazindol was used.

* $p < 0.05$

Chapter 5. Discussion and Future Directions

5.1 Pharmacophore-based Drug Design

The pharmacophore is a valuable concept in rational drug design, defining active molecules that possess particular chemical features and geometry favoring the binding at a specific target (Marriott et al., 1999). However, despite the simplicity of pharmacophoric representations they cannot fully explain the biophysical nature of ligand-protein interactions (Seidel et al., 2010). As such, in the current study, out of the over 800 compounds in the hit database and of the six screened compounds, none showed any significant inhibition at any of the MATs. This is not a surprising result given that the percentage of “hit” compounds found from pharmacophore modeling and virtual screening is typically less than 1% of all compounds screened (Bailey and Brown, 2001; Schneider and Bohm, 2002).

In the present investigation, pharmacophore-based drug design was used to search for novel NET inhibitors. With this method, several problems always arise: How/where to set the boundary between active and inactive compounds? How many so-called *false positives* (biologically inactive compounds falsely disguised as active compounds by matching model features) were present in the hit list, and how many *false negatives* (compounds not matched by pharmacophore query but are able to cause biological activity) were missed in the virtual screen, if only a subset of retrieved hit compounds was tested? (Langer, 2010). The answer to these questions is generally subjective in that each computational biologist may have a different response to such challenges.

An advantage of using a simple pharmacophore model is that it can lead to the discovery of novel lead compounds possessing great structural diversity. For example, each of the six synthesized reagents chosen for pharmacological screening is unique in structural scaffold. Conversely, a potential disadvantage in pharmacophore-based drug design is that because many compounds will be identified as “hits”, there is disagreement as to which criteria to use in selecting compounds for pharmacological testing. In short, there is still much room for research aimed at the improvement of pharmacophore-based methods (Langer, 2010).

In this chapter, a variety of factors affecting the creation of the pharmacophore model, the ranking mechanism of hit compounds and finally, the quality of retrieved hits attained from the virtual screen will be discussed.

5.2 Choosing Training Set Compounds

A challenge lies in the seemingly simple procedure of selecting proper compounds to comprise the training set. In order to avoid analog bias, in which the pharmacophore model tends ignore all compounds different from the single scaffold from which it has been derived, it is important to choose structurally diverse training set compounds. The four training set compounds used in this study were carefully chosen such that they would each be structurally-dissimilar: mazindol, milnacipran, reboxetine and “8d”. Their IUPAC names are listed in Table 5.1

Table 5.1. The four training set compounds and their IUPAC names.

Compound	IUPAC Name
Mazindol	(±)-5-(4-chlorophenyl)-3,5-dihydro-2 <i>H</i> -imidazo[2,1- <i>a</i>]isoindol-5-ol
8d	3 <i>R</i> -(3-fluoro-4-methylphenyl)nortropane-2-carboxylic acid methyl ester (Carroll 2005).
Reboxetine	(<i>R</i> *, <i>R</i> *)-2-[(2-ethoxyphenoxy)-phenyl-methyl]morpholine
Milnacipran	(1 <i>R</i> *,2 <i>S</i> *)-2-(aminomethyl)- <i>N,N</i> -diethyl-1-phenylcyclopropanecarboxamide

Please refer to Table 3.1 for structures.

As can be examined from the names of these compounds, each is of a different chemical scaffold. For example, mazindol contains the “isoindole” group; compound 8d has a tropane moiety; reboxetine contains the morpholine structure; and milnacipran has a cyclopropane carboxamide group.

5.3 Pharmacophore Features

5.3.1 Choosing the Optimal Alignment based on Pharmacophore Features

The alignment in the present study was chosen based on the features MOE developed. A general rule for choosing the features in this investigation was the “one group—one type” policy (Horvath, 2011), meaning that a pharmacophore feature should contain one chemical feature such as “Donor” or “Hydrophobic”, rather than a “one

group—many types” policy such as a “Donor / Hydrophobic” group. The type of chemical features might differ between two queries, but the most specific feature is generally favored (Triballeu et al., 2006). In the current study, when an aromatic ring was deemed an “Aromatic / Hydrophobic” group, it was refined to be more specific as an “Aromatic” group.

Moreover, based on the observations of Horvath, no two authors ever came up with the same set of pharmacophoric queries. While some authors allow atoms to carry more than one pharmacophore “flag” (such as a carboxylate group being both an “anion” and a “hydrogen bond acceptor”), others limit a chemical group to one pharmacophore type (Horvath, 2011). Sanders and colleagues asserted that in order to obtain an optimal binding mode, it is important to select only those features that correlate, or are believed to correlate, with biological activity (Sanders et al., 2012b). Although simply stated, it is quite a difficult task to carry out.

5.3.2 External Volumes

The selectivity of pharmacophores can also be increased by the addition of shape restraints (Sanders et al., 2012b). Greenidge et al. (1998) showed that the number of false positives could be decreased by a factor of 2–5 with the addition of a shape restraint, while the number of true positives remained nearly unchanged. Using a shape restraint often ensures that molecules with many interacting groups can only match the pharmacophore features in a conformation that is complementary to the protein binding site (Sanders et al., 2012b). The generated model in this study included an exterior volume feature in order to make the virtual screen more restrictive. After the addition of

the shape restraint, there was a general reduction in the number of retrieved hits from the virtual screen. Further, when an exterior volume was added in the refinement/validation process the number of inactive compounds retrieved were reduced from three to two.

5.4 Validation Test Set

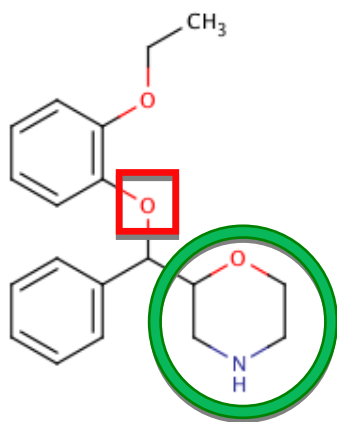
When choosing compounds to comprise the test set, an important point to consider is that they should be chemically different from those comprising the training set. The problem lies in defining “diverse”. If the molecules of the training set are too similar to those of the test set, this aspect of the validation is not very challenging for the model; conversely, if they are too different, there is a risk of depriving the training set of some key SAR (structure activity relation) information. Therefore, molecules kept for the test set should be neither too similar nor too different from training set compounds (Triballeu et al., 2006).

In the present study, the ten compounds comprising the test set (listed in Table 5.2 according to their IUPAC names) were structurally different from the training set compounds, with the exception of compound “3”, a reboxetine analog. Because reboxetine was part of the training set, there is little diversity between it and “3” (Figure 5.1). Based on the above assertion of Triballeu and colleagues, including structurally similar compounds between the training set and the test set may not challenge the model, causing a bias for a particular chemical scaffold and therefore lead to improper validation. If a compound other than the reboxetine analog had been included in the test set, it is likely that different feature characteristics would have evolved from the refinement step, and different hit compounds would have been retrieved. Conversely,

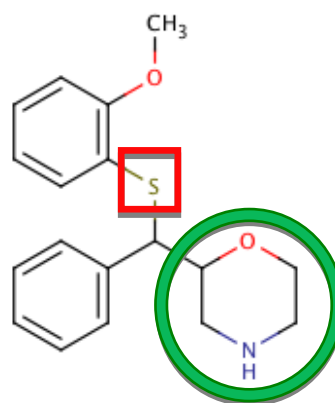
the chemical structures of the training and active test set compounds did not differ greatly as each molecule represents a NET inhibitor and there was no structural information lost. In other words, because the training set compounds were not completely unrelated in terms of structural scaffold, MOE was capable of finding common pharmacophore features among the four compounds without missing a particular chemical moiety.

Table 5.2. IUPAC names of test set compounds. Ten test set compounds included five high-affinity NET inhibitors (atomoxetine, duloxetine, nisoxetine, paroxetine, reboxetine analog “3”) and low-affinity compounds at NET (bupropion, citalopram, sertraline, venlafaxine, zimelidine).

Compound	IUPAC Name
Atomoxetine	(3 <i>R</i>)- <i>N</i> -methyl-3-(2-methylphenoxy)-3-phenylpropan-1-amine; (<i>R</i>)- <i>N</i> -methyl-3-phenyl-3-(<i>o</i> -tolylxy)propan-1-amine
Duloxetine	(+)-(<i>S</i>)- <i>N</i> -Methyl-3-(naphthalen-1-yloxy)-3-(thiophen-2-yl)propan-1-amine
Nisoxetine	(<i>RS</i>)-3-(2-methoxyphenoxy)- <i>N</i> -methyl-3-phenylpropan-1-amine
Paroxetine	(3 <i>S</i> ,4 <i>R</i>)-3-[(2 <i>H</i> -1,3-benzodioxol-5-yloxy)methyl]-4-(4-fluorophenyl)piperidine
“3”	2-([(2-methoxyphenyl)sylfanyl](phenyl)methyl)morpholine
Bupropion	(±)-2-(<i>tert</i> -Butylamino)-1-(3-chlorophenyl)propan-1-one
Citalopram	(<i>RS</i>)-1-[3-(dimethylamino)propyl]-1-(4-fluorophenyl)-1,3-dihydroisobenzofuran-5-carbonitrile
Sertraline	(1 <i>S</i> ,4 <i>S</i>)-4-(3,4-dichlorophenyl)- <i>N</i> -methyl-1,2,3,4-tetrahydronaphthalen-1-amine
Venlafaxine	(<i>RS</i>)-1-[2-dimethylamino-1-(4-methoxyphenyl)-ethyl]cyclohexanol
Zimelidine	<i>Z</i> -3-(4-bromophenyl)- <i>N,N</i> -dimethyl-3-(pyridin-3-yl)prop-2-en-1-amine



Reboxetine



Reboxetine Analog, Compound "3"

Figure 5.1. Comparison of the structures of reboxetine and its analogue, compound "3". Both compounds have the morpholine moiety (green circles). Compound "3" has a thiol group in the place of the oxygen in reboxetine (red squares), and a methylbenzyl moiety replaces the ethylbenzyl moiety.

5.5 Influence of pKa on Pharmacophore Features

A source of pharmacophore error is the presence of several ionizable groups within one molecule, which could influence each other's pKa values (Horvath, 2011). The recent development of a pharmacophore flagging approach based on calculated predictions of pKa values of ionizable groups showed that some structurally similar compounds with diverging activities may be explained by subtle changes in pKa values of ionizable groups (Horvath, 2011) and could ultimately lead to significant changes in acidic/basic species of hit compounds. It is worth noting that in this study the alignment of the four training set compounds revealed the presence of either a donor or acceptor group; choosing one feature over the other was by trial-and-error. The pharmacophore center containing either an acceptor group or a donor group was changed in accordance to the relative number of active and inactive compounds that were retrieved from the test set database. Yet, it would certainly be appealing if a software feature were able to calculate an approximate pKa at these centers, creating a fundamental method for defining how to label a particular pharmacophore group – acceptor, donor, or just “ionizable”.

5.6 Virtual Screening

5.6.1 ZINC Database

In the current study, the ZINC database was used to screen for compounds matching the pharmacophore query. An advantage of using the ZINC database is that it is comprised of over 20 million purchasable compounds from over 150 vendors and

represents the largest database of commercially available compounds for virtual screening (VS). However, a consequence of screening such an extensive molecular database is encountering irrelevant molecules. Despite this disadvantage, the creator of the database, John Irwin, believes that in order to be relevant for research, a database for ligand discovery should be big, and the compounds purchasable and biologically appropriate (i.e., able to bind to the target structure) (Irwin et al., 2012). Further, the aim of the virtual screen is to decrease the enormous number of small molecule candidates to a manageable number of compounds that have the greatest chance of modulating a particular protein target (Tondi et al., 1999). Based on the above assertions, ZINC performs these functions and was deemed an adequate database for use in this investigation.

5.7 Ranking of Hit Compounds

5.7.1 RMSD versus Overlay Methods

In this study an alignment-based (or overlay) method was used to rank hit compounds. Scoring functions are divided into two classes, RMSD-based and overlay-based (Sanders et al., 2012a). In the RMSD-based method, the distance between the feature group of a hit compound and the pharmacophore feature center is calculated. Overlay-based approaches measure how the radii of the pharmacophore features match (or overlay) to the atoms/centers of hit compounds (known as the “S” score). Conversely, RMSD scoring does not consider the feature radii (Sanders et al., 2012a).

While RMSD-based approaches generally return hits due to the high number of poses, overlay-based methods provide the more appropriate biophysical binding mode of hit compounds. Moreover, the stricter criteria of overlay-based methods retrieve the more relevant compounds, as this approach is better at discriminating between active and inactive compounds (Sanders et al., 2012a). Choosing which ranking technique to use for evaluating hit compounds was an area of uncertainty in this project. After conducting searches through the literature, the overlay approach was determined to be the better alternative.

5.7.2 Strain Energy versus Overlay Methods

Another approach to ranking hit compounds involves using strain energy. Here, based on visual inspection, it was found that compounds with strain energies greater than 4 kcal/mol deviated from the alignment of the training set compounds. Thus, during the conformational sampling process all compounds containing strain energies greater than 4 kcal/mol were discarded. Strain energy and the degree of overlap are often conflicting parameters given that energetically-implausible geometric deformations may ultimately align exactly two compounds containing pharmacologically similar groups (Hovarth, 2011). In this work, by discarding compounds with large strain energies, hits containing these geometrical deformations may have been avoided. Therefore, ranking hit compounds based on strain energies could be another useful parameter, with the compounds containing the most favorable strain energies chosen for pharmacological assessment. Although in this study compounds were chosen based on their overlay scores, strain energy is certainly an important ranking criterion.

On the other hand, setting the threshold for which energy values are unacceptable in the screening process is an indefinite approach. Like many other criteria to be decided on in pharmacological-based screening, choosing where to set the limit for acceptable strain energies is subjective and at the discretion of the computational chemist.

5.7.3 Clustering by Chemical Scaffold

Organizing molecules by their chemical scaffolds is another technique for ranking hit compounds. Although in this study maximal overlap with the alignment of the training set compounds was used to sort hits, an interesting approach known as clustering could also have been taken into consideration. If the hit compounds are only analogs of one scaffold and are structurally similar to known biologically active molecules, the results of the virtual screen will not be of interest for further drug development. Clustering of compounds with respect to scaffold represents another important tool for organizing the hit list (Markt et al., 2011). In summary, it appears that a combination of such approaches are likely to result in more diverse active compounds (Sanders et al., 2012b).

5.8 Future Directions

5.8.1 Altering the Training Set

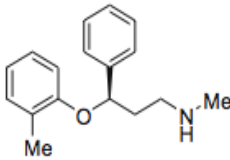
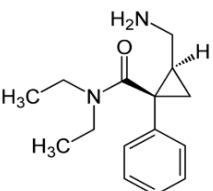
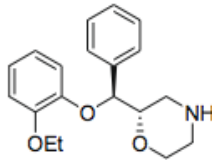
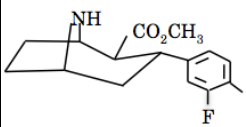
Although none of the purchased six reagents showed any significant activity, only compound AC-1 displayed detectable inhibition of the dopamine transporter (~15%).

This result suggests that the created pharmacophore model, if slightly refined, may prove to be useful in the discovery of active MAT inhibitors. One approach would be to alter the original training set. Perhaps different compounds may generate models consisting of different pharmacophore features. A suggestion for future work would be to choose compounds based on their selectivity at the MATs.

5.8.2 NET-selective TS Compounds

Compound 8d shows a preference for NET but is also quite potent at the other MATs. Similarly, mazindol, though known as a norepinephrine reuptake inhibitor (Kim et al., 2009), is only about 2.5 times more NET-selective relative to SERT and DAT. Milnacipran is NET and SERT selective, with no appreciable DAT activity. Conversely, reboxetine can be considered NET-*specific* (Table 5.3). Therefore, future directions could entail replacing the training set compounds milnacipran, mazindol and 8d with ligands of greater NET-selectivity.

Table 5.3. MAT binding affinities of training set compounds, and the selectivity of each compound relative to NET. Based on literature accounts, the selectivity of each NET inhibitor is shown with SERT relative to NET and DAT relative to NET.

Compound	Binding Affinity, Ki (nM)			Selectivity Ratio	
	hDAT	hSERT	hNET	SERT/NET	DAT/NET
1: Mazindol 	45±1	50±15	18±2	2.8	2.5
2: Milnacipran 	>100,000	8.44±1.57	22±2.58	0.4	4545.5
3: Reboxetine 	>10,000	440	11	40	909.1
4: 8d 	9.0±2.5*	23.8±4.4	0.43±0.02	55.3	N/A

* Values represent IC₅₀ (nM) affinities

1: Houlihan 2002

2: Vaishnavi 2004

3: Bymaster 2002

4: Carroll 2005

5.8.3 Examining Analogs of AC-1

In order to examine whether modest structural modification of the hit compound AC-1 would show greater inhibition at any of the MATs, analogs were built in MOE and ranked according to their “S” scores. Fifteen AC-1 analogs were created (Table 5.4), and conformers for each were generated. The “S” score was calculated for these compounds relative to the original training set molecules. As a result, the structure of the original AC-1 compound exhibited the best “S” score compared to the analogs. Table 5.5 shows all AC-1 analogs with an “S” score of -114 or less. Although none of the AC-1 analogs exhibited a better “S” score than the original compound, this could be a useful method in studying how altering structural substituents can change a particular score and possibly lead to a different percent inhibition at a protein target.

Table 5.4. Analogs of compound AC-1. Analogs were created computationally and assessed for their overlay scores.

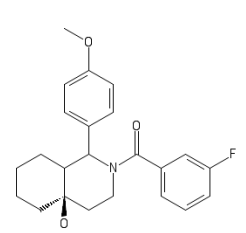
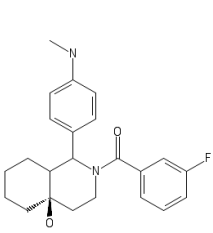
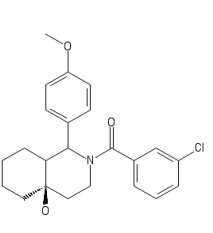
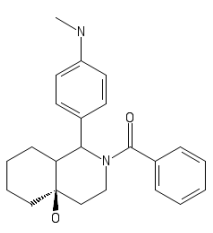
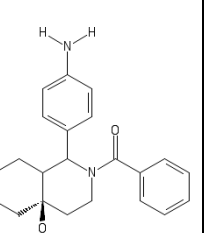
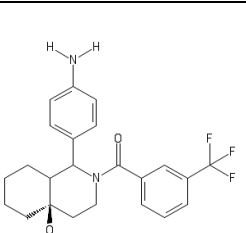
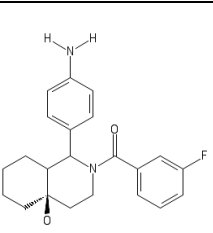
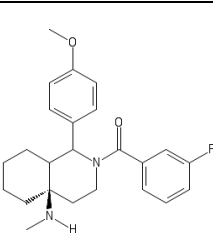
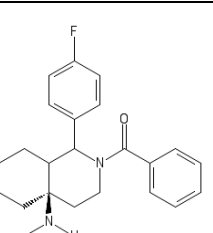
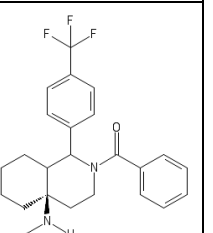
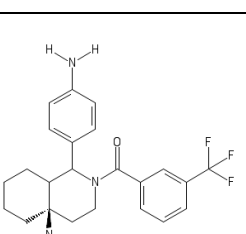
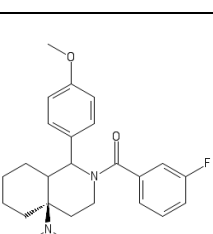
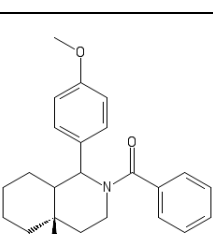
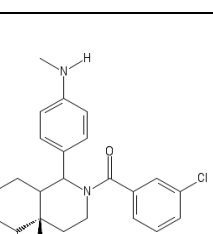
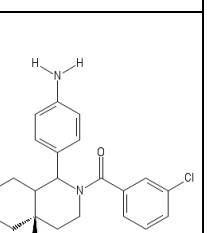
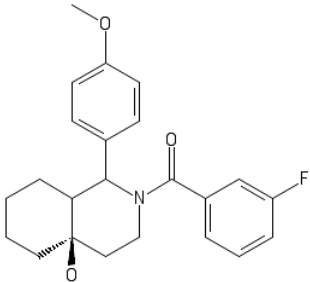
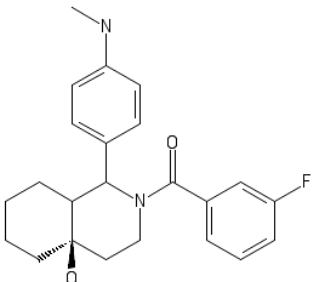
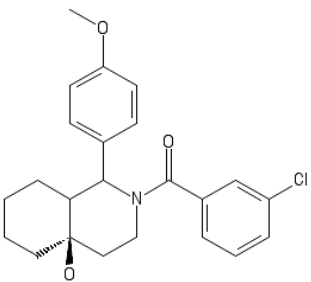
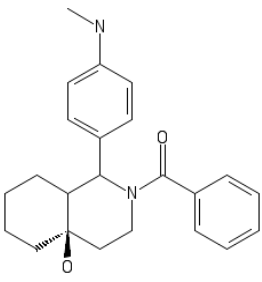
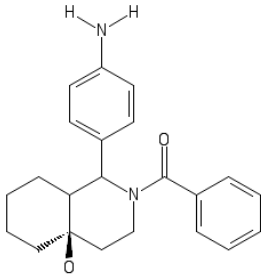
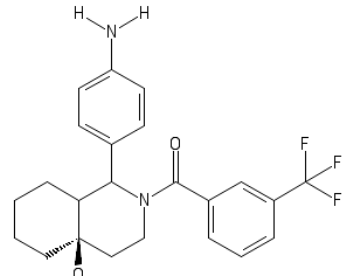
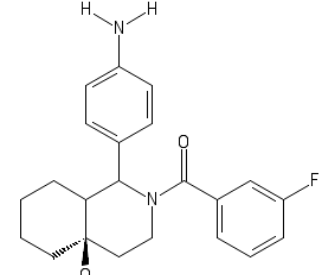
AC-1 Analogs				
				
AC-1	AC-10	AC-11	AC-12	AC-13
				
AC-14	AC-15	AC-16	AC-17	AC-18
				
AC-19	AC-20	AC-21	AC-22	AC-23

Table 5.5. Analogs of AC-1 with an “S” score better than -114.

Structure	“S” Score
<p>AC-1</p> 	-116
<p>AC-10</p> 	-116
<p>AC-11</p> 	-116
<p>AC-12</p> 	-115

<p>AC-13</p> 	<p>-115</p>
<p>AC-14</p> 	<p>-115</p>
<p>AC-15</p> 	<p>-115</p>

5.8.4 Amine groups in CNS Drugs

The majority of CNS-active drugs tend to have a basic nitrogen located approximately 5 Å from an aromatic ring (Guner, 2005). It was, therefore, interesting to examine the distances between the same features of the model in the present investigation. To measure the distances, the AC-1 analog AC-10 was aligned with the refined pharmacophore query (Figure 5.2). The rationale for using AC-10 rather than AC-1 was that because the methoxy group of AC-1 was changed to a methylamine group to become compound AC-10, it was important to understand where the donor group would position itself on AC-10. Alteration of the methoxy group did not change the

orientation of the donor group, which remained aligned with the isoquinolinol hydroxyl group. Despite this, based on Figure 5.2, the distances between the aromatic groups and the donor group are approximately 5 Å, or 5.67 Å and 4.27 Å to be exact. If the alcohol group were to be converted to an amine, it would meet the above criterion: to contain a basic nitrogen about 5 Å from an aromatic feature. In Table 1, it could be detected that such a structure was created, but because its “S” score value was lower than expected, it was not considered. In view of the fact that the “S” score is not an exact measure of activity, future directions could certainly entail synthesizing such an analog and testing it *in vitro* at the MATs.

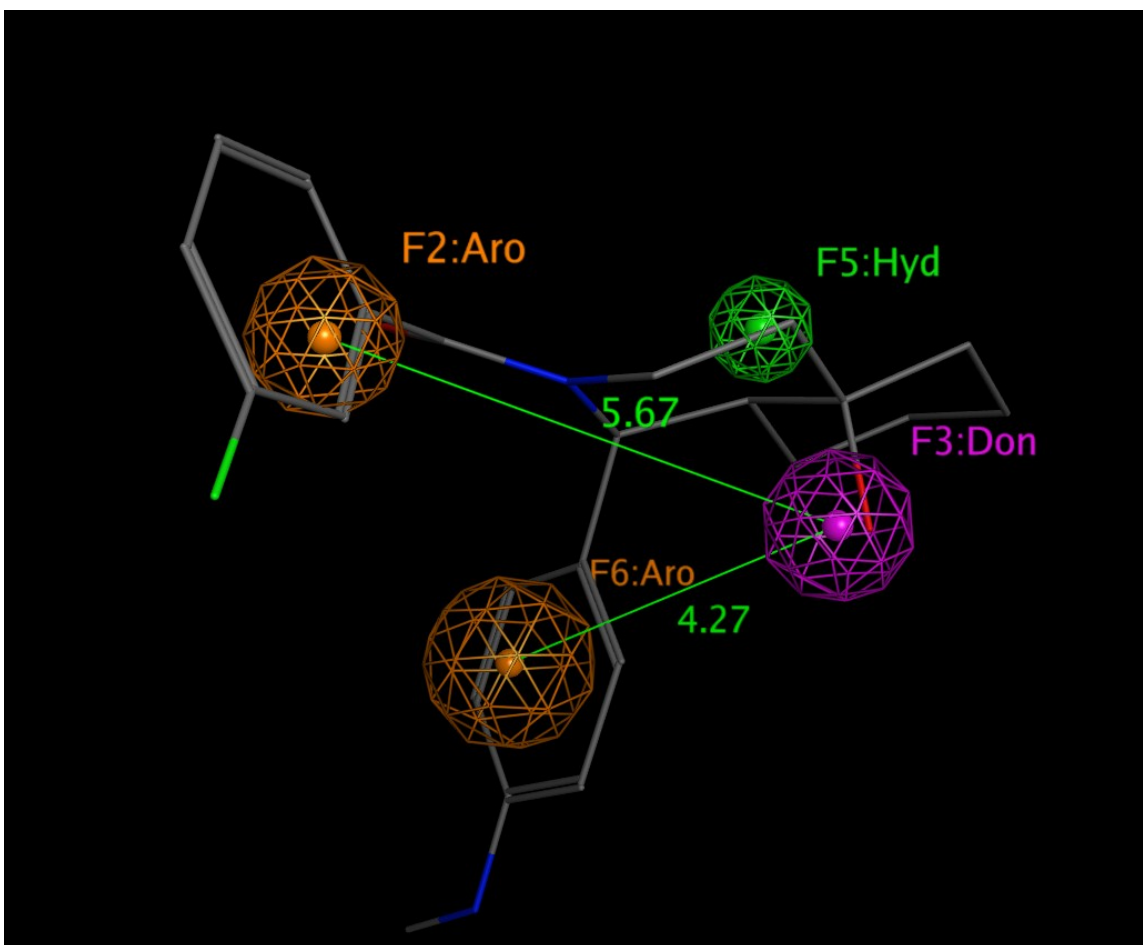


Figure 5.2. Compound AC-10 demonstrating the distances in Angstroms from the donor feature to the two aromatic features. The distance from the donor group to the F2 aromatic group is 5.67 Å; the distance from the donor group to the F6 aromatic group is 4.27 Å. Both values are close to 5 Å, indicating that if the alcohol group in the isoquinolinol moiety were to be converted to a basic amine, there is great potential for this compound to be active at the MATs.

5.8.5 Revision to Pharmacophore Model

Because the synthesized compounds (AC-1 – AC-6) did not show any significant inhibition at any of the MATs, it was interesting to examine what effect altering the pharmacophore model would have on the hit compounds. As mentioned in the computational chapter, a validation test set containing five active and five inactive compounds at the NET was used to confirm that the created model was functional. The generated model selected all five actives and one inactive, sertraline. Yet, there was no *internal validation* performed. With internal validation a database of compounds is created containing conformations of the original training set compounds. Therefore, this approach examines whether a pharmacophore model could pick out training set compounds. The model selected only one training set compound. This is a logical outcome given that the pharmacophore features were based on the alignment of the training set compounds but were refined from their original states. Thus, it was interesting to explore which features were necessary to return to their original forms in order to retrieve all four training set compounds.

As in the previous query modification, each feature was systematically altered one at a time until the original compounds were returned. The first step involved changing the aromatic feature (the larger of the two aromatic features) back to its original form, “Aro|Hyd”. From this change, milnacipran and reboxetine were selected. Therefore, this change was retained. Two more of the TS compounds still needed to be retrieved: reboxetine and 8d. Changing the radius of the 0.89 Å “Aro|Hyd” feature back to the original 1.55 Å did not increase the number of retrieved TS compounds, so the radius was returned to 0.89 Å. Both of the PiN features were then included one at a time, which did

not retrieve any of the TS compounds, and were again removed. The hydrophobic feature was then changed back from its small radius of 0.55 Å to 1.41 Å. This modification produced no change, as milnacipran and reboxetine were still the only two training set compounds retrieved.

When the exterior volume feature was ignored, milnacipran and reboxetine were again selected, but not mazindol or 8d. As changing the “Aro” back to “Aro|Hyd” produced the effect of retrieving milnacipran and reboxetine, the exterior volume remained part of the model.

The next step was to vary the donor feature, which was initially an acceptor feature. Switching “Don” to “Acc” retrieved two of the TS compounds, only this time reboxetine and mazindol were retrieved. Thus, this change was implemented. Next, it was interesting to revisit previous alterations, but with the acceptor feature replacing the donor feature. When the hydrophobic feature radius was changed back to its original 1.41 Å, all of the TS compounds were selected.

As a result, it was necessary for three features to be returned to their original state: the “Aro” feature previously found between the PiNs was changed back to “Aro|Hyd”, the “Hyd” feature radius was again 1.41 Å, and the “Don” feature was changed back to “Acc”. These changes also retrieved one active compound (#3) and two inactives (venlafaxine and zimelidine). For future work, some additional refinement may be necessary for the model in order for it to select more active and less inactive compounds, while still selecting all four TS compounds.

From these results, it appeared as if the hydrophobic feature was a major factor contributing to which TS compounds were retrieved. Small increments of change to its

radius were experimented with to determine which test set compounds would be selected. It was found that decreasing the “Hyd” radius to 1 Å from 1.41 Å retrieved all four TS compounds: one active compound (3), and this time, only one inactive (venlafaxine). But considering that venlafaxine is moderately inactive at NET (approximately 3 μM; (Tsuruda et al., 2010)), it was deemed acceptable that the new “semirefined” model selected it. The new model is illustrated in Figure 5.3.

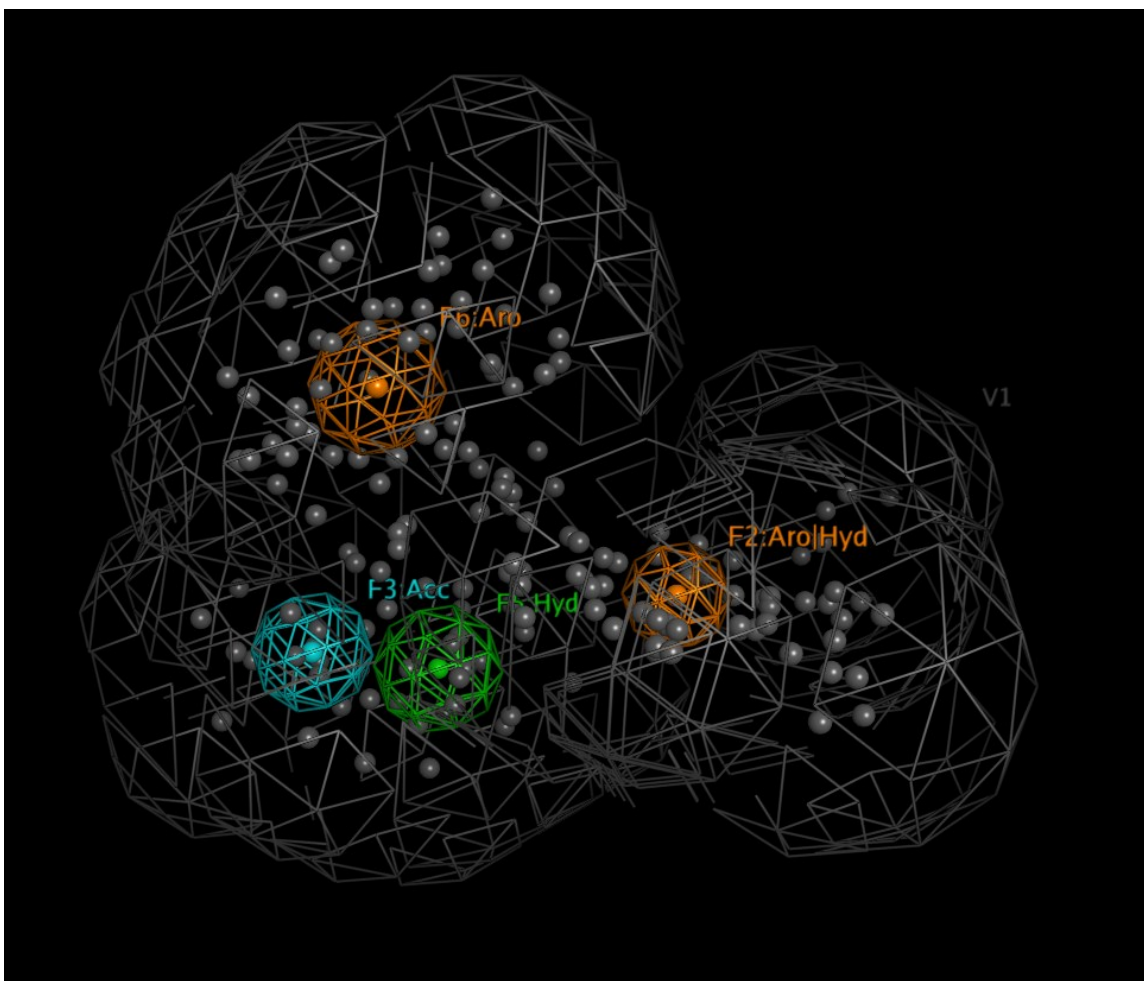
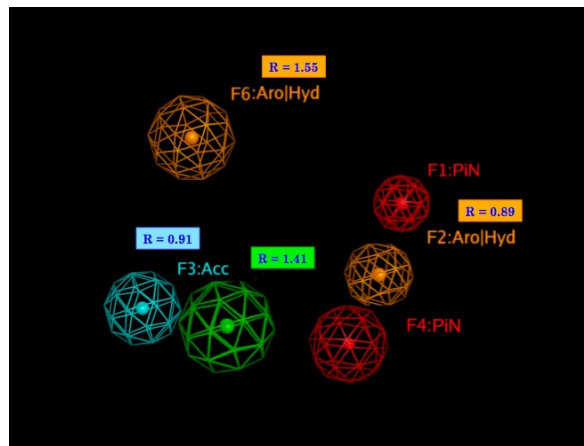


Figure 5.3. Semi-refined model. Several features were restored to the original model in such a way that the original training set compounds would be selected. The aromatic (Aro) as well as the aromatic / hydrophobic (Aro|Hyd) features are both shown in orange; the hydrophobic (Hyd) feature is shown in green; the acceptor (Acc) feature is shown in cyan. The exterior volume is represented by gray netting around the accessible area of the training set compounds (not shown). The small gray spheres represent pharmacophore annotation points.

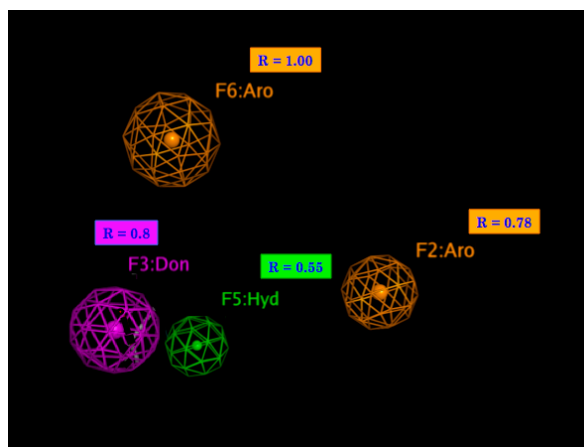
A comparison of the three models including the original pharmacophore query, the refined query and the “semi-refined” query, described above, is shown in Figure 5.4. The features in the original pharmacophore query (Figure 5.4a) were refined to create the “refined query” (Figure 5.4b) by changing several pharmacophore features. The “Aro|Hyd” features was changed to “Aro” features. The radius was decreased from 1.55 Å to 1.00 Å and from 0.89 Å to 0.78 Å in the F6 “Aro|Hyd” and F2 “Aro|Hyd” features, respectively. The PiN features became ignored in the refined query; the “Hyd” feature radius was decreased from 1.41 Å to 0.55 Å; the acceptor feature was amended to become a donor feature and its radius decreased from 0.91 Å to 0.80 Å. An exterior volume feature was also added to the refined query (shown in Figure 3.4) with a radius of 2.14 Å.

Several features in the refined query were returned to their original states, generating the semi-refined query (Figure 5.4c). Feature F2 was changed from “Aro” in the refined query (Figure 5.4b) back to “Aro|Hyd” while keeping the radius constant; the “Hyd” feature radius was increased from 0.55 Å to become 1.00 Å; the “Don” feature and its radius was changed back to its original state to become “Acc” with a radius of 0.91 Å; the exterior volume and its radius were not changed.

(a)



(b)



(c)

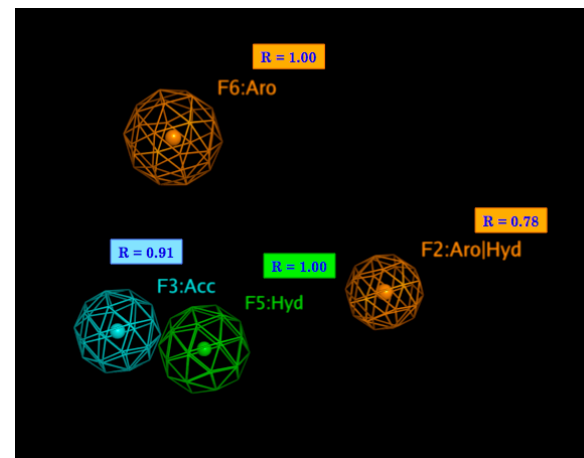


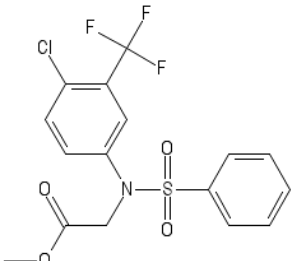
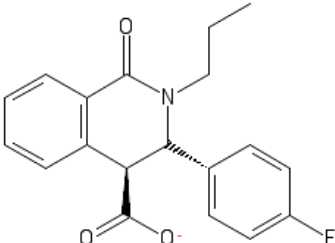
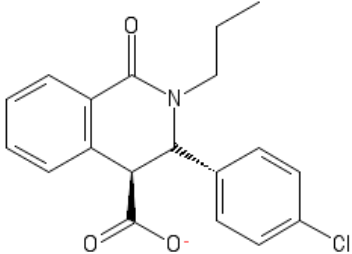
Figure 5.4. Comparison of three generated pharmacophore models. The original query (a), refined query (b) and semi-refined query (c).

5.8.6 Rescreening the ZINC Database

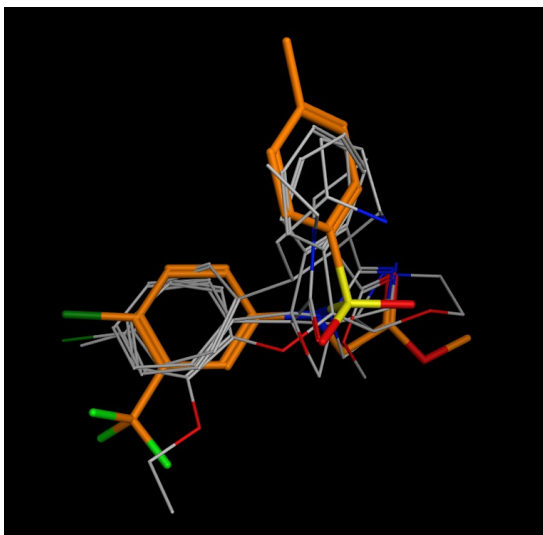
The ZINC database was rescreened with the newly-refined pharmacophore query, and the “S” score svl code was reentered into MOE in order to rank the new hits. This time the score appeared to be better than for the previous screen. The numbers were significantly smaller, with the best score being -120, compared to -116 seen with AC-1, the best score attained in the previous screen. This time, all hits with an “S” score greater than -115 were discarded from the output database. As a result, there were 73 new hits that appeared to overlay better to the original training set alignment than previously. The top hits, with “S” scores of -120 and -119 are shown in Table 5.6 and as overlays to the original training set alignments in Figure 5.5. If visually compared to the AC-1 hit, shown in Figure 5.6, compounds, AC-7 and AC-8, align significantly better to the original training set alignment. Future research could include synthesizing these three compounds and pharmacologically assessing them at the three MATs.

Table 5.6. Structures and “S” Scores of the top three new hit compounds.

Compounds AC-7, AC-8 and AC-9 were retrieved from a second virtual screen using the semi-refined pharmacophore model.

Structure	“S” Score
<p data-bbox="250 506 321 537">AC-7</p> 	-120
<p data-bbox="250 810 321 842">AC-8</p> 	-119
<p data-bbox="250 1115 321 1146">AC-9</p> 	-119

(a)



(b)

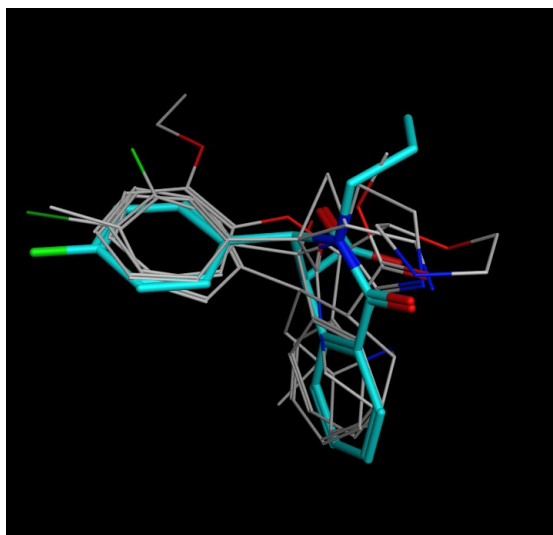


Figure 5.5. Overlay of top new hits from the semi-refined query to the alignment of the original training set compounds. Compound AC-7, shown in orange (a), generated an “S” score of -120; compound AC-8, in cyan (b), produced an “S” score of -119.



Figure 5.6. Overlay of AC-1 to the original training set alignment. AC-1 is shown in orange, with an “S” score of -116. By visual inspection, it can be seen that AC-1 aligns poorly to the training set compounds as compared to AC-7 and AC-8 (Figure 5.5).

As another internal control to determine whether the deviations in “S” score are representative of good or poor overlays, it was interesting to examine what the worst “S” score overlay would look like. Figure 5.7 illustrates the compound AC-0 with an “S” score of -88 overlaid on the training set alignment. It is clear that there is a poor correlation to the original alignment. From these results, it can be concluded that the higher the “S” score, the better the alignment and therefore, the more potential for a hit compound to show activity at the NET.

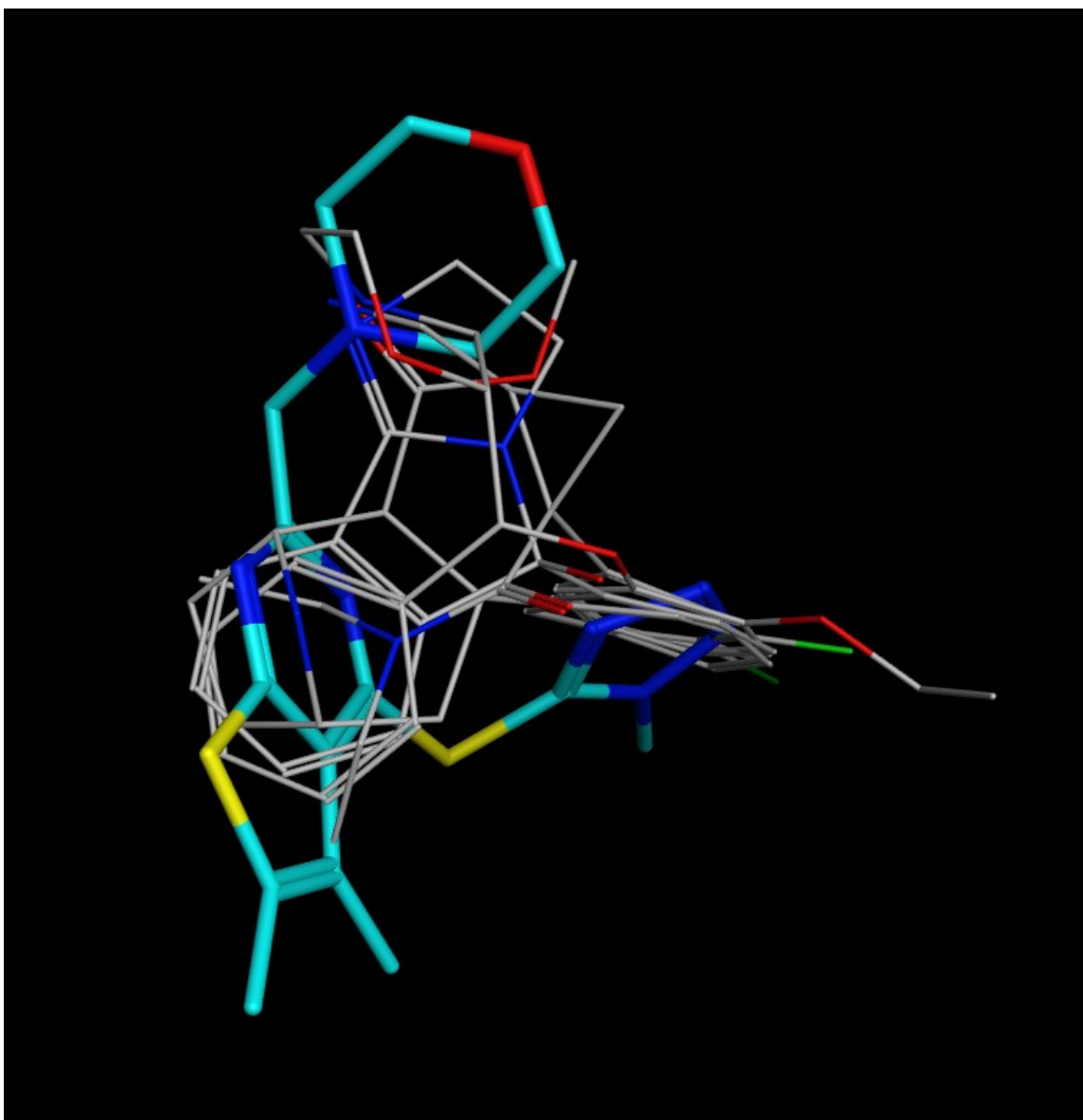


Figure 5.7. Illustration of poorest alignment. Compound AC-0 has an “S” score of -88 and is illustrated overlaying the training set alignment. It can be seen that there is a generally poor alignment between AC-0 and the four active set compounds, and it is defined by having a poor overlay score.

5.8.7 Selecting Compounds Based on RMSD versus Overlay Score

Another approach for future work would be to choose several top-ranking compounds having the best overlay, or “S” score, as well as several compounds exhibiting the best (or lowest) RMSD score for pharmacological studies. Rather than solely choosing hits by their overlay score, as in this study, it may be possible to determine which ranking criteria are most helpful in selecting compounds for competition binding assays. Further, it may also be possible to select compounds based on the combination of RMSD value and “S” score. In the second virtual screen, all hits having an “S” score greater than -115 were discarded, leaving 73 compounds to choose from, with scores ranging from -115.00 to -120 . Among these compounds the RMSD score ranged from 0.299 Å to 0.751 Å. Given that all of these 73 compounds exhibited good alignment to the training set compounds, it may be beneficial to choose compounds with a relatively lower RMSD score. Interestingly, the top three hits (AC-7, AC-8 and AC-9) all have relatively lower RMSD scores, ranging from 0.419 Å to 0.494 Å. Therefore, these three compounds show great potential at inhibiting any of the MATs.

5.8.8 Unique structure of hit compounds

Heterocyclic compounds, particularly nitrogen heterocycles, are a valuable class of compounds in the pharmaceutical industry and consist of about 60% of all drug substances. In particular, the tetrahydroisoquinoline ring structure is a chemical scaffold common to many biologically active natural products and pharmacologically relevant therapeutic agents (Sridharan et al., 2011). The structures of AC-1, AC-8 and AC-9 all contain the isoquinoline scaffold. Isoquinoline is one of the most broadly distributed

alkaloids with established therapeutic benefit. Their development as effective therapeutics is an area of continued study (Bhadra and Kumar, 2011).

5.8.9 Refining the Structure of New Hit Compounds

Based on the review by Guner (2005) regarding active CNS drugs containing a basic amine group located about 5 Å from an aromatic pharmacophore group, it may be constructive to refine the structure of new hit compound AC-7 accordingly. As seen in Figure 5.2 with compound AC-10, the distances from the aromatic groups to the donor group (Figure 5.2) or the acceptor group (Figure 5.8) are the same given that the spatial orientation of the pharmacophore features in the semirefined model were not changed. In Figure 5.8, compound AC-7 is overlaid with the semirefined query. The acceptor group is located on the carboxylic acid. However, if this substituent were to be replaced with a basic amine group, it would be located ~ 5 Å from an aromatic group. Therefore, by making structural changes to compound AC-7 it may lead to an active drug at the MATs.

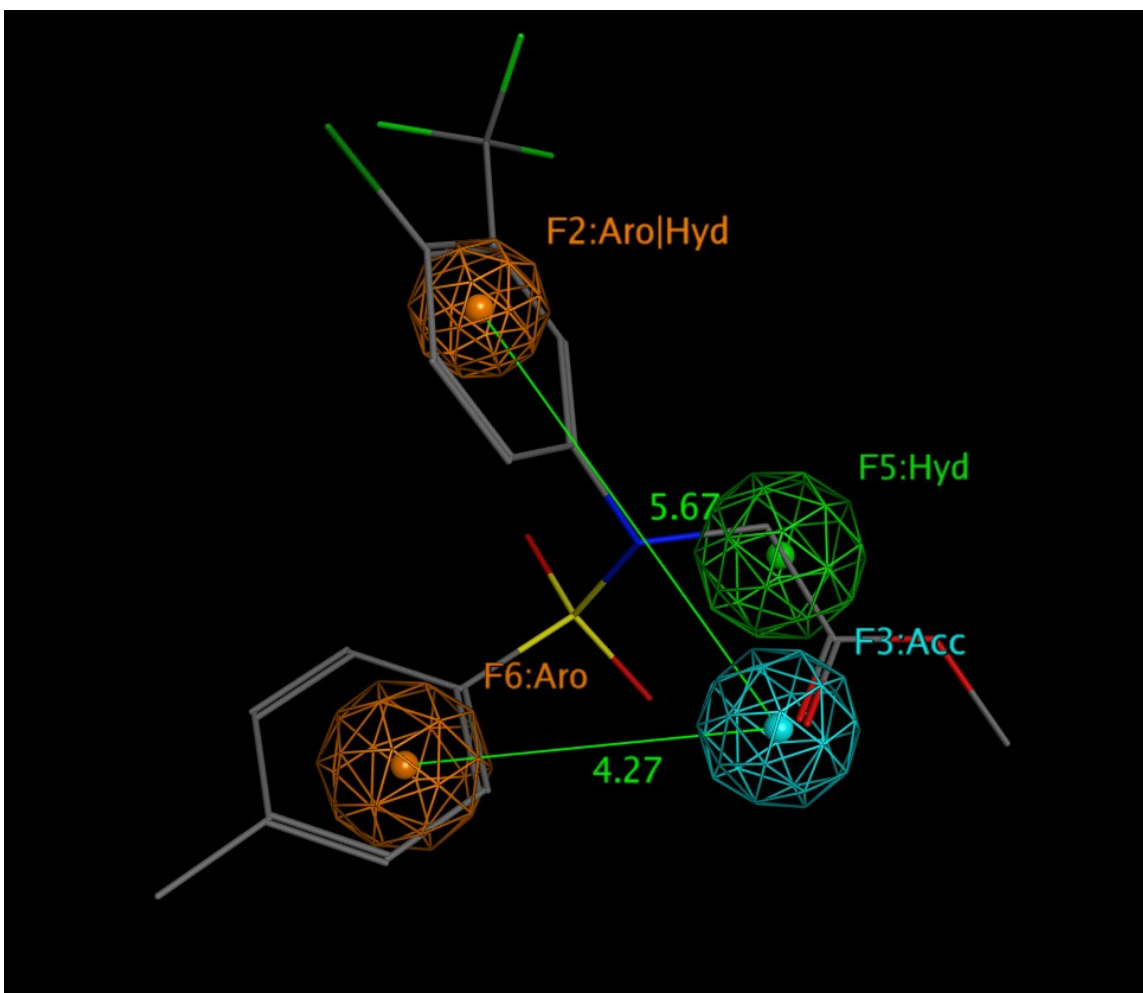


Figure 5.8. Compound AC-7 demonstrating the distances in Angstroms from the acceptor feature to the two aromatic features. The distance from the acceptor group to the F2 “Aro|Hyd” group is 5.67 Å; the distance from the acceptor group to the F6 aromatic group is 4.27 Å. Both values are close to 5 Å, indicating that if the ester group were to be converted to a basic amine, there is potential for this compound to be active at the MATs.

5.9 Conclusion

Computational chemistry and structural biology are playing a progressively more significant role in drug discovery. Pharmacophore-based drug design can present a preliminary representation of the different aspects involved in the binding interactions between a ligand and its receptor protein. Using this information, chemists could rationally design molecules with specific chemical characteristics necessary for the proper interaction to a binding site (Wang and Lewis, 2010). Yet, pharmacophore modeling is not based on a fundamental theory, and, as such, is intrinsically error-prone (Horvath, 2011). Despite the prosperity of pharmacophore techniques there is room for improvement, such in the creation of more optimal pharmacophore models.

In regard to choosing the proper approach for the creation, alignment or ranking of the pharmacophore model, the “best” pharmacophore scheme is the one maximizing the retrieval of active and minimizing the retrieval of inactive hit compounds. In the end, it is less important to understand whether one method is slightly “better” than another, statistically speaking, rather which approach can lead to biologically relevant hits. (Horvath, 2011).

In this investigation, although none of the tested hit compounds showed significant inhibition at any of the MATs, the new hits attained with the “semirefined” model show potential as novel MAT inhibitors since they have a better overall alignment to the original training set compounds, as demonstrated by their higher overlay score. Furthermore, using a combination of ranking criteria may prove to be beneficial in selecting hit compounds from a pharmacophore-based virtual screening study. In the present study, the new hits (AC-7 – AC-9) exhibit the best overlay to the original training

set compounds and also have relatively low RMSD values. Future directions could entail synthesizing and evaluating compounds AC-7, AC-8 and AC-9 with in vitro pharmacology, to attain their activity profiles at the monoamine transporters.

Considering the difficulties involved in attaining protein target information, ligand-based drug design approaches are anticipated to have a significant impact on drug design in the near future (Tropsha and Wang, 2006; Costanzi et al., 2009). In summary, the pharmacophore concept has truly stood the test of time and is likely to play an important role in drug development for years to come (Langer, 2010).

References

- Andersen, J., Kristensen, A. S., Bang-Andersen, B., and Stromgaard, K. (2009). Recent advances in the understanding of the interaction of antidepressant drugs with serotonin and norepinephrine transporters. [Research Support, Non-U.S. Gov't Review]. *Chemical Communications* (25), 3677-3692.
- Andersen, J., Stuhr-Hansen, N., Zachariassen, L., Toubro, S., Hansen, S. M., Eildal, J. N., et al. (2011). Molecular determinants for selective recognition of antidepressants in the human serotonin and norepinephrine transporters. *Proceedings of the National Academy of Sciences of the United States of America*, 108(29), 12137-12142.
- Anderson, I. M. (2000). Selective serotonin reuptake inhibitors versus tricyclic antidepressants: a meta-analysis of efficacy and tolerability. [Comparative Study Meta-Analysis]. *Journal of Affective Disorders*, 58(1), 19-36.
- Axelrod, J. (1974) Regulation of the neurotransmitter norepinephrine in The Neurosciences. Third Study Program. F.O Schmitt, F.G Worden, eds., MIT Press, Cambridge, 863-76.
- Azima, H., and Vispo, R. H. (1958). Imipramine; a potent new anti-depressant compound. *The American Journal of Psychiatry*, 115(3), 245-246.
- Bailey, D., and Brown, D. (2001). High-throughput chemistry and structure-based design: survival of the smartest. *Drug Discovery Today*, 6(2), 57-59.
- Beer, M., Hacker, S., Poat, J., and Stahl, S. M. (1987). Independent regulation of beta 1-

- and beta 2-adrenoceptors. [In Vitro]. *British Journal of Pharmacology*, 92(4), 827-834.
- Beuming, T., Shi, L., Javitch, J. A., and Weinstein, H. (2006). A comprehensive structure-based alignment of prokaryotic and eukaryotic neurotransmitter/Na⁺ symporters (NSS) aids in the use of the LeuT structure to probe NSS structure and function. [Research Support, N.I.H., Extramural]. *Molecular Pharmacology*, 70(5), 1630-1642.
- Bhadra, K., and Kumar, G. S. (2011). Therapeutic potential of nucleic acid-binding isoquinoline alkaloids: binding aspects and implications for drug design. [Research Support, Non-U.S. Gov't Review]. *Medicinal Research Reviews*, 31(6), 821-862.
- Bielska, E.; Lucas, X.; Czerwoniec, A.; Kasprzak, J.M.; Kaminska, K.H. and Bujnicki, J.M. (2011) Virtual screening strategies in drug design – methods and applications. *Jour of Biotech, Comp Biol and Bionanotech*, 92, 249-264.
- Bonisch, H., and Bruss, M. (2006). The norepinephrine transporter in physiology and disease. [Review]. *Handbook of Experimental Pharmacology* (175), 485-524.
- Boschmann, M., Schroeder, C., Christensen, N. J., Tank, J., Krupp, G., Biaggioni, I., et al. (2002). Norepinephrine transporter function and autonomic control of metabolism. [Clinical Trial Randomized Controlled Trial Research Support, Non-U.S. Gov't]. *The Journal of Clinical Endocrinology and Metabolism*, 87(11), 5130-5137.
- Boyer, E. W., and Shannon, M. (2005). The serotonin syndrome. [Research Support, U.S. Gov't, P.H.S. Review]. *The New England Journal of Medicine*, 352(11), 1112-

1120.

- Brown, A. S., and Gershon, S. (1993). Dopamine and depression. [Review]. *Journal of Neural Transmission*, General section, *91*(2-3), 75-109.
- Bylund, D. B., Eikenberg, D. C., Hieble, J. P., Langer, S. Z., Lefkowitz, R. J., Minneman, K. P., et al. (1994). International Union of Pharmacology nomenclature of adrenoceptors. [Review]. *Pharmacological Reviews*, *46*(2), 121-136.
- Bymaster, F. P., Dreshfield-Ahmad, L. J., Threlkeld, P. G., Shaw, J. L., Thompson, L., Nelson, D. L., et al. (2001). Comparative affinity of duloxetine and venlafaxine for serotonin and norepinephrine transporters in vitro and in vivo, human serotonin receptor subtypes, and other neuronal receptors. [Comparative Study]. *Neuropsychopharmacology : Official Publication of the American College of Neuropsychopharmacology*, *25*(6), 871-880.
- Bymaster, F. P., Katner, J. S., Nelson, D. L., Hemrick-Luecke, S. K., Threlkeld, P. G., Heiligenstein, J. H., et al. (2002). Atomoxetine increases extracellular levels of norepinephrine and dopamine in prefrontal cortex of rat: a potential mechanism for efficacy in attention deficit/hyperactivity disorder. *Neuropsychopharmacology: Official Publication of the American College of Neuropsychopharmacology*, *27*(5), 699-711.
- Carroll, F. I., Tyagi, S., Blough, B. E., Kuhar, M. J., and Navarro, H. A. (2005). Synthesis and monoamine transporter binding properties of 3alpha-(substituted phenyl)nortropine-2beta-carboxylic acid methyl esters. Norepinephrine transporter selective compounds. [In Vitro Research Support, N.I.H., Extramural

- Research Support, U.S. Gov't, P.H.S.]. *Journal of Medicinal Chemistry*, 48(11), 3852-3857.
- Chan, S. L., and Labute, P. (2010). Training a scoring function for the alignment of small molecules. *Journal of Chemical Information and Modeling*, 50(9), 1724-1735.
- Chen, N. H., Reith, M. E., and Quick, M. W. (2004). Synaptic uptake and beyond: the sodium- and chloride-dependent neurotransmitter transporter family SLC6. [Research Support, U.S. Gov't, P.H.S. Review]. *Pflugers Archiv : European Journal of Physiology*, 447(5), 519-531.
- Cooper, J.R.; Bloom, F.E.; Roth, R.H. (2003) The biochemical basis of neuropharmacology. Vol. 8. Oxford University Press; Oxford; New York.
- Costanzi, S., Tikhonova, I. G., Harden, T. K., and Jacobson, K. A. (2009). Ligand and structure-based methodologies for the prediction of the activity of G protein-coupled receptor ligands. [Research Support, N.I.H., Intramural]. *Journal of Computer-Aided Molecular Design*, 23(11), 747-754.
- Crassous, P. A., Denis, C., Paris, H., and Senard, J. M. (2007). Interest of alpha2-adrenergic agonists and antagonists in clinical practice: background, facts and perspectives. [Review]. *Current Topics in Medicinal Chemistry*, 7(2), 187-194.
- Dash, R. C., Bhosale, S. H., Shelke, S. M., Suryawanshi, M. R., Kanhed, A. M., and Mahadik, K. R. (2012). Scaffold hopping for identification of novel D(2) antagonist based on 3D pharmacophore modelling of iloperidone analogs. [Research Support, Non-U.S. Gov't]. *Molecular Diversity*, 16(2), 367-375.
- Dostert, P. L., Strolin Benedetti, M., and Tipton, K. F. (1989). Interactions of monoamine

- oxidase with substrates and inhibitors. [Research Support, Non-U.S. Gov't Review]. *Medicinal Research Reviews*, 9(1), 45-89.
- Drews, J. (2000). Drug discovery: a historical perspective. [Historical Article Portraits]. *Science*, 287(5460), 1960-1964.
- Duman, R. S., and Monteggia, L. M. (2006). A neurotrophic model for stress-related mood disorders. [Research Support, U.S. Gov't, Non-P.H.S. Research Support, U.S. Gov't, P.H.S. Review]. *Biological Psychiatry*, 59(12), 1116-1127.
- Ehrlich, P., (1909) Über den jetzigen Stand der Chemotherapie. *Dtsch. Chem. Ges.*, 42, 17-47.
- Eshleman, A.J., Carmolli, M., Cumbay, M., Martens, C.R., Neve, K.A., and Janowsky, A. (1999) Characteristics of drug interactions with recombinant biogenic amine transporters expressed in the same cell type [Research Support, Non-U.S. Gov't Research Support, U.S. Gov't, Non-P.H.S. Research Support, U.S. Gov't, P.H.S.]. *The Journal of Pharmacology and Experimental Therapeutics*, 289(2), 877-885.
- Esposito, E.X., Hopfinger, A.J., and Madura, J.D. (2004) Methods for applying the quantitative structure-activity paradigm in Chemoinformatics: Concepts, Methods, and Tools for Drug Discovery, J. Bajorath, ed., Humana Press Inc., Totowa, NJ.
- Evers, A., Hessler, G., Matter, H., and Klabunde, T. (2005). Virtual screening of biogenic amine-binding G-protein coupled receptors: comparative evaluation of protein- and ligand-based virtual screening protocols. [Comparative Study Evaluation Studies]. *Journal of Medicinal Chemistry*, 48(17), 5448-5465.
- Gasteiger, J. and Engel, T. (2003) Chemoinformatics. Wiley-VCH: Weinheim.

- Gillman, P. K. (2007). Tricyclic antidepressant pharmacology and therapeutic drug interactions updated. [Comparative Study Review]. *British Journal of Pharmacology*, 151(6), 737-748.
- Gould, G. G., Pardon, M. C., Morilak, D. A., and Frazer, A. (2003). Regulatory effects of reboxetine treatment alone, or following paroxetine treatment, on brain noradrenergic and serotonergic systems. [Comparative Study Research Support, Non-U.S. Gov't Research Support, U.S. Gov't, P.H.S.]. *Neuropsychopharmacology : Official Publication of the American College of Neuropsychopharmacology*, 28(9), 1633-1641.
- Gund, P. (1977) Three-dimensional Pharmacophoric Pattern Searching. *Prog Mol Subcell Biol*, 11, 117–143.
- Guner, O.F. (2000) Pharmacophore perception, development, and use in drug design. Int. Univ. Line.
- Guner, O. F. (2002). History and evolution of the pharmacophore concept in computer-aided drug design. [Historical Article Review]. *Current Topics in Medicinal Chemistry*, 2(12), 1321-1332.
- Guner, O. F. (2005). The impact of pharmacophore modeling in drug design. [Review]. *IDrugs : the Investigational Drugs Journal*, 8(7), 567-572.
- Haenisch, B., and Bonisch, H. (2011). Depression and antidepressants: insights from knockout of dopamine, serotonin or noradrenaline re-uptake transporters. [Review]. *Pharmacology & Therapeutics*, 129(3), 352-368.
- Hahn, M. K., and Blakely, R. D. (2007). The functional impact of SLC6 transporter genetic variation. [Research Support, N.I.H., Extramural Review]. *Annual Review*

- of Pharmacology and Toxicology*, 47, 401-441.
- Heffernan, G. D., Coghlan, R. D., Manas, E. S., McDevitt, R. E., Li, Y., Mahaney, P. E., et al. (2009). Dual acting norepinephrine reuptake inhibitors and 5-HT(2A) receptor antagonists: Identification, synthesis and activity of novel 4-aminoethyl-3-(phenylsulfonyl)-1H-indoles. *Bioorganic & Medicinal Chemistry*, 17(22), 7802-7815.
- Hoglund, P. J., Adzic, D., Scicluna, S. J., Lindblom, J., and Fredriksson, R. (2005). The repertoire of solute carriers of family 6: identification of new human and rodent genes. [Research Support, Non-U.S. Gov't]. *Biochemical and Biophysical Research Communications*, 336(1), 175-189.
- Horvath, D. (2011). Pharmacophore-based virtual screening. [Review]. *Methods in Molecular Biology*, 672, 261-298.
- Houlihan, W. J., Kelly, L., Pankuch, J., Koletar, J., Brand, L., Janowsky, A., et al. (2002). Mazindol analogues as potential inhibitors of the cocaine binding site at the dopamine transporter. [In Vitro Research Support, U.S. Gov't, P.H.S.]. *Journal of Medicinal Chemistry*, 45(19), 4097-4109.
- Huotari, M., Gogos, J. A., Karayiorgou, M., Koponen, O., Forsberg, M., Raasmaja, A., et al. (2002). Brain catecholamine metabolism in catechol-O-methyltransferase (COMT)-deficient mice. [Research Support, Non-U.S. Gov't]. *The European Journal of Neuroscience*, 15(2), 246-256.
- Irwin, J. J., Sterling, T., Mysinger, M. M., Bolstad, E. S., and Coleman, R. G. (2012). ZINC: A Free Tool to Discover Chemistry for Biology. *Journal of Chemical Information and Modeling*, 52(7), 1757-1768.

- Iversen, L. (2000). Neurotransmitter transporters: fruitful targets for CNS drug discovery. [Review]. *Molecular Psychiatry*, 5(4), 357-362.
- Keating, G. M., and Lyseng-Williamson, K. A. (2005). Tolcapone: a review of its use in the management of Parkinson's disease. [Review]. *CNS Drugs*, 19(2), 165-184.
- Keiser, M. J., Roth, B. L., Armbruster, B. N., Ernsberger, P., Irwin, J. J., and Shoichet, B. K. (2007). Relating protein pharmacology by ligand chemistry. [Evaluation Studies Research Support, N.I.H., Extramural Research Support, U.S. Gov't, Non-P.H.S.]. *Nature Biotechnology*, 25(2), 197-206.
- Kier, L.B. (1967) Molecular orbital calculation of preferred conformations of acetylcholine, muscarine, and muscarone. *Mol Pharmacol.* 3:487-494.
- Kier, L. B. (1973) The prediction of molecular conformation as a biologically significant property. *Pure Appl Chem*, 35, 509–520.
- Kim, S. S., Lee, H. W., and Lee, K. T. (2009). Validated method for determination of mazindol in human plasma by liquid chromatography/tandem mass spectrometry. [Research Support, Non-U.S. Gov't Validation Studies]. *Journal of Chromatography. B, Analytical technologies in the biomedical and life sciences*, 877(10), 1011-1016.
- Kristensen, A. S., Andersen, J., Jorgensen, T. N., Sorensen, L., Eriksen, J., Loland, C. J., et al. (2011). SLC6 neurotransmitter transporters: structure, function, and regulation. [Review]. *Pharmacological Reviews*, 63(3), 585-640.
- Kuhn, R. (1958). The treatment of depressive states with G 22355 (imipramine hydrochloride). *The American Journal of Psychiatry*, 115(5), 459-464.
- Langer, T. and Hoffmann, R.D. (2006) Pharmacophores and pharmacophore searches in

- Methods and Principles in Medicinal Chemistry, vol. 32 R. Manhold, H. Kubinyi, and G. Folkers, eds., Wiley-VCH Verlag GmbH, Weinheim.
- Langer, T. (2010) Pharmacophores in drug research. *Mol Inf*, 29: 470-475.
- Leach, A.R.; Gillet, V.J.; Lewis, R.A. and Taylor, R. (2010) Three-Dimensional Pharmacophore methods in drug discovery. *J Med Chem*, 53, 539-558.
- Lee, C. H., Huang, H. C., and Juan, H. F. (2011). Reviewing ligand-based rational drug design: the search for an ATP synthase inhibitor. *International Journal of Molecular Sciences*, 12(8), 5304-5318.
- Limmroth, V., and Michel, M. C. (2001). The prevention of migraine: a critical review with special emphasis on beta-adrenoceptor blockers. [Review]. *British Journal of Clinical Pharmacology*, 52(3), 237-243.
- Lin, Z., Canales, J. J., Bjorgvinsson, T., Thomsen, M., Qu, H., Liu, Q. R., et al. (2011). Monoamine transporters: vulnerable and vital doorkeepers. [Research Support, N.I.H., Extramural Research Support, N.I.H., Intramural Research Support, Non-U.S. Gov't Review]. *Progress in Molecular Biology and Translational Science*, 98, 1-46.
- Macdougall, I. J., and Griffith, R. (2008). Pharmacophore design and database searching for selective monoamine neurotransmitter transporter ligands. *Journal of Molecular Graphics & Modeling*, 26(7), 1113-1124.
- Manepalli, S., Geffert, L. M., Surratt, C. K., and Madura, J. D. (2011). Discovery of novel selective serotonin reuptake inhibitors through development of a protein-based pharmacophore. [Research Support, N.I.H., Extramural Research Support, U.S. Gov't, Non-P.H.S.]. *Journal of Chemical Information and Modeling*, 51(9),

- 2417-2426.
- Markt, P.; Schuster, D.; Langer, T. (2011) Pharmacophore Models for Virtual Screening in Methods and Principles in Med. Chem. Vol. 48 pgs. 115-152.
- Marriott, D. P., Dougall, I. G., Meghani, P., Liu, Y. J., and Flower, D. R. (1999). Lead generation using pharmacophore mapping and three-dimensional database searching: application to muscarinic M(3) receptor antagonists. [In Vitro]. *Journal of Medicinal Chemistry*, 42(17), 3210-3216.
- Martin, Y.C. (2000) Pharmacophore Perception, Development and Use in Drug Design O.F.Guner, ed., La Jola, CA, pp. 49-68.
- Mill, J., and Petronis, A. (2007). Molecular studies of major depressive disorder: the epigenetic perspective. [Research Support, N.I.H., Extramural Research Support, Non-U.S. Gov't Review]. *Molecular Psychiatry*, 12(9), 799-814.
- Millan, M. J., Gobert, A., Lejeune, F., Newman-Tancredi, A., Rivet, J. M., Auclair, A., et al. (2001). S33005, a novel ligand at both serotonin and norepinephrine transporters: I. Receptor binding, electrophysiological, and neurochemical profile in comparison with venlafaxine, reboxetine, citalopram, and clomipramine. [Comparative Study]. *The Journal of Pharmacology and Experimental Therapeutics*, 298(2), 565-580.
- Molecular Operating Environment (MOE)*, Chemical Computing Group Inc.: Montreal, QC, Canada H3A 2R7, 2010.
- Moon, J. B., and Howe, W. J. (1991). Computer design of bioactive molecules: a method for receptor-based de novo ligand design. *Proteins*, 11(4), 314-328.
- Moore, R. Y., and Bloom, F. E. (1979). Central catecholamine neuron systems: anatomy

- and physiology of the norepinephrine and epinephrine systems. [Comparative Study Research Support, U.S. Gov't, P.H.S. Review]. *Annual Review of Neuroscience*, 2, 113-168.
- Nelson, N. (1998). The family of Na⁺/Cl⁻ neurotransmitter transporters. [Research Support, Non-U.S. Gov't Research Support, U.S. Gov't, Non-P.H.S. Review]. *Journal of Neurochemistry*, 71(5), 1785-1803.
- Nemeroff, C. B., and Owens, M. J. (2002). Treatment of mood disorders. [Research Support, U.S. Gov't, P.H.S. Review]. *Nature neuroscience*, 5 Suppl, 1068-1070.
- Ong, H. T. (2007). Beta blockers in hypertension and cardiovascular disease. [Review]. *BMJ*, 334(7600), 946-949.
- Owens, M. J., Morgan, W. N., Plott, S. J., and Nemeroff, C. B. (1997). Neurotransmitter receptor and transporter binding profile of antidepressants and their metabolites. [Research Support, Non-U.S. Gov't Research Support, U.S. Gov't, P.H.S.]. *The Journal of Pharmacology and Experimental Therapeutics*, 283(3), 1305-1322.
- Pacholczyk, T., Blakely, R. D., and Amara, S. G. (1991). Expression cloning of a cocaine- and antidepressant-sensitive human noradrenaline transporter. [Research Support, Non-U.S. Gov't]. *Nature*, 350(6316), 350-354.
- Pandit, D., So, S. S., and Sun, H. (2006). Enhancing specificity and sensitivity of pharmacophore-based virtual screening by incorporating chemical and shape features--a case study of HIV protease inhibitors. [Research Support, Non-U.S. Gov't]. *Journal of Chemical Information and Modeling*, 46(3), 1236-1244.
- Piscitelli, C. L., Krishnamurthy, H., and Gouaux, E. (2010). Neurotransmitter/sodium symporter orthologue LeuT has a single high-affinity substrate site. [Research

- Support, N.I.H., Extramural Research Support, Non-U.S. Gov't]. *Nature*, 468(7327), 1129-1132.
- Posey, D. J., and McDougle, C. J. (2007). Guanfacine and guanfacine extended release: treatment for ADHD and related disorders. [Research Support, N.I.H., Extramural Research Support, Non-U.S. Gov't Review]. *CNS Drug Reviews*, 13(4), 465-474.
- Raistrick, D., West, D., Finnegan, O., Thistlethwaite, G., Brearley, R., and Banbery, J. (2005). A comparison of buprenorphine and lofexidine for community opiate detoxification: results from a randomized controlled trial. [Comparative Study Randomized Controlled Trial Research Support, Non-U.S. Gov't]. *Addiction*, 100(12), 1860-1867.
- Ramos, B. P., and Arnsten, A. F. (2007). Adrenergic pharmacology and cognition: focus on the prefrontal cortex. [Research Support, N.I.H., Extramural Review]. *Pharmacology & Therapeutics*, 113(3), 523-536.
- Rasmussen, S. G., and Gether, U. (2005). Purification and fluorescent labeling of the human serotonin transporter. *Biochemistry*, 44(9), 3494-3505.
- Rohrer, S. G., and Baumann, K. (2009). Maximum unbiased validation (MUV) data sets for virtual screening based on PubChem bioactivity data. [Validation Studies]. *Journal of Chemical Information and Modeling*, 49(2), 169-184.
- Roth, B. L., Sheffler, D. J., and Kroeze, W. K. (2004). Magic shotguns versus magic bullets: selectively non-selective drugs for mood disorders and schizophrenia. [Research Support, U.S. Gov't, P.H.S. Review]. *Nature Reviews. Drug Discovery*, 3(4), 353-359.
- Sanders, M.P.; Barbosa, A.J.; Zarzycka, B.; Nicolaes, G.A.; Klomp, J.P.; de Vlieg,

- J. and Del Rio, A. (2012a) Comparative analysis of pharmacophore screening tools. *J Chem Inf Model*, 52:1607-1620.
- Sanders, M.P.; McGuire, R.; Roumen, L.; de Esch, I.J.; de Vlieg, J.; Klomp, J.P. and de Graaf, C. (2012b) From the protein's perspective: the benefits and challenges of protein structure-based pharmacophore modeling. *Med Chem Commun*, 3, 28-38.
- Schlessinger, A., Geier, E., Fan, H., Irwin, J. J., Shoichet, B. K., Giacomini, K. M., et al. (2011). Structure-based discovery of prescription drugs that interact with the norepinephrine transporter, NET. [Research Support, N.I.H., Extramural Research Support, Non-U.S. Gov't]. *Proceedings of the National Academy of Sciences of the United States of America*, 108(38), 15810-15815.
- Schneider, G., and Bohm, H. J. (2002). Virtual screening and fast automated docking methods. [Review]. *Drug Discovery Today*, 7(1), 64-70.
- Schneider, G.; Baringhaus, K.; Kubinyi, H. (2008) Molecular Design: Concepts and Applications, Wiley-VCH: Weinheim.
- Seidel, T.; Ibis, G.; Bedix, F. and Wolber, G. (2010) Strategies for 3D pharmacophore-based virtual screening. *Drug Discovery Today*, 7, 221-8.
- Shoichet, B. K. (2004). Virtual screening of chemical libraries. [Research Support, U.S. Gov't, P.H.S. Review]. *Nature*, 432(7019), 862-865.
- Sleno, L., and Emili, A. (2008). Proteomic methods for drug target discovery. [Research Support, Non-U.S. Gov't Review]. *Current Opinion in Chemical Biology*, 12(1), 46-54.
- Sneider, W. (2005) Drug Discovery: A History. John Wiley & Sons, Ltd.: Chichester,

UK.

- Sridharan, V., Suryavanshi, P.A., and Menendez, C.J. (2011) Advances in the chemistry of tetrahydroquinolines. [Review]. *Chem Rev*, *111*, 7157-7259.
- Starke, K. (2001). Presynaptic autoreceptors in the third decade: focus on alpha2-adrenoceptors. [Review]. *Journal of Neurochemistry*, *78*(4), 685-693.
- Sun-Edelstein, C., Tepper, S. J., and Shapiro, R. E. (2008). Drug-induced serotonin syndrome: a review. [Research Support, Non-U.S. Gov't Review]. *Expert Opinion on Drug Safety*, *7*(5), 587-596.
- Tanoue, A., Koshimizu, T. A., Shibata, K., Nasa, Y., Takeo, S., and Tsujimoto, G. (2003). Insights into alpha1 adrenoceptor function in health and disease from transgenic animal studies. [Review]. *Trends in Endocrinology and Metabolism: TEM*, *14*(3), 107-113.
- Tate, C. G. (2001). Overexpression of mammalian integral membrane proteins for structural studies. [Review]. *FEBS letters*, *504*(3), 94-98.
- Tate, C. G., and Blakely, R. D. (1994). The effect of N-linked glycosylation on activity of the Na(+)- and Cl(-)-dependent serotonin transporter expressed using recombinant baculovirus in insect cells. [Research Support, Non-U.S. Gov't Research Support, U.S. Gov't, P.H.S.]. *The Journal of Biological Chemistry*, *269*(42), 26303-26310.
- Tate, C. G., Haase, J., Baker, C., Boorsma, M., Magnani, F., Vallis, Y., et al. (2003). Comparison of seven different heterologous protein expression systems for the production of the serotonin transporter. [Comparative Study Research Support, Non-U.S. Gov't]. *Biochimica et Biophysica Acta*, *1610*(1), 141-153.
- Tatsumi, M., Groshan, K., Blakely, R. D., and Richelson, E. (1997). Pharmacological

- profile of antidepressants and related compounds at human monoamine transporters. [In Vitro Research Support, Non-U.S. Gov't Research Support, U.S. Gov't, P.H.S.]. *European Journal of Pharmacology*, 340(2-3), 249-258.
- Tellioglu, T., and Robertson, D. (2001). Genetic or acquired deficits in the norepinephrine transporter: current understanding of clinical implications. [News]. *Expert Reviews in Molecular Medicine*, 2001, 1-10.
- Thangapandian, S., John, S., Sakkiah, S., and Lee, K. W. (2010). Ligand and structure based pharmacophore modeling to facilitate novel histone deacetylase 8 inhibitor design. [Research Support, Non-U.S. Gov't]. *European Journal of Medicinal Chemistry*, 45(10), 4409-4417.
- Tondi, D., Slomczynska, U., Costi, M. P., Watterson, D. M., Ghelli, S., and Shoichet, B. K. (1999). Structure-based discovery and in-parallel optimization of novel competitive inhibitors of thymidylate synthase. [Research Support, Non-U.S. Gov't Research Support, U.S. Gov't, P.H.S.]. *Chemistry & Biology*, 6(5), 319-331.
- Triballeau, N.; Bertrand, H.O. and Acher, F. (2006) Are you sure you have a good model in Pharmacophores and pharmacophore searches. Vol. 32 T. Langer and R.D. Hoffmann, eds., Wiley-VCH Verlag GmbH, Weinheim.
- Tropsha, A., and Wang, S. X. (2006). QSAR modeling of GPCR ligands: methodologies and examples of applications. [Research Support, N.I.H., Extramural Research Support, Non-U.S. Gov't Review]. *Ernst Schering Foundation Symposium Proceedings* (2), 49-73.
- Tsigos, C., and Chrousos, G. P. (2002). Hypothalamic-pituitary-adrenal axis, neuroendocrine factors and stress. [Review]. *Journal of Psychosomatic Research*,

53(4), 865-871.

- Tsuruda, P. R., Yung, J., Martin, W. J., Chang, R., Mai, N., and Smith, J. A. (2010). Influence of ligand binding kinetics on functional inhibition of human recombinant serotonin and norepinephrine transporters. *Journal of Pharmacological and Toxicological Methods*, 61(2), 192-204.
- Vaishnavi, S. N., Nemeroff, C. B., Plott, S. J., Rao, S. G., Kranzler, J., and Owens, M. J. (2004). Milnacipran: a comparative analysis of human monoamine uptake and transporter binding affinity. [Comparative Study Research Support, Non-U.S. Gov't]. *Biological Psychiatry*, 55(3), 320-322.
- van Drie, J. H. (2003). Pharmacophore discovery--lessons learned. [Review]. *Current Pharmaceutical Design*, 9(20), 1649-1664.
- Varnek, A. and Tropsha, A. (2008) Chemoinformatics Approaches to Virtual Screening. RSC Publishing: Cambridge.
- Vetulani, J., and Nalepa, I. (2000). Antidepressants: past, present and future. [Review]. *European Journal of Pharmacology*, 405(1-3), 351-363.
- Vyas, V.; Jain, An.; Jain, Av. and Gupta, A. (2008) Virtual screening: a fast tool for drug design. *Sci Pharm*, 76, 333-360.
- Wagstaff, R., Hedrick, M., Fan, J., Crowe, P. D., and DiSepio, D. (2007). High-throughput screening for norepinephrine transporter inhibitors using the FLIPRTetra. *Journal of Biomolecular Screening*, 12(3), 436-441.
- Walters, W.P., Stahl, M.T. and Murcko, M.A. (1998) Virtual Screening-An Overview. *Drug Discovery Today*, 3, 160-178.
- Wang, C. I., and Lewis, R. J. (2010). Emerging structure-function relationships defining

- monoamine NSS transporter substrate and ligand affinity. [Research Support, Non-U.S. Gov't Review]. *Biochemical Pharmacology*, 79(8), 1083-1091.
- Waszkowycz, B. (2002). Structure-based approaches to drug design and virtual screening. [Review]. *Current Opinion in Drug Discovery & Development*, 5(3), 407-413.
- Wermuth, C.G. and Langer, T. (1993) Pharmacophore Identification. In 3D QSAR in Drug Design. Theory Methods and Applications. H.Kubinyi, ed, Leiden: ESCOM Science Publishers, 117-136.
- Wolber, G., Seidel, T., Bendix, F., and Langer, T. (2008). Molecule-pharmacophore superpositioning and pattern matching in computational drug design. [Review]. *Drug Discovery Today*, 13(1-2), 23-29.
- Yang, S. Y. (2010). Pharmacophore modeling and applications in drug discovery: challenges and recent advances. [Review]. *Drug Discovery Today*, 15(11-12), 444-450.
- Young, J.B. and Landsberg, L. (1998) Catecholamines and the adrenal medulla in Willimas Textbook of Endocrinology, 9th Ed. J.D. Wilson and D.W. Foster, eds., W.B. Saunders Co., Philadelphia, 680-2.
- Zeng, F., Jarkas, N., Stehouwer, J. S., Voll, R. J., Owens, M. J., Kilts, C. D., et al. (2008). Synthesis, in vitro characterization, and radiolabeling of reboxetine analogs as potential PET radioligands for imaging the norepinephrine transporter. [Research Support, N.I.H., Extramural Research Support, Non-U.S. Gov't]. *Bioorganic & Medicinal Chemistry*, 16(2), 783-793.
- Zhou, J. (2004). Norepinephrine transporter inhibitors and their therapeutic potential.

Drugs of the Future, 29(12), 1235-1244.

Zhou, Z., Zhen, J., Karpowich, N. K., Law, C. J., Reith, M. E., and Wang, D. N. (2009).

Antidepressant specificity of serotonin transporter suggested by three LeuT-SSRI structures. [Research Support, N.I.H., Extramural Research Support, Non-U.S. Gov't]. *Nature Structural & Molecular Biology*, 16(6), 652-657.